# Deepwater Wind South Fork Wind Farm:
## Hydrodynamic and Sediment Transport Modeling Results

**Prepared for:** Jacobs
18 Tremont St., Suite 700
Boston, MA 03861

**On behalf of:** Deepwater Wind
56 Exchange Terrace
Providence, RI 02903

**Submitted By:** RPS
**Date Submitted:** 23 May 2018
**Report Authors:** Nathan Vinhateiro, Deborah Crowley, Daniel Mendelsohn
**Project POC:** Nathan Vinhateiro
55 Village Square Drive, South Kingstown, RI 02879
P: 401.789.6224; E: Nathan.Vinhateiro@rpsgroup.com

## Executive Summary

Deepwater Wind (DWW) is proposing to develop the South Fork Wind Farm (SFWF) within the Outer Continental Shelf (OCS) waters offshore Rhode Island and Massachusetts Wind Energy Area (RI-MA WEA). The project is located approximately 31 kilometers (km) southeast of Block Island, RI and consists of up to 15 wind turbine generators (WTG) connected by an inter-array cable network, and an offshore substation. Power generated from the SFWF will be delivered to Long Island, NY via the South Fork Export Cable (SFEC), which will run from the offshore substation to a landfall location in East Hampton, NY. Collectively, the SFWF and SFEC are referred to within this report as the Project.

Several aspects of project construction will require temporary seabed disturbing activities (e.g. suction dredging and jet plow trenching associated with cable installation) each of which has the potential to produce suspended sediment plumes and deposition. RPS has performed hydrodynamic and sediment dispersion modeling study to help assess potential environmental impacts of Project-related activities in support of the Project's Construction and Operations Plan (COP). Specifically, the analysis included two interconnected modeling tasks:

1. The development and calibration of a three-dimensional hydrodynamic model application for the southern New England OCS.
2. Simulations of the suspended sediment fate and transport from submarine trenching and dredging activities associated with the Project. (Current fields developed in the first modeling task were used as the primary forcing for the sediment dispersion model.)

A hydrodynamic model of the study area was first developed using RPS' HYDROMAP modeling system. The model grid was mapped to the shoreline and extended between New York Harbor at the westernmost extent, Cape Cod to the east, and south along the continental shelf approximately 75 km from Montauk. The model was forced at its open boundaries using tides and along the full water surface boundary with surface winds. The model was validated over a one-month period in 2001 when a range of synoptic datasets were collected off the coast of southeastern Long Island from a series of short-term oceanographic instrument deployments (measuring tides and currents). When compared with instrument records, the model was able to accurately reproduce tidal amplitude and phase throughout the domain and was able to capture the general patterns in circulation and trends in current speeds near the Project components. Since the sediment construction activities will primarily occur near the seabed, the validation focused on reproducing accurate current fields in the lower water column.

Following the model validation, additional HYDROMAP simulations were developed to generate a large window of time that could be used as forcing for the sediment dispersion modeling task. The simulations were run for time periods seasonally consistent with anticipated construction timeframes using a recent year (2016) to represent typical conditions in the study area. This period was selected after analyzing long-term records of local wind speed for the region. In the study area, currents vary due to tides and winds, which do not change substantially on an inter-annual basis but may exhibit variations in monthly-averages due to episodic meteorological events or river flow. The analysis showed monthly wind speeds during 2016 remain close to the long-term averages of the typical offshore conditions in the study area with no extreme outliers. Hydrodynamic fields from this period were therefore used as forcing for the predictive modeling of the sediment transport and dispersion associated with the Project.

Simulations of the suspended sediment fate and transport (including evaluation of seabed deposition and sediment plumes) were performed using RPS' SSFATE modeling system. SSFATE uses a Lagrangian (or particle-based) scheme to represent the total mass of sediments resuspended from a range of marine construction equipment including mechanic dredges, ploughs, hydraulic trenchers, and suction pumps. Working with DWW and Jacobs, RPS developed three independent modeling scenarios to evaluate patterns of sediment dispersion from:

1. Burial of the SFEC between the sea-to-shore transition offshore Long Island and the SFWF offshore substation (approximately 98.3 km) using a hydraulic trencher/mechanical plow (Scenario 1). Results from this activity are further divided to distinguish between impacts to NY state waters (SFEC-NYS) and federal waters (SFEC-OCS).
2. Burial of a representative segment of the inter-array cable between two potential WTG locations (approximately 1.4 km) using a hydraulic trencher/mechanical plow (Scenario 2). Results from this activity are entirely within federal waters.
3. Excavation of the HDD exit pit at the sea-to-shore transition site using a suction/vacuum dredger (Scenario 3). Results from this activity are entirely within NY state waters.

A total of 187 sediment grain size samples (139 by sieve analysis, 48 by hydrometer) from 66 sediment cores collected across the study area were used to develop the modeling input files. Other model inputs included volumes of the trenching/dredging areas, dredge production rates, and rates of sediment resuspension for each activity. For the simulation of the SFEC burial, the duration of construction (2 months) was sufficient to adequately capture variability of the tides and currents in the region. Simulations of the inter-array cable burial and the HDD pit excavation were notably shorter (both are less

than a day long) and therefore both activities were simulated twice, with each period sampling a different tidal regime.

Total suspended sediment (TSS) in the water column and seabed deposition from each of the above scenarios were computed on a grid with resolution of 20 meters (m) x 20 m in the horizontal dimension and 0.5 m in the vertical dimension. General findings from the sediment modeling scenarios are summarized below.

- Sediment plumes that arise during Project-related trenching or dredging activities are transient. For all scenarios, TSS concentrations are predicted to return to ambient levels within 1.4 hours of the completion of the construction activity.
- The orientation of the sediment plume oscillates with the tide at each of the scenario locations. In New York waters (near the start of the SFEC route) the plume is oriented in a NE/SW configuration, reflecting the tidal current patterns near the site, which are aligned with the nearshore topography. For construction areas in deeper waters, (east of Montauk) the plume assumes more of a N/S orientation.
- The extent and orientation of plumes from each activity is largely controlled by the hydrodynamic field and the model period. For that reason, it is important to consider that in actuality the plume may extend away from the source in multiple directions depending on the phase of the tide during construction. Considering all three scenarios, plumes exceeding 100 milligrams per liter (mg/L) are predicted to extend up to 340 m from the source; plumes above 50 mg/L may extend up to 460 m.
- During the SFEC installation (Scenario 1), the highest TSS concentrations are predicted to occur in locations where the hydro-plow passes over pockets of finer sediments (e.g. between VC-217 and VC-220, and again between VC-235 and the end of the route). Peak concentrations in these areas exceed 1,000 mg/L and plumes exceeding 100 mg/L extend several hundred meters from the trencher. Elsewhere, sediment concentrations above 30 mg/L remain within approximately 100 m of the source during the simulation.
- TSS concentrations from both the inter-array cable burial and the HDD pit excavation (Scenarios 2 and 3) are notably lower than the SFEC burial scenario, which encompasses more variability in hydrodynamics and sedimentary environments due to its scale.
- For all model runs, elevated TSS concentrations are predicted to remain very close to the seabed. Plumes above 10 mg/L are not predicted to extent vertically beyond three meters of the source at any time during each of the simulations.

- Sediments across the study area are generally coarse-grained. As a result, a large portion of the sediment mass which is resuspended is predicted to settle rapidly after its release (all scenarios). The sediments which remain in suspension and produce the broad oscillating water column plumes, disperse widely, settling on the seabed at concentrations below detection by the model (<0.1 millimeters [mm]).
- The thickest levels of sediment deposition are predicted to arise during the HDD pit excavation (Scenario 3), where the dredge and side-cast operation will occur within a relatively confined area (e.g. a single point within the model domain).
- The maximum predicted TSS concentration from portions of the SFEC burial that cross NY state waters (Scenario 1, SFEC-NYS) is 587 mg/L. TSS concentrations are predicted to return to ambient levels 1.3 hours after the trencher crosses into federal waters. The maximum predicted deposition is 9.9 mm.
- The maximum predicted TSS concentration from portions of the SFEC burial that cross federal waters (Scenario 1, SFEC-OCS) is 1,347 mg/L. TSS concentrations are predicted to return to ambient levels 1.4 hours after the conclusion of trenching. The maximum predicted deposition is 11.4 mm.
- The maximum predicted TSS concentration from the inter-array cable burial simulation (Scenario 2) is 100 mg/L. TSS concentrations are predicted to return to ambient levels within 0.3 hours following the conclusion of trenching. The maximum predicted deposition is 10.8 mm.
- The maximum predicted TSS concentration from suction dredging at the HDD pit (Scenario 3) is 562 mg/L. TSS concentrations are predicted to return to ambient levels within 1.1 hours following the conclusion of dredging. The maximum predicted deposition is 318.3 mm.

Figure EX-1 shows the cumulative footprint of excess TSS resulting from all model simulations; additional results are summarized in Table EX-1.

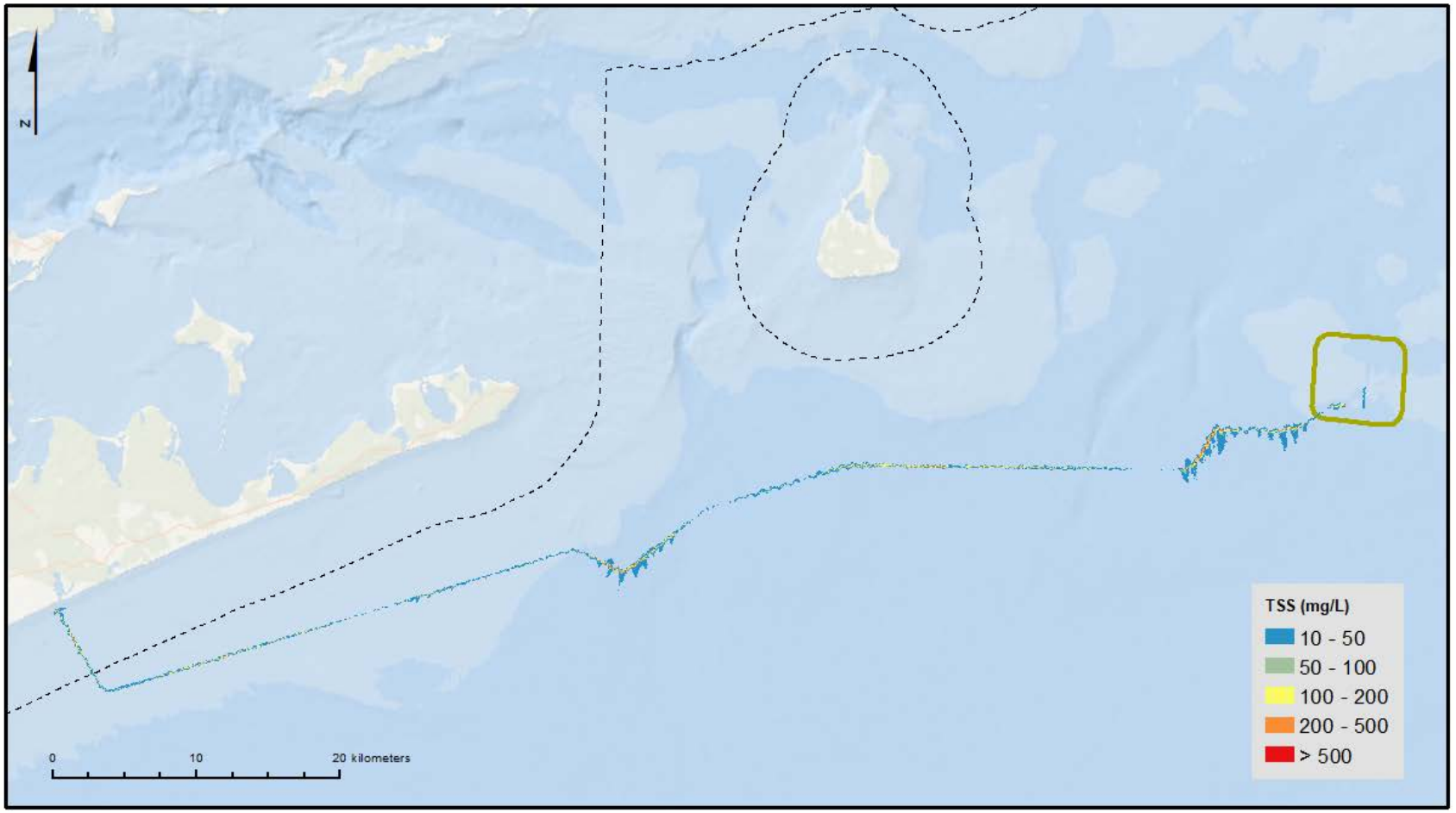


Figure EX-1. Cumulative footprint of excess TSS (> 10 mg/L) from all offshore construction simulations. Dashed line shows the Submerged Lands Act (SLA) boundary – 5.6 km seaward of the coastline – marking the transition between federal waters on the OCS and state territorial waters.

Table EX- 1. Summary of model-predicted TSS and deposition results

| Scenario | Construction Activity | Total Sediment Volume ($m^3$) | Duration of TSS plume (hrs) | Time For TSS to return to ambient (hrs) | Max Distance of TSS Plume exceeding ambient (m) | | Peak TSS concentration (mg/L) | Maximum Extent of Deposition > 1 cm (m) | Areal Extent of Deposition > 1 cm (ha) | Max deposition thickness (mm) |
|---|---|---|---|---|---|---|---|---|---|---|
| | | | | | 50 mg/L | 100 mg/L | | | | |
| Scenario 1 | SFEC installation - NYS | 8,426 | 76.7 | 1.3 | 135 | 120 | 578 | -- | -- | 9.9 |
| | SFEC installation - OCS | 155,940 | 1,388.7 | 1.4 | 460 | 340 | 1,347 | 9 | 1.72 | 11.4 |
| Scenario 2 | Burial of inter-array cable between WTG 11 and WTG 9 | 2,342 | 21.0 | 0.3 | 90 | 40 | 100 | 8 | 0.04 | 10.8 |
| Scenario 3 | Excavation of seafloor for access to HDD pilot hole offshore Beach Lane | 650 | 8.3 | 1.1 | 260 | 145 | 562 | 54 | 0.56 | 318.3 |

## Table of Contents

## List of Figures

## List of Tables

# 1 Introduction

## 1.1 Project Background

Deepwater Wind (DWW) is proposing to develop the South Fork Wind Farm (SFWF) within the Outer Continental Shelf (OCS) waters offshore Rhode Island and Massachusetts Wind Energy Area (RI-MA WEA). The project will be located approximately 31 km southeast of Block Island, RI. The wind farm will occupy approximately 3,600 hectares (ha) (6 km by 6 km) near Cox's Ledge, covering portions of OCS Blocks 6965, 6966, 7015, and 7016, and will be comprised of up to 15 wind turbine generators connected by an inter-array cable network, and an offshore substation. Power generated from the SFWF will be delivered to Long Island, NY via the South Fork Export Cable (SFEC), which will run from the offshore substation to a landfall location in East Hampton, NY (Figure 1). Currently, DWW is considering two landing sites for the SFEC: the preferred landing site at Wainscott Beach (Beach Lane) and an alternative landing site at Hither Hills. Collectively, the SFWF and SFEC are referred to as the Project.

A major component of the Project will be the installation and burial of the SFEC, which will connect the SFWF with the Long Island Power Authority transmission and delivery system. The cable route will extend approximately 99 km, with 5.6 km passing through NY state waters and the remainder in federal waters. At the shore crossing, horizontal directional drilling (HDD) will be used to install the cable between a land-side entry point and a tie-in location approximately 650 m offshore. A temporary cofferdam may be installed at the point where the HDD conduit exits from the sea bed (approximately 12 m water depth). Between this point and the offshore substation at the SFWF, the cable will be buried using a jet trenching method (hydro-plow) to a depth of 1.8 m below the seabed. Except for the shore approach segment, the water depth in the SFEC burial corridor is generally between 30 and 45 meters (Fugro, 2018).

Aspects of the Project will require a range of dredging and burial techniques (e.g. suction dredging, jet trenching) each of which has the potential to produce seabed disturbances, suspended sediment plume formation, and smothering due to sedimentation. Accordingly, hydrodynamic and sediment transport and dispersion simulations have been developed to help assess potential environmental impacts of Project-related activities. This report describes the computer modeling systems and approach being used to evaluate the Project and provides predictions of suspended sediment concentrations and deposition from a set of initial construction scenarios.

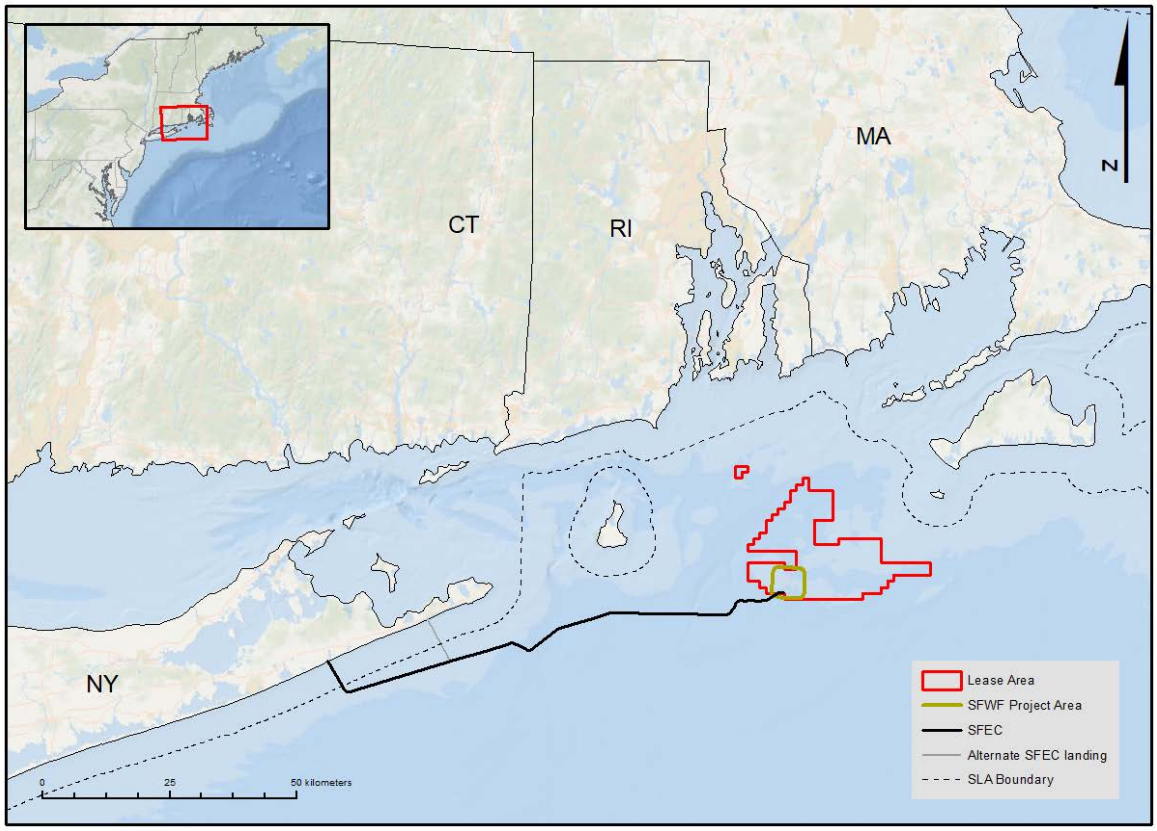


Figure 1. Offshore study area for the proposed SFWF and SFEC. Dashed line shows the Submerged Lands Act (SLA) boundary – 5.6 km seaward of the coastline – marking the transition between federal waters on the OCS and state territorial waters.

## 1.2 Overview of the Study Area

The study area is broadly situated within the southern New England OCS, which lies south of Massachusetts, Rhode Island, and Long Island, New York, and extends from the Hudson Shelf Canyon in the west to Nantucket Shoals in the east. Components of the Project that have potential for sediment disturbance span a relatively large distance, with the export cable proposed to run from one of two locations near East Hampton, NY, extending approximately 99 km east to the SFWF south of Rhode Island Sound. The general ocean circulation (currents) across these Project components (the cable route and the wind farm) is complex and influenced to some extent by wind-driven processes, tides, and density gradients that arise from combined interaction with adjacent estuaries, solar effects, and heat flux through the air-sea interface (Codiga and Ullman, 2010). Yet over most of the region, tidal currents are the dominant form of circulation (Spaulding & Gordon, 1982;) with wind and density variations playing a smaller role.

Tides in the study area are predominately semi-diurnal (twice per day) with influences from diurnal (once per day) constituents; this results in approximately two high tides and two low tides daily with a ramp to peak speeds four times a day as the current ebbs and floods in response to the changing water levels. In most locations the current direction also reverses four times a day with the ebbs and floods, however in some areas the tidal signal is present as a strengthening and weakening of currents that move predominately in the same direction as opposed to flooding in one direction and ebbing in the opposite. The currents vary spatially and temporally throughout the domain, and across portions of the study area where the Project construction will occur.

Sediments in the study area are characterized by modern marine deposits and reworked glacial and post-glacial outwash deposits. Marine deposits in this region are typically comprised of silty fine sand and are typically up to 2 to 3 meters thick. Closer to the shoreline, sediments are predominantly sandy and highly mobile due to transport from nearshore currents and waves (Fugro, 2017).

## 1.3 Objectives and Tasks

To address potential impacts from sediment resuspension during Project-related activities, RPS has been contracted to develop and apply customized hydrodynamic, and sediment transport and dispersion models to the study area. Specifically, the analysis includes two interconnected modeling tasks:

1. The development and calibration of a three-dimensional hydrodynamic model application for the southern New England OCS, including portions of Long Island Sound, Block Island Sound, Narragansett Bay, Rhode Island Sound, Buzzards Bay, Vineyard Sound, Nantucket Sound, and nearby waters of the Atlantic Ocean using the HYDROMAP modeling system.
2. Simulations of the suspended sediment fate and transport (including evaluation of seabed deposition and sediment plumes) using the SSFATE modeling system. SSFATE was applied to simulate offshore construction activities including suction dredging at the HDD exit location and cable burial by hydraulic trenching. Current fields developed using the HYDROMAP model are used as the primary forcing for the sediment dispersion model.

A description of the hydrodynamic model and its application to the study area are presented in Section 2. Section 3 provides an overview of the SSFATE sediment model and results from the application of SSFATE for a range of initial construction scenarios. References for both modeling systems are provided in Section 4.

# 2 Hydrodynamic Modeling

The initial modeling task was the development, validation, and application of a three-dimensional hydrodynamic model application for the southern New England OCS. RPS' HYDROMAP model system (Isaji et al., 2001) was used to model the circulation pattern and water volume flux through the study area and to provide hydrodynamic conditions (spatially and temporally varying currents) for input to the sediment dispersion model.

To adequately cover the full SFWF and SFEC route, the hydrodynamic model domain spans from the offshore wind energy area in the east, along the entire proposed export cable route and beyond the cable landing locations on Long Island, to the west. Since the sediment construction activities are active near the seabed and resuspended sediments are introduced to the water column close to the seabed, a three-dimensional characterization of the currents that had good representation of the bottom waters was necessary.

The hydrodynamic modeling task included gathering and analyzing environmental data, development of the model grid and boundary conditions, validation of model performance for a period coincident with observations of water levels and currents, and development of currents for two scenario timeframes to be used in the sediment transport simulations. The two different scenario timeframes coincide with anticipated installation timeframes and typical wind conditions; wind was used to define the scenario timeframe since tides do not vary seasonally.

## 2.1 HYDROMAP Model Description

HYDROMAP is a globally re-locatable hydrodynamic model capable of simulating complex circulation patterns due to tidal forcing, wind stress and fresh water flows, quickly and efficiently, anywhere on the globe. HYDROMAP employs a novel step-wise-continuous-variable rectangular (SCVR) gridding strategy with up to six levels of resolution. The term "step-wise-continuous" implies that the boundaries between successively smaller and larger grids are managed in a consistent integer step. The advantage of this approach is that large areas of widely differing spatial scales can be addressed within one consistent model application. Grids constructed by the SCVR are still "structured," so that arbitrary locations can be easily located to corresponding computational cells. This mapping facility is particularly advantageous when outputs of the hydrodynamics model are used in subsequent application programs (e.g., Lagrangian particle transport model) that use another grid or grid structure.

The hydrodynamic model solves the three-dimensional conservation equations in spherical coordinates for water mass, density, and momentum, with the Boussinesq and hydrostatic assumptions applied. These equations are solved subject to the following boundary conditions:

1) At land boundaries the normal component of velocity is set to zero;
2) At the open boundaries the sea surface elevation is specified by the dominant tidal constituents, each with its own amplitude and phase from a reference time zone, or as a time series of total surface elevation defined relative to the local surface elevation;
3) At the sea surface the applied stress due to the wind is matched to the local stress in the water column and the kinematic boundary condition is satisfied; and
4) At the sea floor a quadratic stress law, based on the local bottom velocity, is used to represent frictional dissipation and a friction coefficient parameterizes the loss rate.

The numerical solution methodology follows that of Davies (1977) and Owen (1980). The vertical variations in horizontal velocity are described by an expansion of Legendre polynomials. The resulting equations are then solved by a Galerkin-weighted residual method in the vertical and by an explicit finite difference algorithm in the horizontal. A space staggered grid scheme in the horizontal plane is used to define the study area. Sea surface elevation and vertical velocity are specified in the center of each cell while the horizontal velocities are given on the cell face. To increase computational efficiency, a "split-mode" or "two mode" formulation is used (Owen, 1980; Gordon, 1982). In the split-mode, the free-surface elevation is treated separately from the internal, three-dimensional flow variables. The free-surface elevation and vertically integrated equations of motion (external mode), for which the Courant-Friedrichs-Lewis (“CFL”) limit must be met, is solved first. The vertical structure of the horizontal components of the current then may be calculated such that the effects of surface gravity waves are separated from the three-dimensional equations of motion (internal mode). Therefore, surface gravity waves no longer limit the internal mode calculations and much longer time steps are possible. Isaji et al. (2001), and Isaji and Spaulding (1984) provide a detailed description of the model physics and numerical implementation.

HYDROMAP output includes spatially and temporally varying fields of current speed and direction. This output is seamlessly integrated as input in RPS’ transport models, including SSFATE (sediment transport and fates model).

## 2.2 Environmental Data Relevant to Hydrodynamic Model Application

Environmental data including shoreline, bathymetry, winds, tidal elevations and currents were acquired in order to understand and characterize the circulation local to the Project components in marine waters. The data were used both in developing model forcing as well as for validating the model predictions. The location of various data sources in relation to the Project components including the SFWF work area and SFEC route are shown in Figure 2; further details on the data sources are provided below.

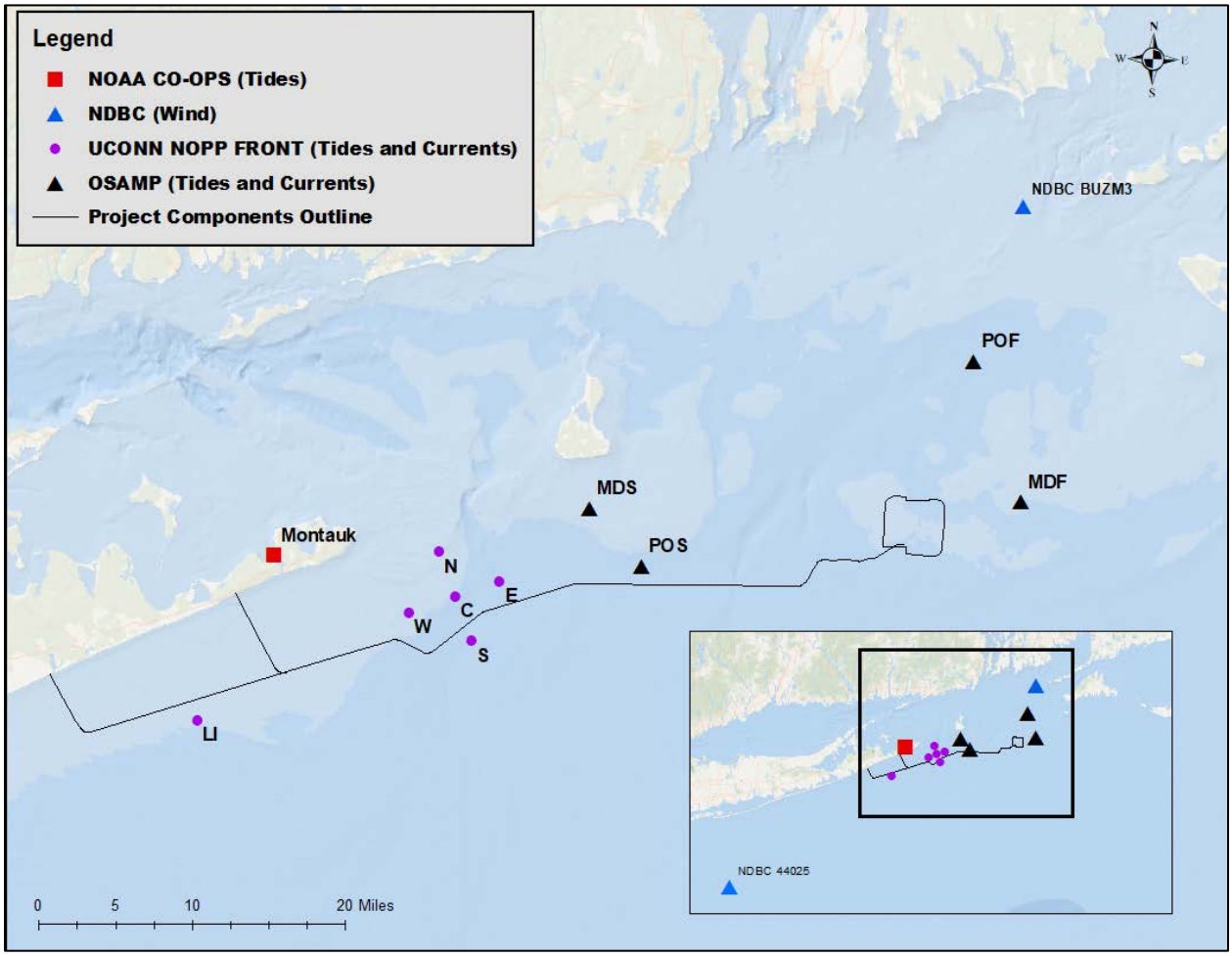


Figure 2. Location of various observations stations shown along with a delineation of the Project components.

### 2.2.1 Shoreline and Bathymetry

The model domain extends from New York City to Cape Cod and is significantly larger than the Project footprint, which was necessary to accurately locate and define open boundary conditions. The shoreline

for the domain was developed based on merging shoreline data from each of the relevant states (MA, RI, CT and NY). Bathymetry data was gathered from publicly available data provided by the National Oceanic and Atmospheric Administration (NOAA) for coastal and offshore waters of MA, CT, RI and NY. NOAA soundings were downloaded from the NOAA's Electronic Navigational Chart (ENC) Direct to GIS portal (https://encdirect.noaa.gov/) and were obtained for the harbor, coastal and approach ENC band levels. Soundings are available from their native positioning, which is irregular in spacing. The combined bathymetry dataset was used to develop the depths for the hydrodynamic model grid as well as the depth grid used in the sediment transport modeling, which is implemented with a finer resolution.

### 2.2.2 Sea Surface Height (Tide) and Current Data

Sea surface height (SSH or tides) and current data were gathered and analyzed for this study. SSH data was used for both developing model forcing and for verification of the hydrodynamic model predictions. Current data was used solely to validate the model predictions.

#### 2.2.2.1 Sea Surface Height

Multiple sources of SSH data were used in this study. The data were available either as time histories of observations of water surface elevation or in the form of harmonic constituents. Harmonic constituents represent the amplitude and phase of defined periodic constituents of the tidal signal (sine waves with different wave lengths), where the tidal signal is the sum of all constituents added together by superposition. The amplitude describes the difference between a mean sea level datum and the peak water level for a constituent, and the phase describes the timing of the signal relative to a time datum. The constituent period determines the time for one full oscillation of the signal. Tidal harmonic constituent's names indicate the approximate period (e.g., M2 is ~twice daily and O1 is ~once daily).

Output from the TPXO7 global tidal model developed by Oregon State University (OSU) was used to characterize the tides at the hydrodynamic model open boundaries. The TPX07 model output contains tidal harmonic constituent data on a ¼ degree resolution across the globe. The model is based on data from the TOPEX/Poseidon and Jason satellites, and the model methodology is documented in Egbert et al. (1994) and Egbert and Erofeeva (2002). A summary of the constituents obtained, and their specific periods, is provided in Table 1. Details on the spatially varying amplitude and phase used as boundary forcing are provided in Section 2.3.2.1.

Table 1. Tidal constituents used as boundary forcing

| Name | Constituent | Speed (degrees/hour) | Period (hours) |
|---|---|---|---|
| M2 | Principal lunar semidiurnal constituent | 28.98 | 12.42 |
| S2 | Principal solar semidiurnal constituent | 30.00 | 12.00 |
| N2 | Larger lunar elliptic semidiurnal constituent | 28.44 | 12.66 |
| K1 | Lunar diurnal constituent | 15.04 | 23.93 |
| O1 | Lunar diurnal constituent | 13.94 | 25.82 |

Observation-based tidal harmonic data was obtained from three different sources, (1) National Oceanographic and Atmospheric Administration (NOAA) published harmonics, (2) published studies associated with the Rhode Island Ocean Special Area Management Plan (OSAMP) and (3) observational data from the University of Connecticut's work through the National Oceanographic Partnership Program (NOPP), Front-Resolving Observation Network with Telemetry (FRONT) project.

Published harmonic constituents from the NOAA CO-OPS Montauk station and from two of the OSAMP offshore buoys (POF and POS) published by Grilli et al. (2010) were used in this study. The locations of these stations are shown in Figure 2 (note that the OSAMP had a total of four buoys but only two collected pressure which was converted to water depth to capture the tides). The amplitude and phase for the M2, N2, S2, K1 and O1 at each of these stations are summarized in Table 2 and Table 3 respectively. These constituents were used to develop the time histories of sea surface height at each location for different periods of time using the publicly available T_Tide Matlab Toolbox; methodologies of the toolbox are described in Pawlowicsz et al. (2002). The generated time history was used for comparisons of the model predictions of water level at these locations. All four OSAMP buoys also had observations of currents throughout the water column for varying durations between fall 2009 and winter 2010, however the model validation period was performed over a different timeframe, where observations were available from instruments closer to the route from the UCONN NOPP FRONT project.

Table 2. Summary of amplitudes of harmonic constituents within the study domain

| Summary of Harmonic Constituent Amplitude (m) | | | | | | |
|---|---|---|---|---|---|---|
| **Location** | **Source** | **M2** | **S2** | **N2** | **K1** | **O1** |
| Montauk | NOAA | 0.302 | 0.065 | 0.079 | 0.074 | 0.054 |
| POS | Grilli et al. | 0.443 | 0.095 | 0.104 | 0.073 | 0.022 |
| POF | Grilli et al. | 0.452 | 0.098 | 0.111 | 0.068 | 0.034 |

Table 3. Summary of phases of harmonic constituents within the study domain

| Summary of Harmonic Constituent Phase (degrees) | | | | | | |
|---|---|---|---|---|---|---|
| **Location** | **Source** | **M2** | **S2** | **N2** | **K1** | **O1** |
| Montauk | NOAA | 46.8 | 56.6 | 22.2 | 178.7 | 209.8 |
| POS | Grilli et al. | 3.9 | 18.7 | 350.5 | 166.8 | 16.3 |
| POF | Grilli et al. | 0.9 | 18.2 | 344.7 | 167.2 | 7.4 |

#### 2.2.2.2 Currents

Measured data from the UCONN NOPP FRONT project (Codiga and Houk, 2002) was used to validate the model predictions. This project involved multiple intermittent deployments of oceanographic instruments within the inner continental shelf between Montauk and Block Island within the period of 1999 - 2002. The same general location was sampled for multiple short-term deployments. One of the deployments included an additional instrument located off the coast of southeastern Long Island, and this deployment period was selected as the period of model validation because it had the greatest number of observations which spanned different relevant portions of the study area. The locations of these stations are shown in Figure 2. The time history of observed pressure from each instrument was converted to water level; these records were then used for comparisons to model predictions at these locations. Additionally, the vertical profile of observed currents was available at each of these stations and was used for comparisons to model predictions of speed and direction at these locations. Based on the availability of synoptic data the model validation period was defined as the period from 8 October 2001 through 7 November 2001.

### 2.2.3 Wind Data

HYDROMAP forcing also includes surface winds and thus record describing the wind speed and direction during the simulation period was needed. While there are multiple buoys that have recorded winds within the domain for varying periods of record, only the National Data Buoy Center (NDBC) Buzzards Bay station BUZM3, and NDBC 44025 had observed winds during the model validation period in 2001; the location of these stations is also shown in Figure 2. At both stations, wind speed and direction were obtained from an anemometer located above mean sea level, approximately 24.8 m for BUZM3 and 5 m for NDBC 44025. (For the purposes of this comparative analysis the wind speeds were not adjusted to a common height since the focus was on the direction and distribution as opposed to absolute value however it should be noted that the speeds at BUZM3 would be lower at a 5 m height, or conversely the speeds at NDBC 44025 would be greater at a 24.8 m height.) Measurements at both stations are recorded on an hourly time step. Since these stations spanned the project, and majority of the domain, the wind records at these two sites were compared for the year 2001 to investigate the variability across the domain. The wind roses for

these sites is presented in Figure 3, which indicates that the trends are similar (although the winds at BUZM3 are a slightly stronger due to the elevation of the anemometer). Since station 44025 is located further offshore south of the model domain and BUZM3 is located within the model domain, and closer to the area of interest, BUZM3 was selected as the primary source for wind forcing.

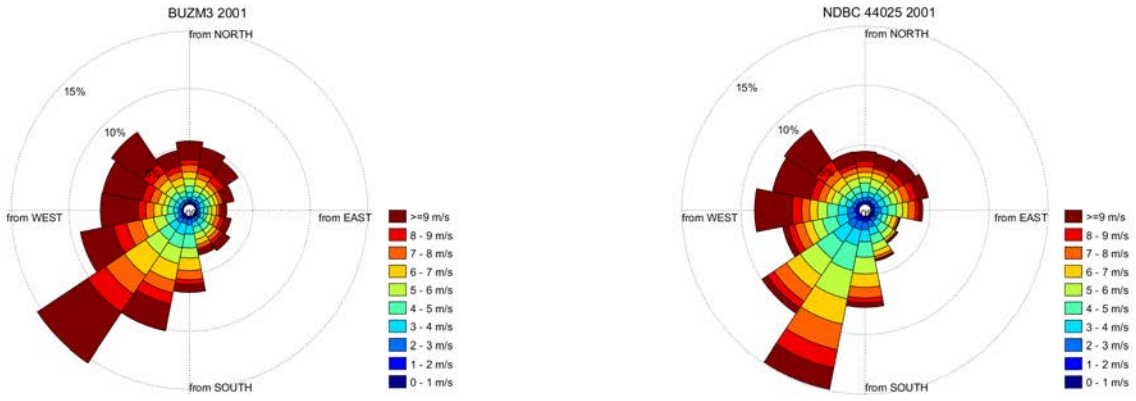


Figure 3. Wind roses for the period of 1 January 2001 through 1 January 2002 at NDBC BUZ3M Buzzards Bay station (left) and NDBC 44025 (right).

#### 2.2.3.1 Selection of Representative Simulation Periods

The primary purpose of the hydrodynamic model was to generate current fields to simulate the effects of Project activities several years into the future. As a result, it was necessary to first establish a period from the historical record representative of the typical offshore conditions in the study area. Currents in the area vary primarily due to tides and winds, and because tides do not vary seasonally, an analysis of monthly wind records was conducted to define the scenario timeframes.

The most complete ten-year record of winds at BUZM3 (2006-2016) was analyzed to evaluate the wind characteristics and to select a typical year. Monthly average speeds were calculated for the full record and were assessed quantitatively and qualitatively to determine which year had monthly averages that most closely represented the full record. The wind rose for the complete 10-year period is shown in Figure 4. The monthly average wind speed ranges from 3.83 m/s to 10.29 m/s and the annual speed at this location is 7.6 m/s. Winds are predominately from the southwest followed by a relatively high frequency of occurrences from the northwest (though the wind rose indicates that the winds blow from all directions for some portions of the year). The trends of individual years were investigated through analysis of the

monthly average winds speeds. A two-plot figure showing (i) the differences in monthly average wind speed from the full 10-year record, and (ii) the selected typical year (2016) along with the record average, is presented in Figure 5. As can be seen in this figure the monthly averages during 2016 remain close to the record averages throughout the year with no extreme outliers.

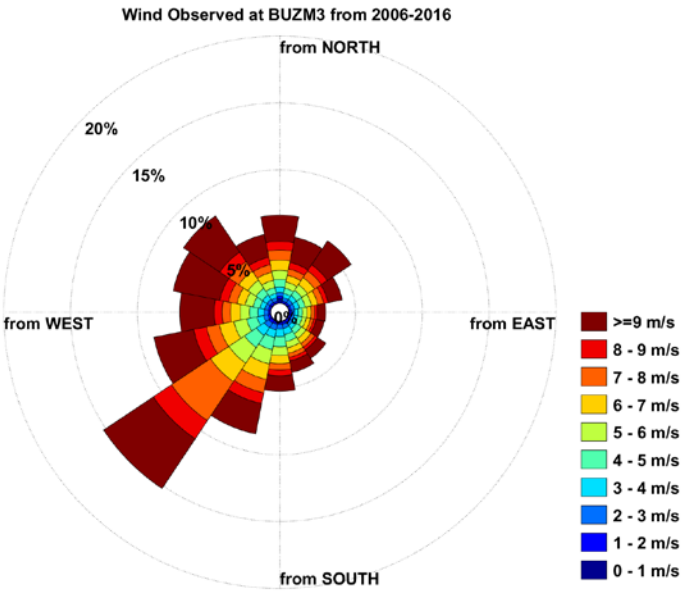


Figure 4. Wind rose for the period of 2006-2016 at NDBC BUZ3M Buzzards Bay station (24.8 m above MSL).

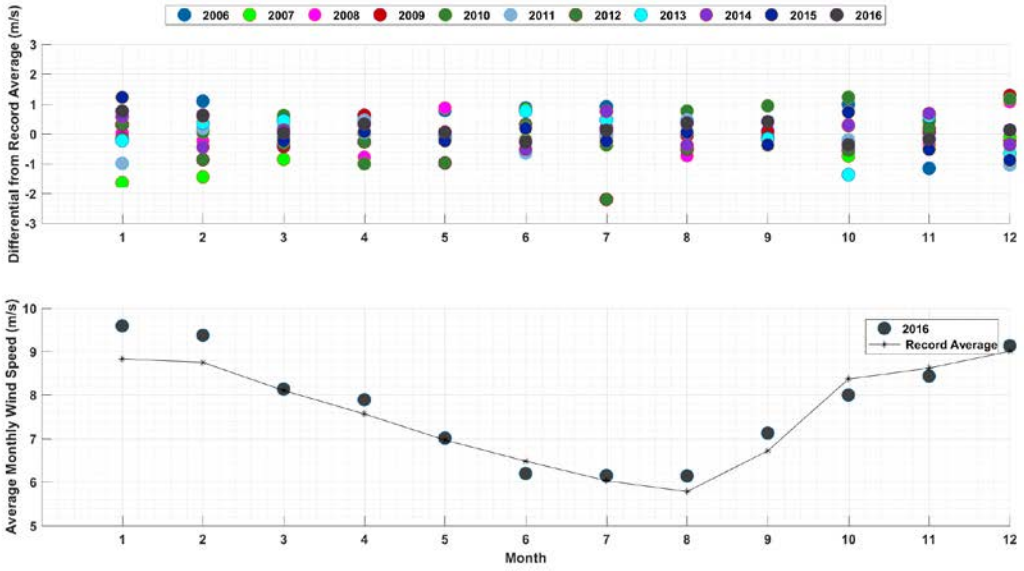


Figure 5. Monthly average wind speeds. Top plot shows the differential between monthly average wind speed for a given year (marked by color) and the record monthly average. Bottom plot shows the monthly average wind speeds for the selected typical year (2016) as well as the record average.

## 2.3 HYDROMAP Model Application

A model application of the study area was developed using the HYDROMAP hydrodynamic model system. This included development of a model grid and grid bathymetry, development of boundary forcing (tides and wind) and selection of numerical parameters. The model set up allows for three-dimensional simulations, which was utilized for this study. The vertical structure is represented by Legendre polynomials; in this instance six polynomials were used to represent the vertical variability in the currents from tidal and wind forcing. The model application was first validated to observations and then subsequently run for periods of time identified as having typical winds within a potential construction season.

### 2.3.1 Model Grid (Resolution/Bathymetry)

The complete model domain extended from New York Harbor at the westernmost extent, to Cape Cod at the eastern extent. Although this domain is significantly larger than the study area, the extent was chosen to best locate and define open boundary conditions. The computational grid for the entire domain, consisting of 23,563 active water cells is shown in Figure 6. The hydrodynamic model grid was mapped to

the shoreline with grid cell resolution ranging from ~1.0 km to 250 m; the resolution is coarse further from the shore and becomes finer in the areas closest to the shore, and local to Project activities (higher resolution grids appear darker in Figure 6), or where otherwise necessary to capture the physical characteristics of the shoreline/bathymetry. The model grid bathymetry was assigned by interpolating a set of individual data points (soundings described in 2.2.1) onto the model grid. For grid cells that contain multiple soundings, the values are averaged; grid cells without soundings are interpolated based on the closest soundings. The final gridded bathymetry is shown in Figure 7.

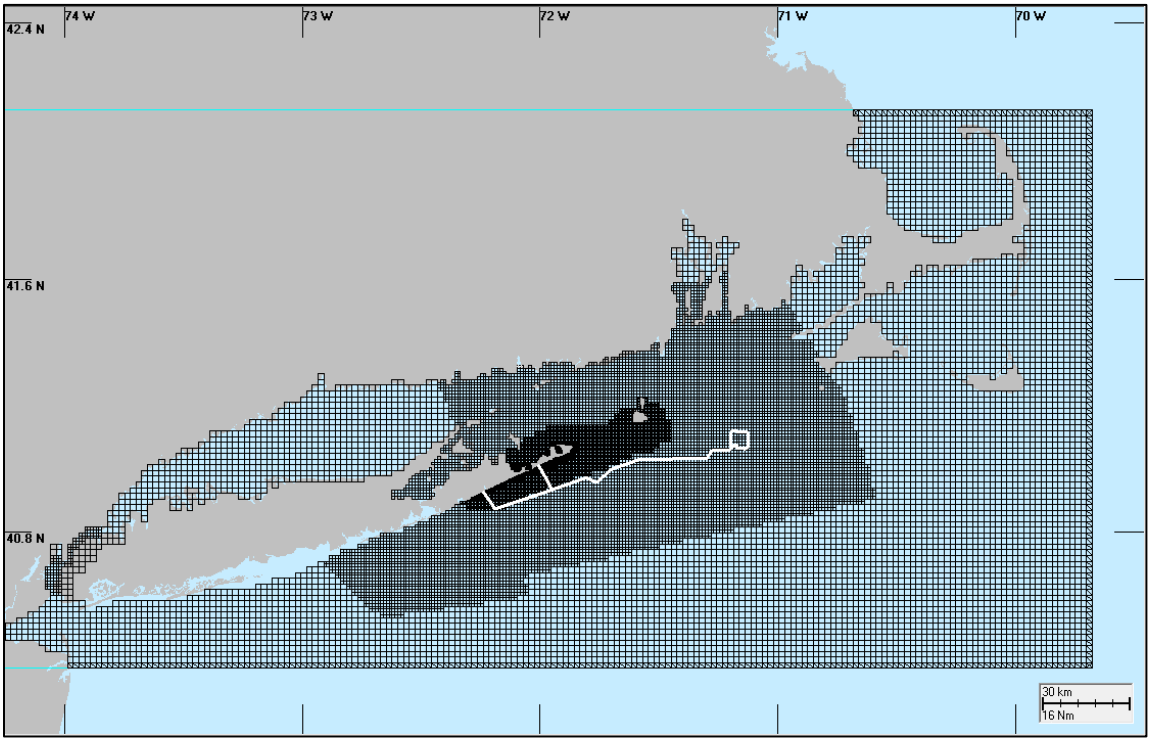


Figure 6. Hydrodynamic model grid. Areas of higher resolution appear darker as the grid becomes more refined. Project components delineated with white line.

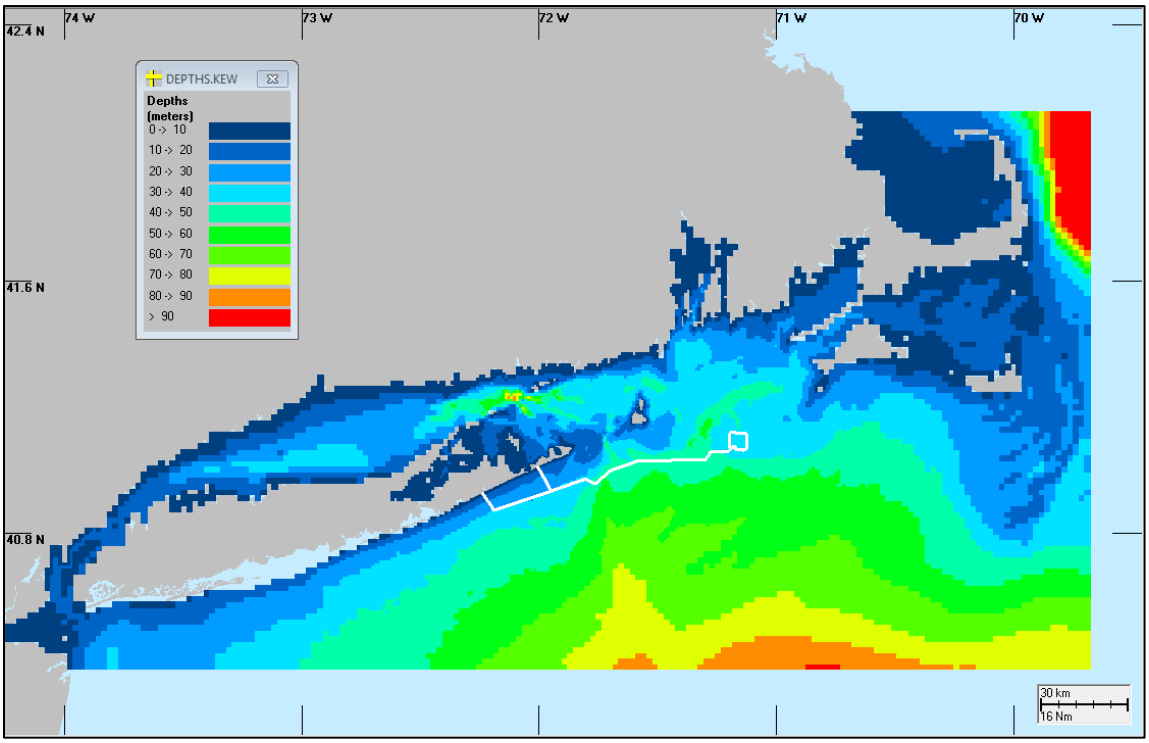


Figure 7. Model grid bathymetry. Project components delineated with white line.

### 2.3.2 Boundary Conditions

Model boundary conditions for this application included specification of tidal characteristics at open boundary water cells at the edge of the domain, and surface winds applied to all cell surfaces.

#### 2.3.2.1 Tidal Boundary Conditions

The circulation in the study area is tidally dominated, and therefore an important feature of the model application is the characterization of tidal boundary conditions. Harmonic constituent data extracted from the TPXO global tidal model was used at the model open boundaries. Each boundary cell was assigned a unique set of the harmonic constituent amplitudes and phases, interpolated from the TOPEX model predictions. In total, the open boundary was specified for the five predominant tidal constituents in the area: three semi-diurnals (M2, N2, and S2) and two diurnals (K1 and O1). HYDROMAP employs a strategy that uses the harmonic construction of astronomic tidal currents where each harmonic (constituent) is simulated individually and the real-time tide is then assembled using the harmonic summation of these simulated constituents. The dominant tidal constituent in this region is the M2-principal lunar semi-diurnal (twice daily) constituent. The M2 causes the sea level to rise and fall approximately twice daily which creates currents that peak and change direction in the areas of reversing currents; rotary currents

complete their rotation approximately twice daily. Illustrations of amplitude and phase along the model grid open boundaries are shown in Figure 8 and Figure 9 respectively. These figures illustrate that the M2 amplitude is greater than 0.4 m in most places with the exception of the southeast region of the domain. The figure also illustrates how the M2 phase is generally similar parallel to Long Island and Narragansett Bay in line with the Project components.

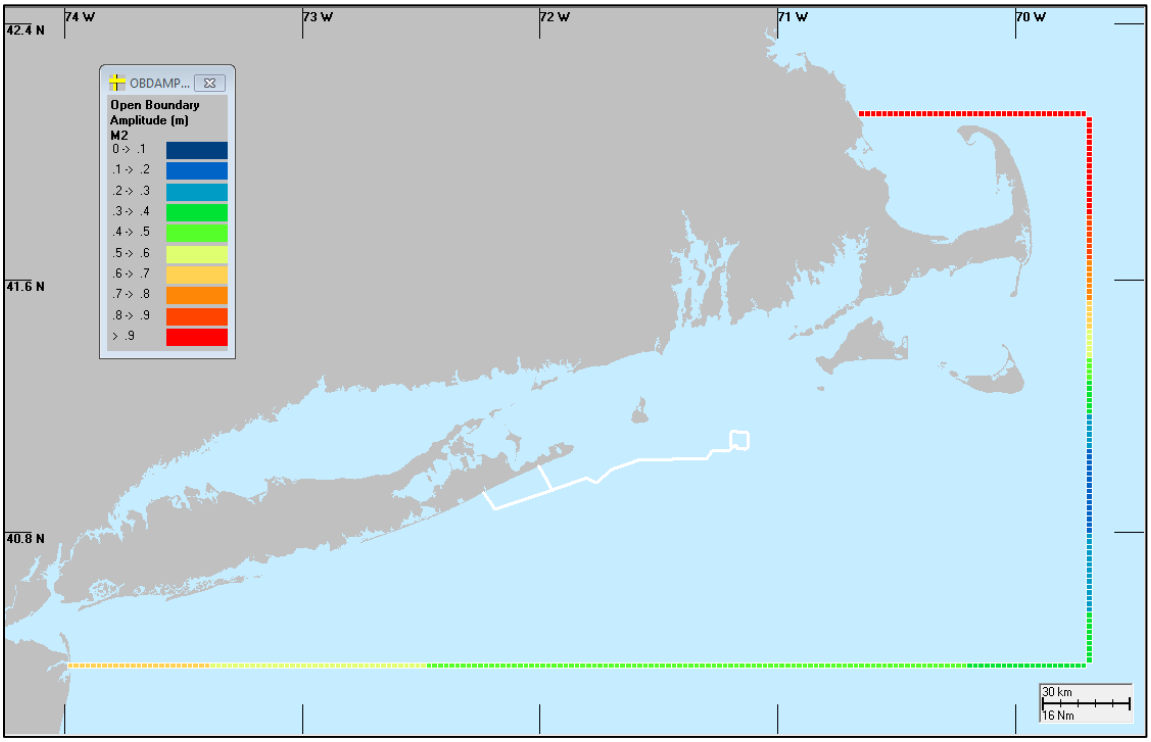


Figure 8. Tidal boundary forcing M2 amplitude. Project components delineated with white line.

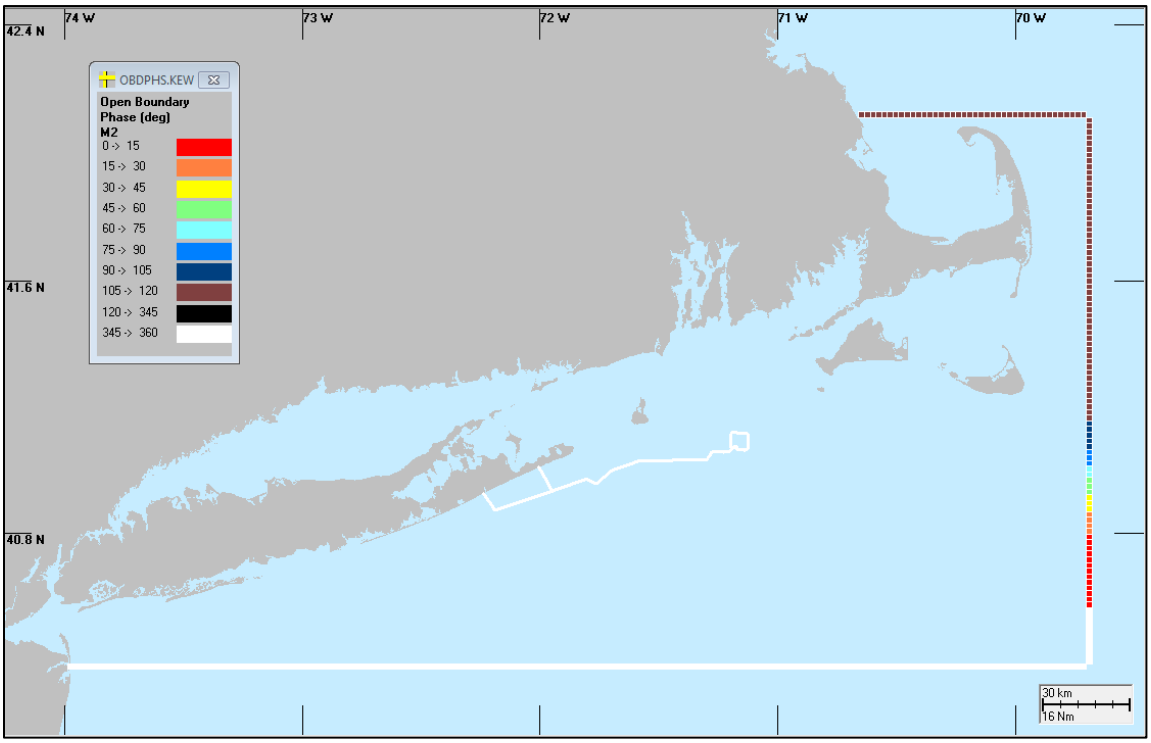


Figure 9. Tidal boundary forcing M2 and phase. Project components delineated with white line. Note that phase is defined between 0-360 degrees (and 360 degrees also equals 0 degrees) and there are no phases between 120-345 degrees which is why there are no black cells per the legend above.

#### 2.3.2.1 Meteorological Boundary Conditions

The water surface boundary covers the entire gridded area and is influenced by wind speed and direction. Meteorological data was obtained from the NDBC Buzzards Bay Station as described in 2.2.3 and was applied to the entire grid surface. The wind rose from the validation period and for the typical wind year (2016) selected are shown in Figure 10.

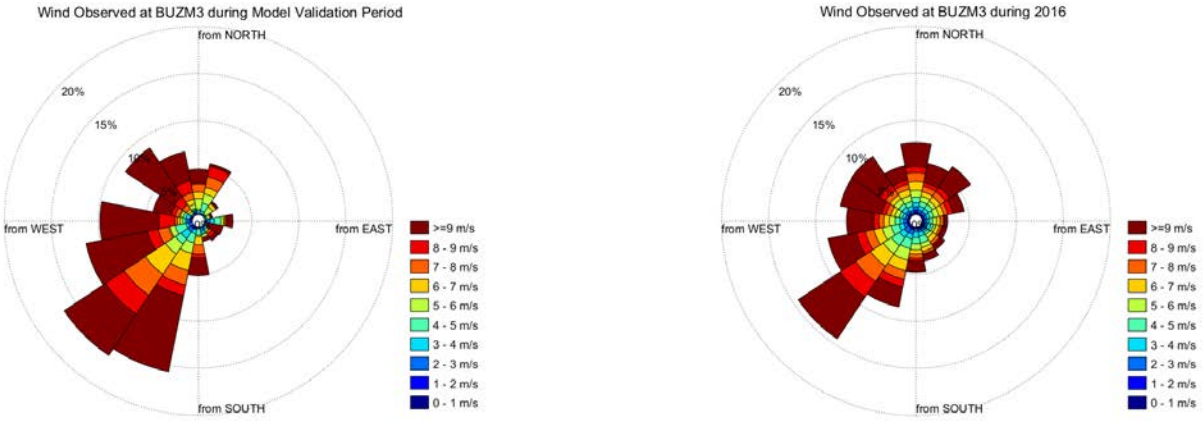


Figure 10. Wind roses from observed winds at BUZM3 (24.8m above MSL) for the model validation period (left) and the typical year 2016 (right).

## 2.4 HYDROMAP Model Results

### 2.4.1 HYDROMAP Model Results for Validation Period

The model was simulated from 8 October through 7 November 2001 and compared to observations of measured water level and currents, as well as reconstructed time histories of water level for stations with harmonic constituents (based on observations – referred herein as observations), for a total of nine stations in the model domain.

Time histories of model predictions versus observations of sea surface height (water level) are shown in Figure 11, which indicates the model is able to accurately reproduce the water elevation tidal signal. The model recreates the amplitude and timing of the tides and reproduces the spring/neap cycle well. Figure 11 also shows that the tidal signal is relatively similar between the observation stations, in the sense that it is predominately semi-diurnal with amplitudes ranging from approximately 0.2 m to 0.8 m during neap and spring tides respectively.

Figure 14 through Figure 19 show a comparison of current roses for the period of observed (left) and modeled (right) currents. The current roses show an integrated summary of the frequency and magnitude of current speeds and directions. The rose petals are sized in accordance to the frequency of time that the currents flow in a certain direction (e.g. north-northeast) and the color-coded bands represent the frequency of speeds in that direction. Reviewing these figures, it can be seen that the model generally does well recreating current directions and reproducing the overall spatial trends as well as the relative trends in current magnitude. In some locations the model does not capture all the directional variability of the record, particularly near the surface, however this is not integral to the sediment transport processes, which are focused at or near the seabed. It is notable that the model reproduced the relatively strong currents at station FA01-N while also reproducing the directionally biased currents (flowing east) at FA01-L1, located offshore southeastern Long Island.

The HYDROMAP-predicted current fields vary in both space and time. Snapshots showing examples of approximate peak ebb and peak flood are shown in Figure 20 and Figure 21 for surface currents, and Figure 22 and Figure 23 for bottom currents. The total number of vectors has been subsampled for clarity of presentation. These figures indicate that bottom currents near the Project components peak at speeds typically less than 0.2 – 0.3 m/s.

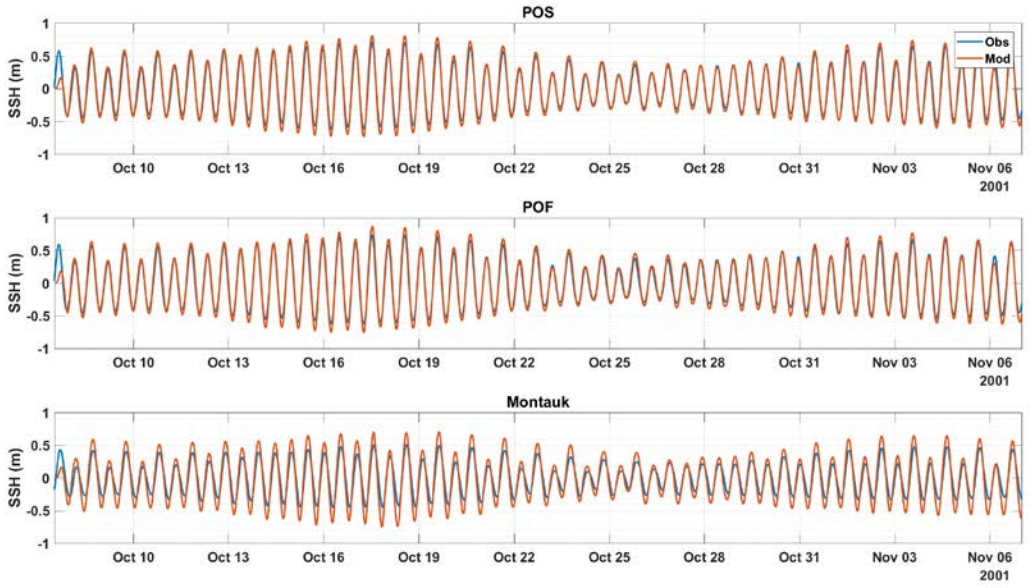


Figure 11. Observed and model predicted sea surface height (SSH) relative to MSL at multiple stations across the model domain for the validation period of 8 October through 7 November 2001. Observed time series shown in blue and model predicted shown in orange. From top to bottom: POS, POF, Montauk. Y-axis in each plot extends from 1 m below MSL (-1) to 1m above MSL (1).

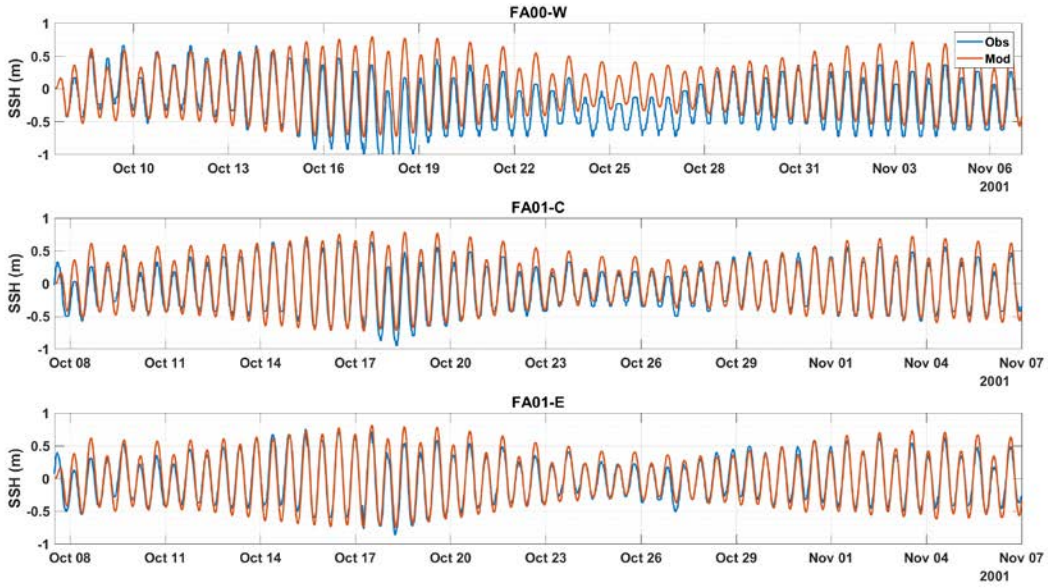


Figure 12. Observed and model predicted sea surface height (SSH) relative to MSL at multiple stations across the model domain for the validation period of 8 October through 7 November 2001. Observed time series shown in blue and model predicted shown in orange. From top to bottom: FA00-W, FA00-C, FA00-E. Y-axis in each plot extends from 1 m below MSL (-1) to 1m above MSL (1).

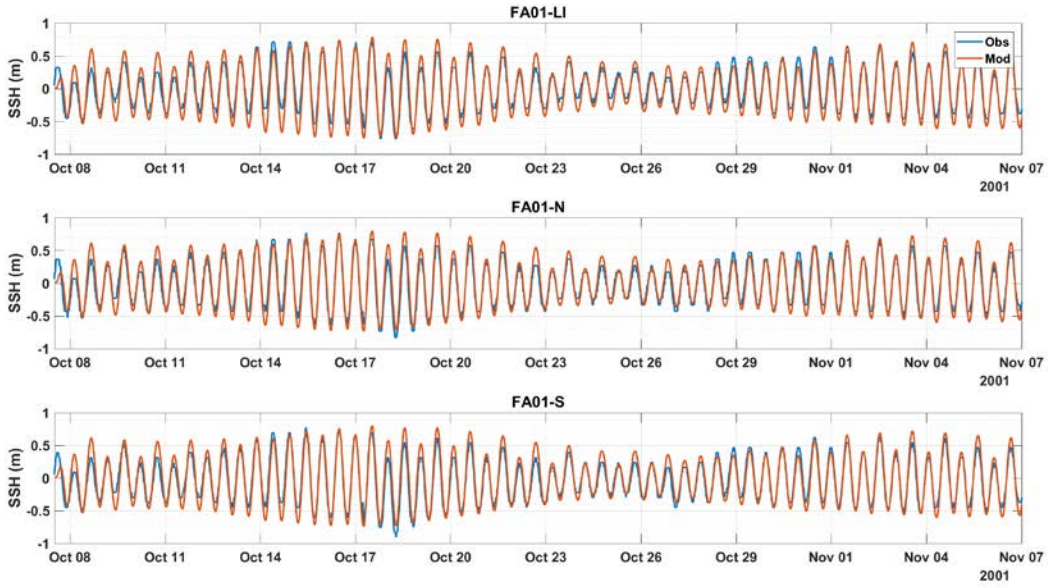


Figure 13. Observed and model predicted sea surface height (SSH) relative to MSL at multiple stations across the model domain for the validation period of 8 October through 7 November 2001. Observed time series shown in blue and model predicted shown in orange. From top to bottom: FA00-LI, FA00-N, FA00-S. Y-axis in each plot extends from 1 m below MSL (-1) to 1m above MSL (1).

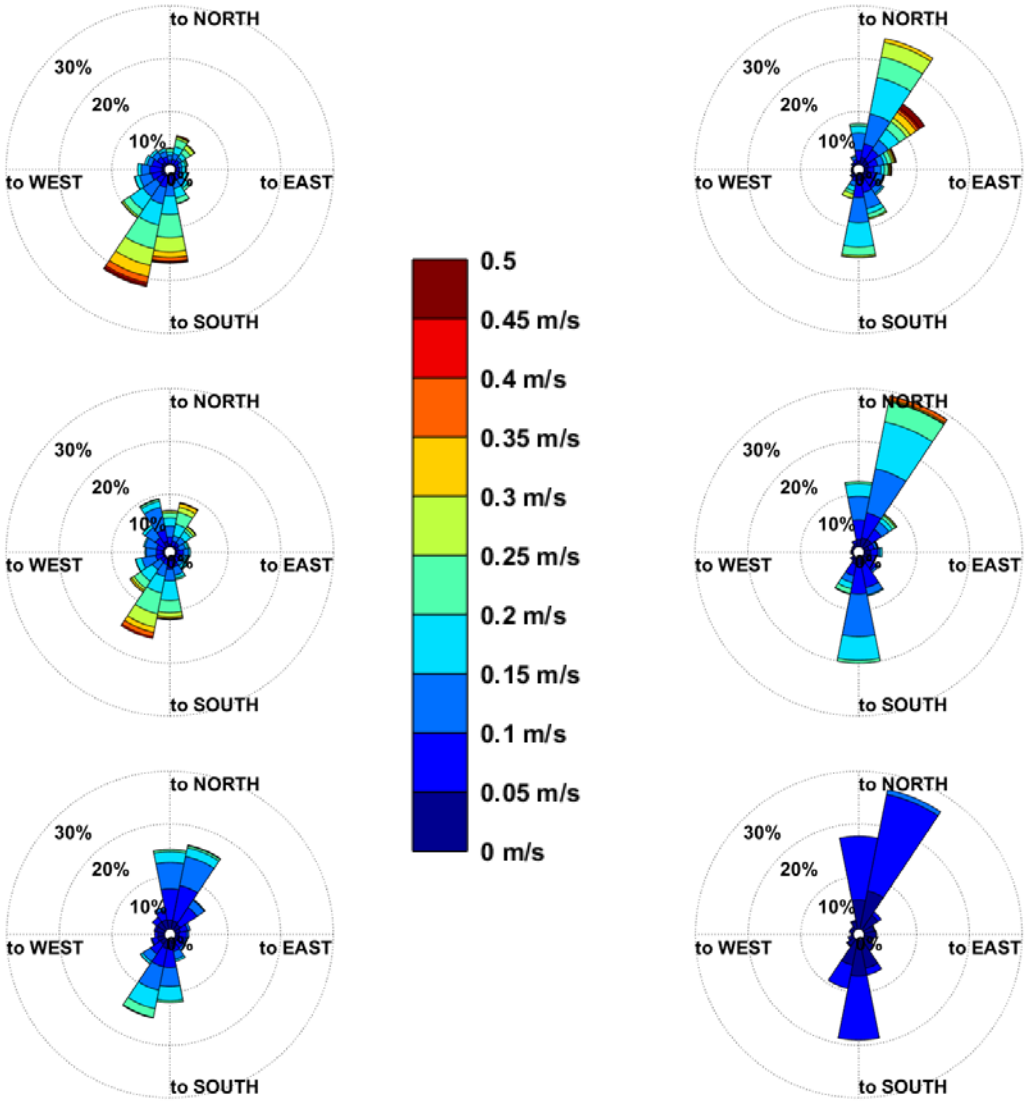


Figure 14. Surface, mid and bottom current roses for observed (left) and modeled (right) currents at FA01-W for the period of 8 October through 7 November 2001.

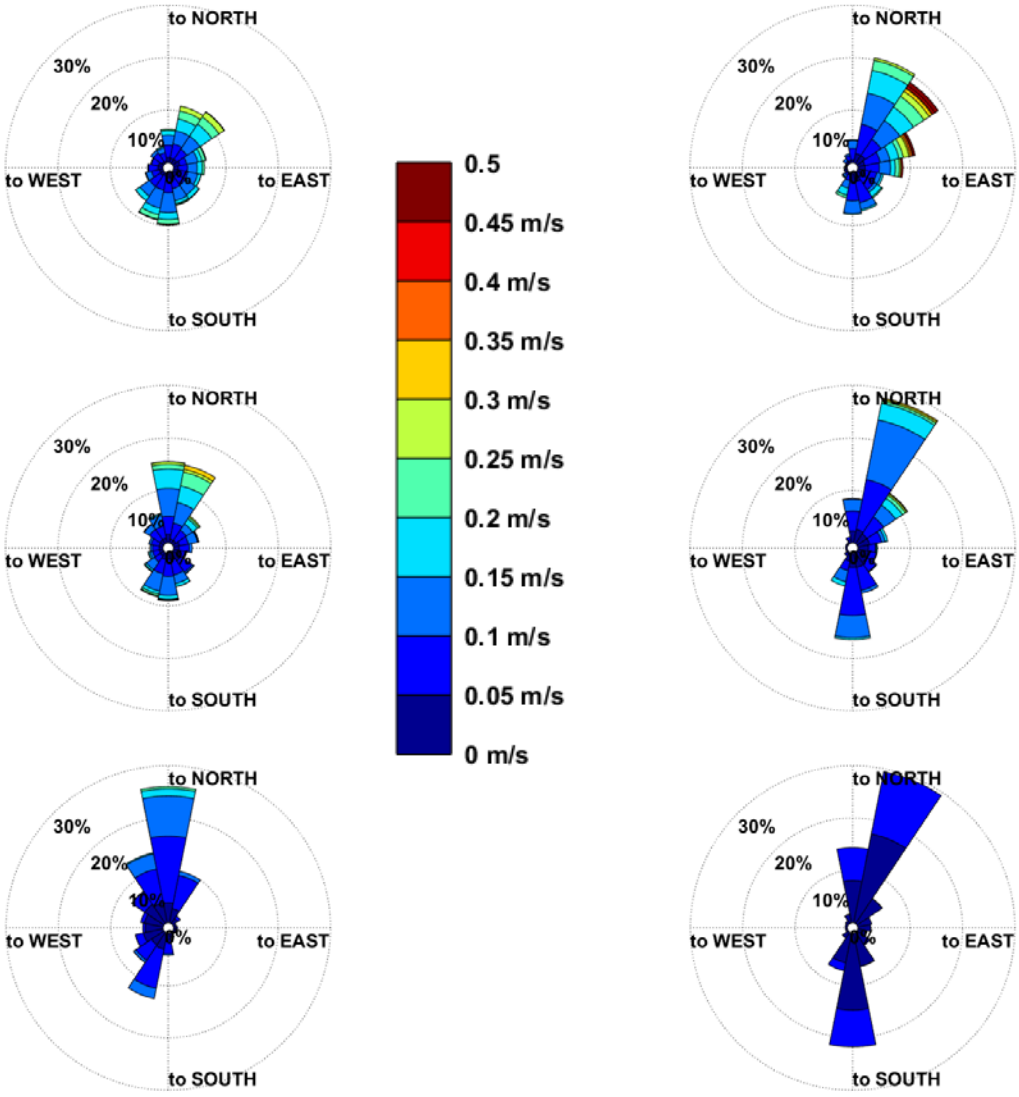


Figure 15. Surface, mid and bottom current roses for observed (left) and modeled (right) currents at FA01-S for the period of 8 October through 7 November 2001.

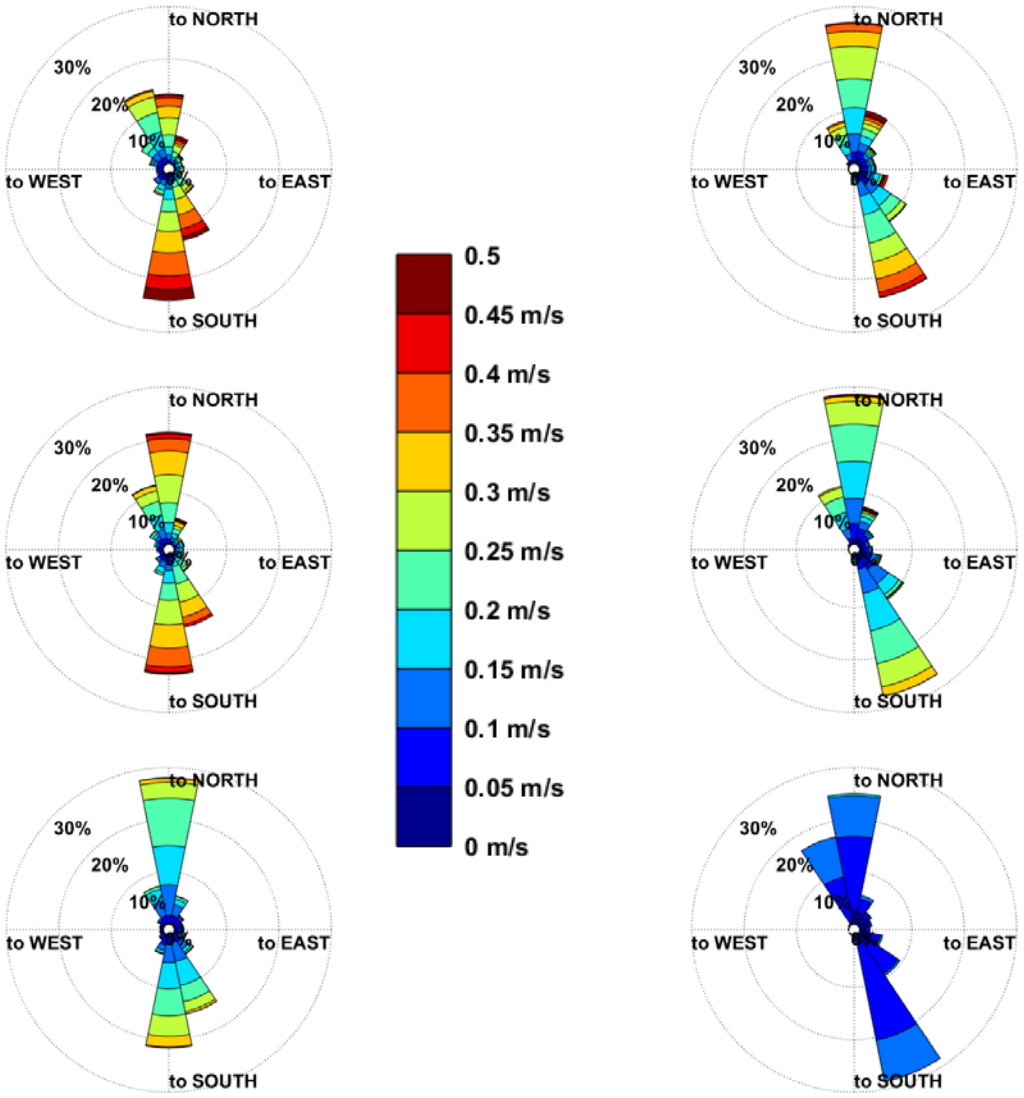


Figure 16. Surface, mid and bottom current roses for observed (left) and modeled (right) currents at FA01-N for the period of 8 October through 7 November 2001.

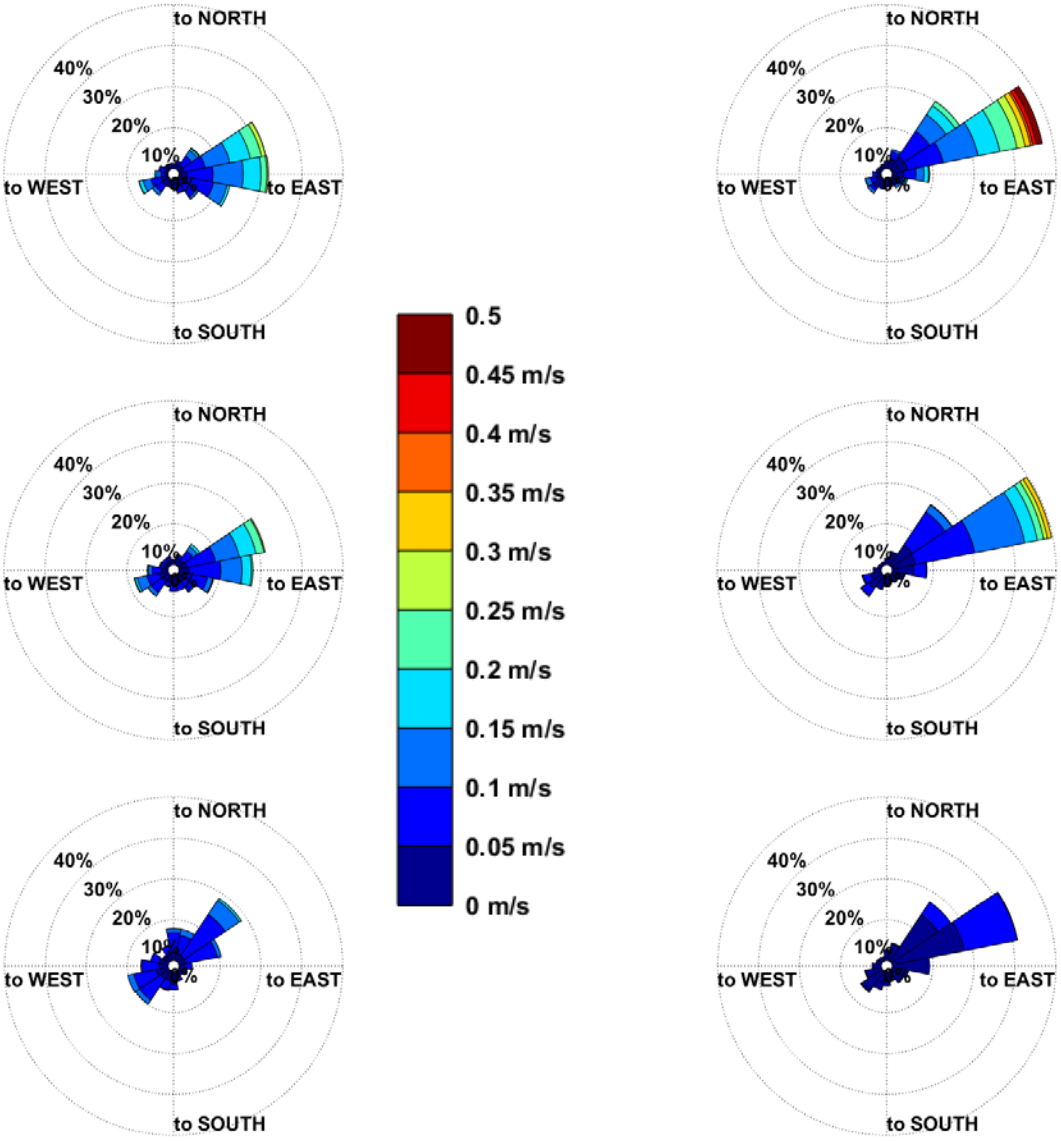


Figure 17. Surface, mid and bottom current roses for observed (left) and modeled (right) currents at FA01-LI for the period of 8 October through 7 November 2001.

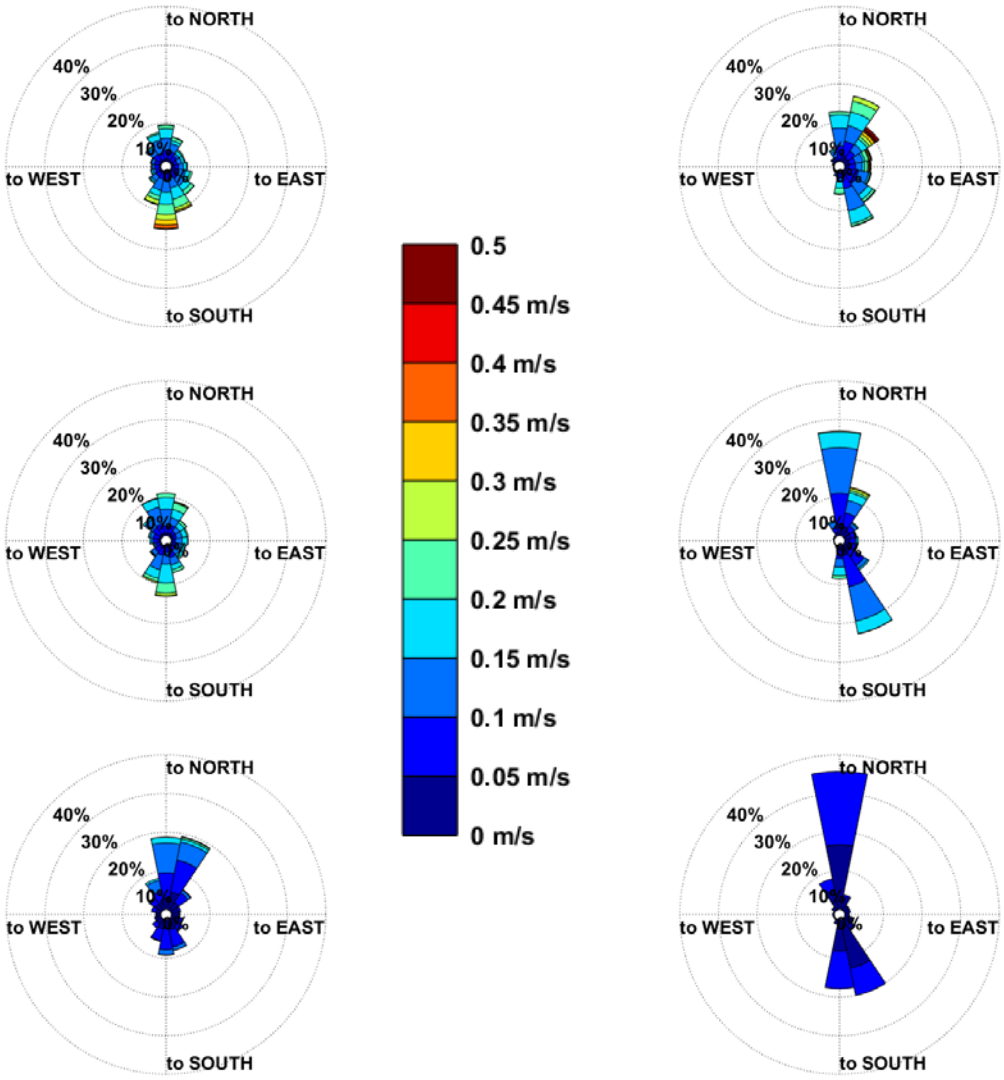


Figure 18. Surface, mid and bottom current roses for observed (left) and modeled (right) currents at FA01-E for the period of 8 October through 7 November 2001.

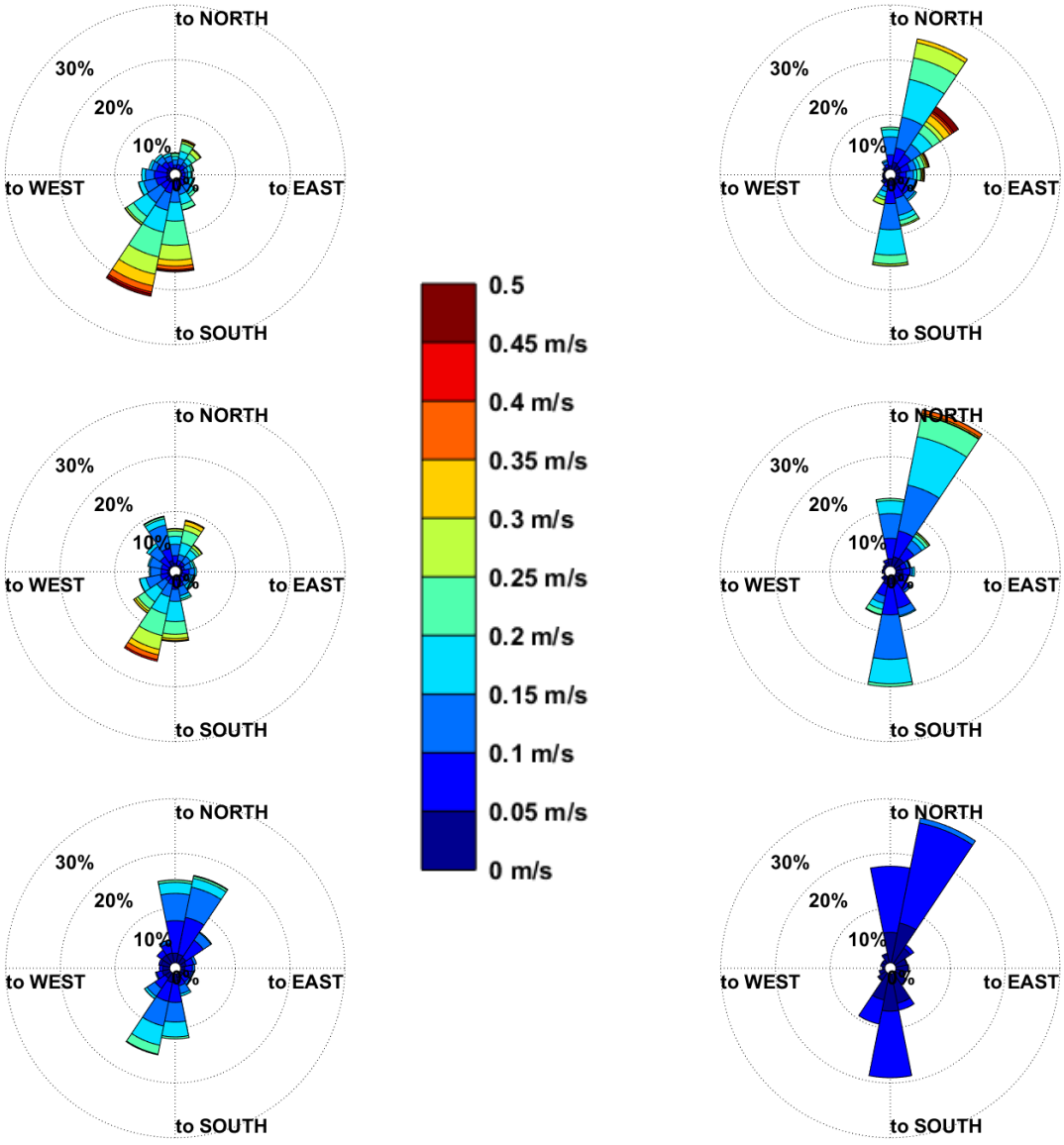


Figure 19. Surface, mid and bottom current roses for observed (left) and modeled (right) currents at FA01-C for the period of 8 October through 7 November 2001.

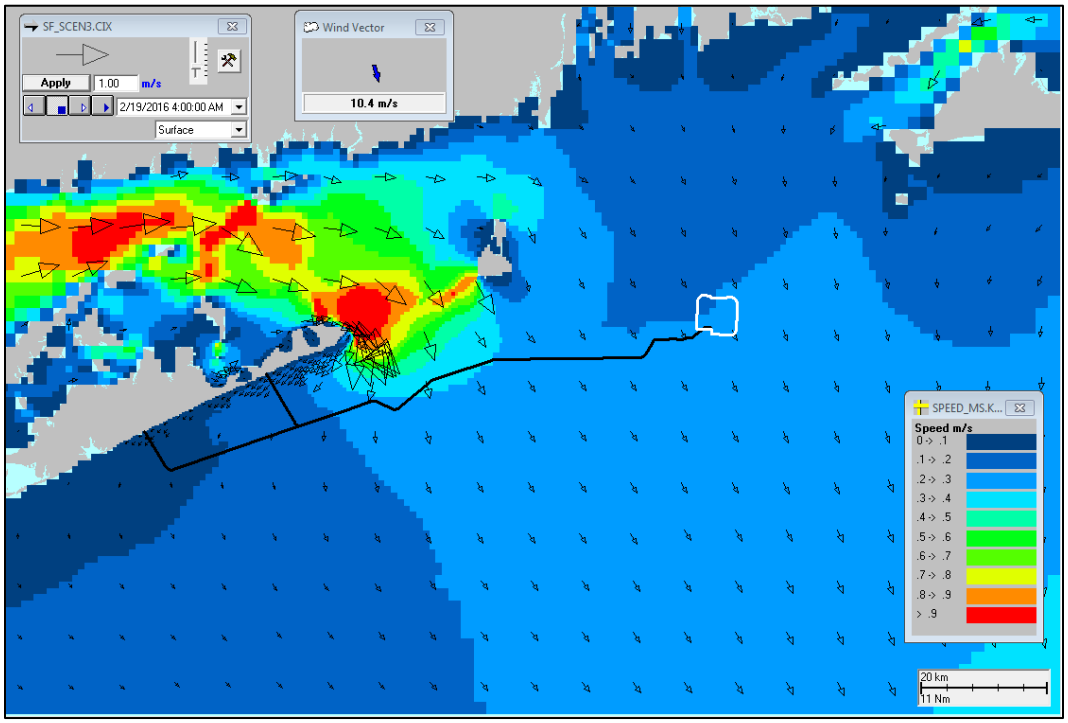


Figure 20. Snapshot showing an example of near peak ebb currents at the surface.

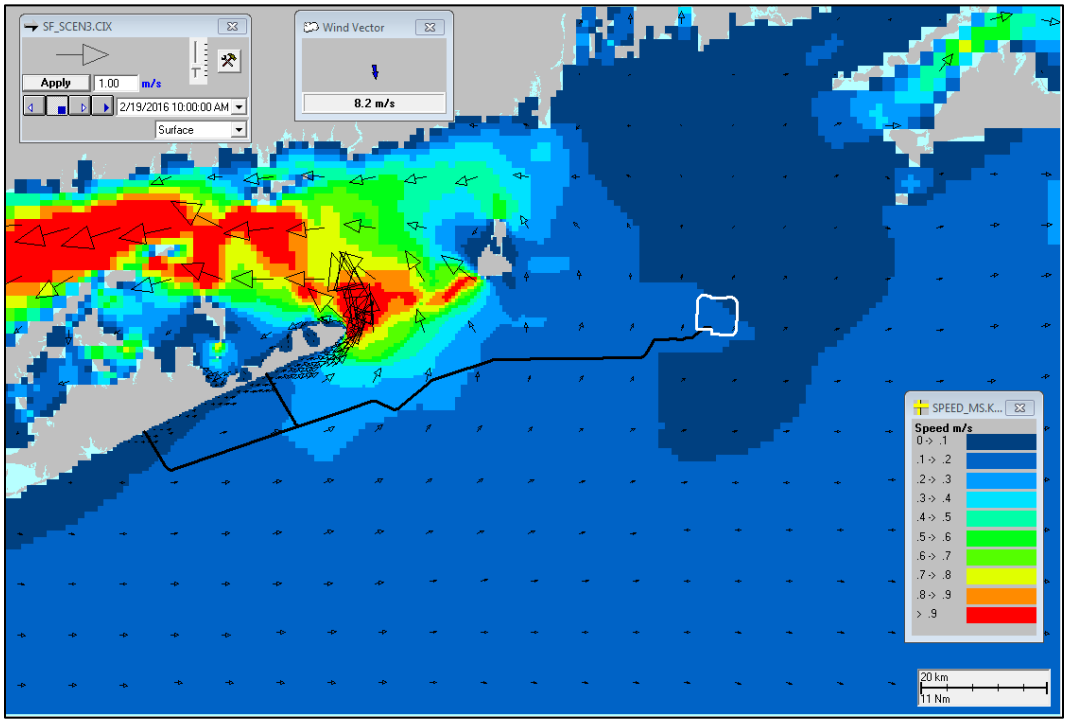


Figure 21. Snapshot showing an example of near peak flood currents at the surface.

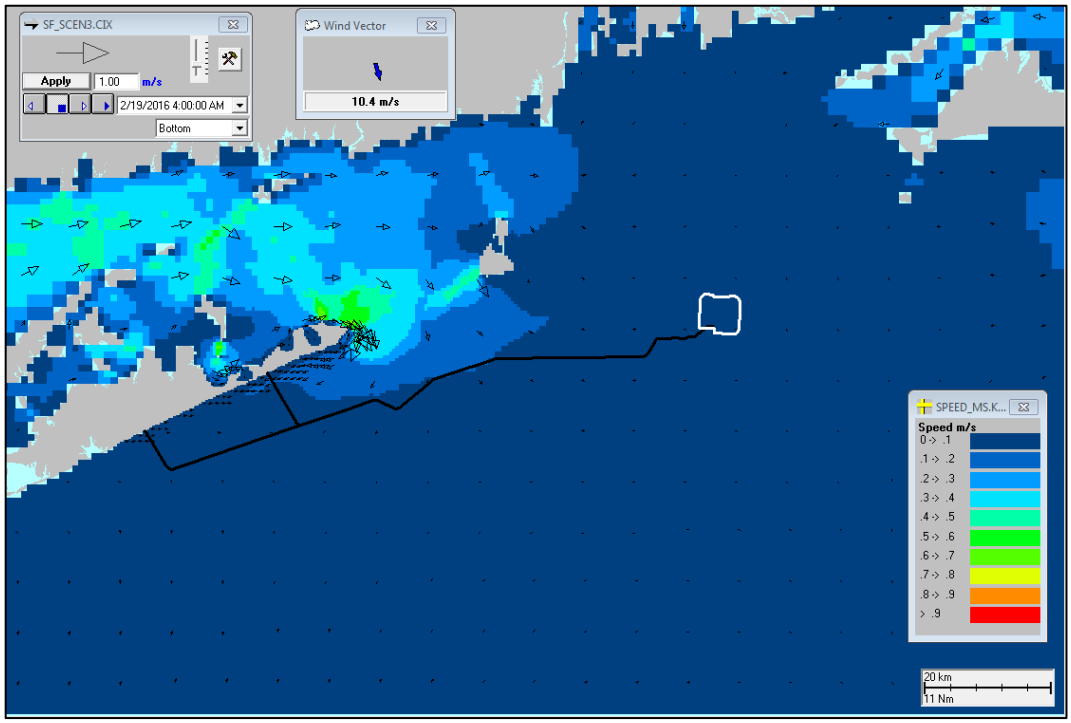


Figure 22. Snapshot showing an example of near peak ebb currents near the seabed.

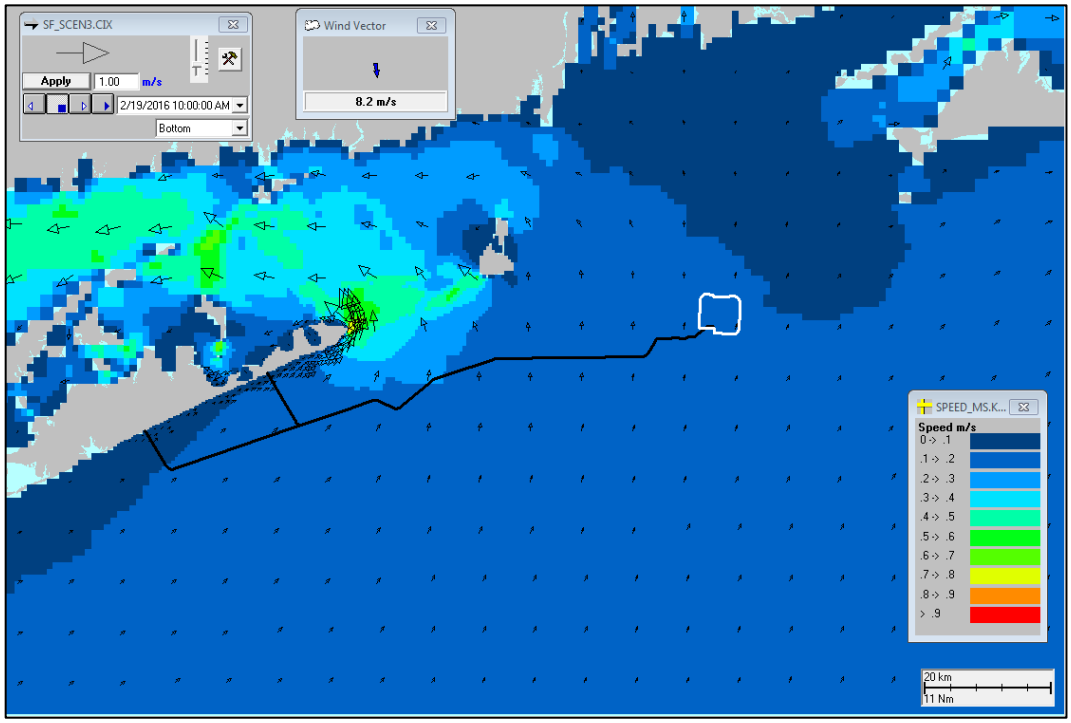


Figure 23. Snapshot showing an example of near peak flood currents near the seabed.

### 2.4.2 HYDROMAP Model Results for Construction Scenarios

Following the model validation, additional HYDROMAP simulations were developed for extended periods within the typical wind year 2016. The purpose of these applications was to generate a large window of time that could be used as forcing for the sediment dispersion modeling. The simulations were run for time periods seasonally consistent with anticipated construction timeframes. Hydrodynamic Simulation 1 was run from May through July covering the approximate installation period for the SFEC and the inter-array cable. Hydrodynamic Simulation 2 covered the period of February through April, corresponding to the proposed schedule for construction at the sea-to-shore transition.

For the simulation of the export cable burial, the duration of construction (2 months) is sufficient to adequately capture variability of the tides and currents in the region. Simulations of the inter-array cable burial and the HDD pit excavation were notably shorter (both are less than a day long) and therefore both activities were simulated twice, with each period sampling a different tidal regime. Figure 25 shows the time history of sea surface height (tides) at a proxy location for each activity (shown in Figure 24). This figure shows the complete simulation period and highlights the actual portion of the hydrodynamic model output that was used for each sediment dispersion scenario. A summary of the sediment dispersion modeling start dates and durations for each construction activity are summarized in Table 4.

Table 4. Summary of start times and duration of simulated construction activities.

| Construction Component | Simulation Start | Duration (Days) |
|---|---|---|
| SFEC cable burial | 5/1/2016 | 61.1 |
| Inter-array cable burial (period 1) | 7/3/2016 | 0.9 |
| Inter-array cable burial (period 2) | 7/12/2016 | 0.9 |
| HDD pit excavation (period 1) | 3/2/2016 | 0.3 |
| HDD pit excavation (period 2) | 4/8/2016 | 0.3 |

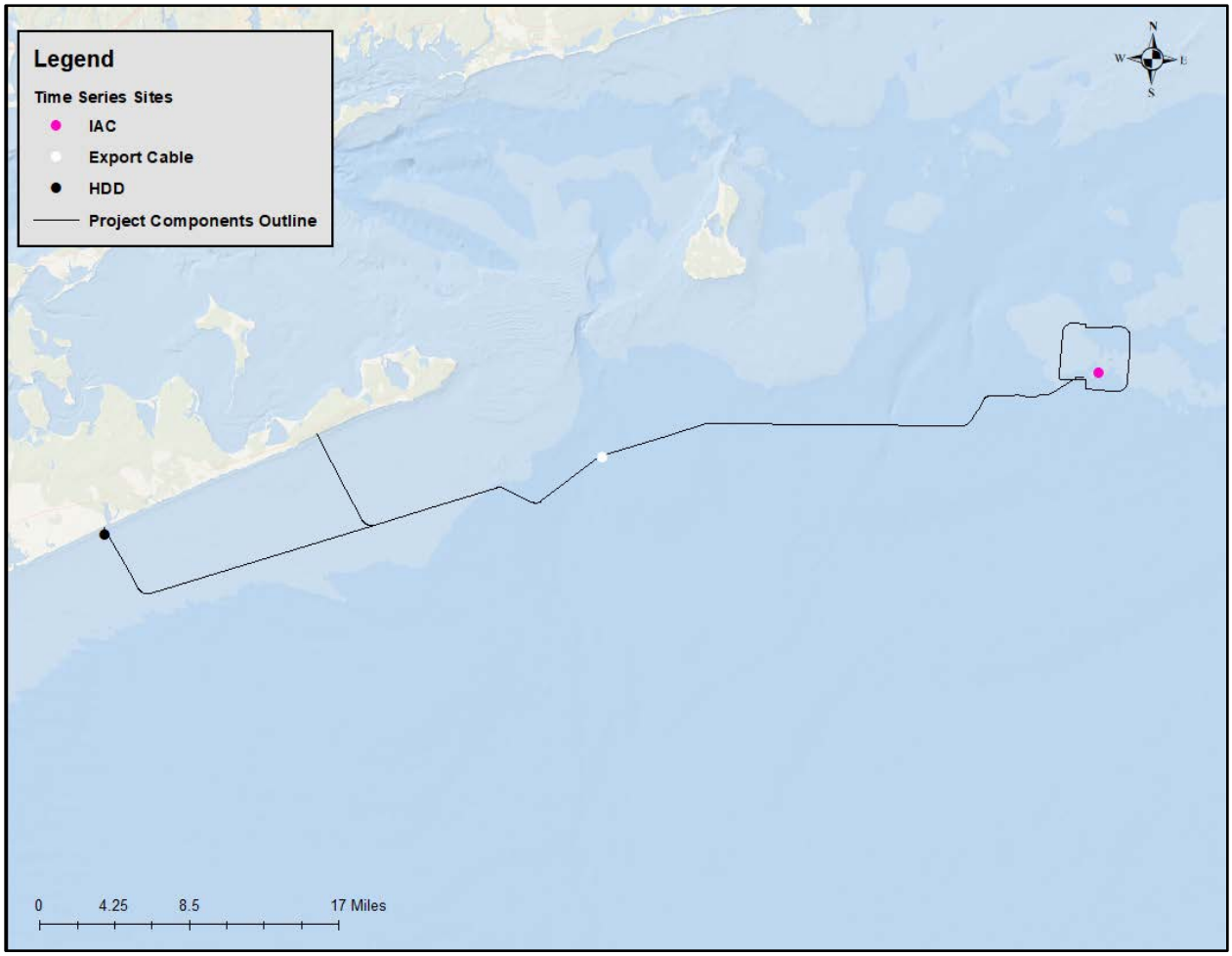


Figure 24. Locations of time series presented in Figure 25.

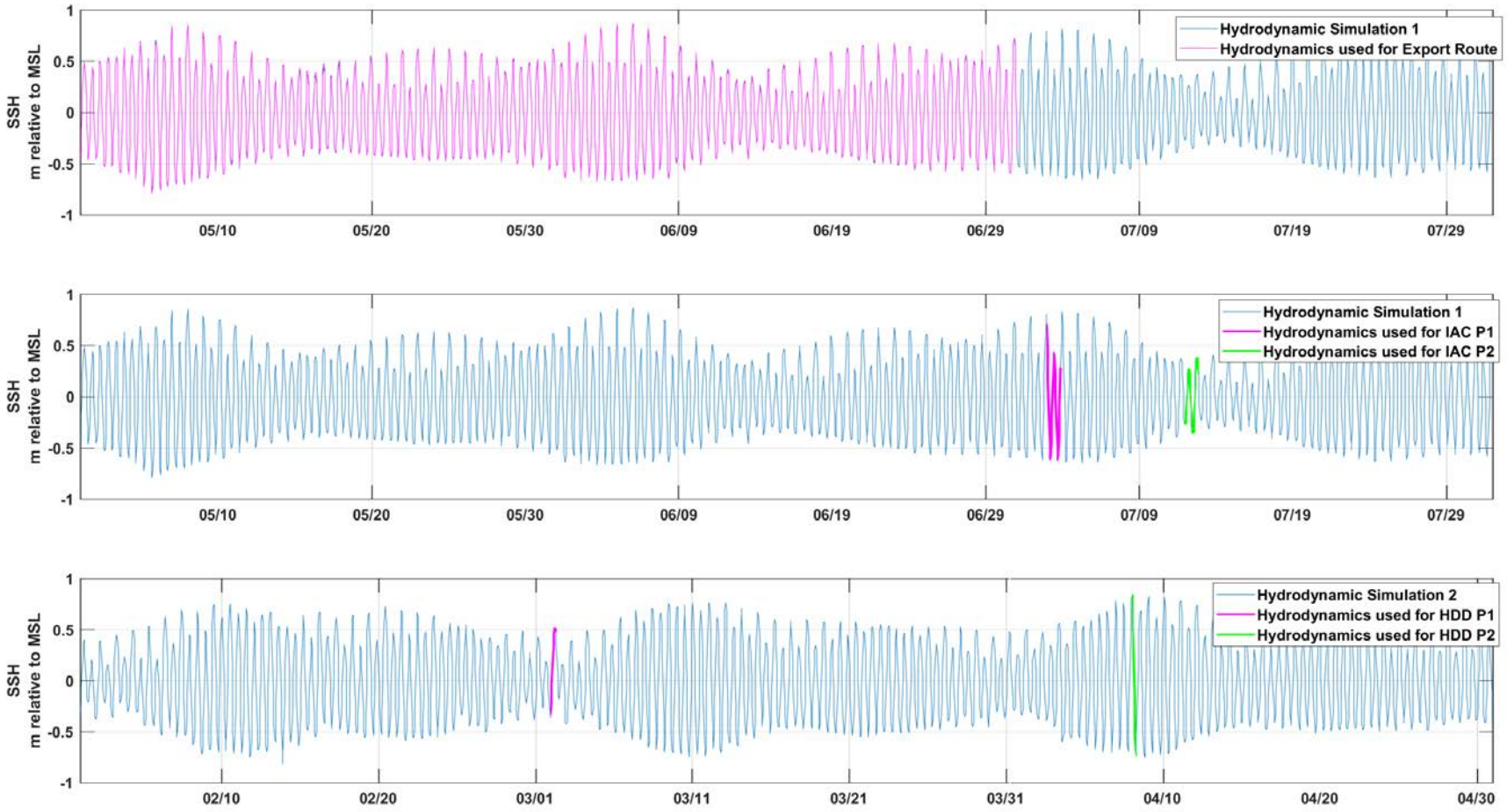


Figure 25. Time series of sea surface height (SSH) at representative locations local to each construction activities. The specific timeframes used for sediment dispersion modeling simulations are shown overlain on the entire simulation time series.

# 3 Suspended Sediment Modeling

## 3.1 SSFATE Description

SSFATE (Suspended Sediment FATE) is a three-dimensional Lagrangian (particle) model developed jointly by the U.S. Army Corps of Engineers (USACE) Environmental Research and Development Center (ERDC) and Applied Science Associates (now part of the RPS group) to simulate sediment resuspension and deposition from marine dredging operations. Model development was documented in a series of USACE Dredging Operations and Environmental Research (DOER) Program technical notes (Johnson et al., 2000; Swanson et al., 2000); at previous World Dredging Conferences (Anderson et al., 2001) and a series of Western Dredging Association Conferences (Swanson et al., 2006; Swanson and Isaji, 2004). Following dozens of technical studies which demonstrated successful application to dredging, SSFATE was further developed to include the simulation of cable and pipeline burial operations using water jet trenchers (Swanson et al., 2006), and mechanical ploughs, as well as sediment dumping and dewatering operations. The current modeling system includes a GIS-based interface for visualization and analysis of model output.

SSFATE computes total suspended sediment (TSS) concentrations and sedimentation patterns resulting from sediment disturbing activities. The model requires a spatial and time varying circulation field (typically from hydrodynamic model output), definition of the water column bathymetry, and parameterization of the sediment disturbance (source) and predicts the transport, dispersion and settling of suspended sediment released to the water column. The focus of the model is on the far-field (i.e. beyond the initial disturbance) processes affecting the fate of suspended sediment. The model uses specifications for the suspended sediment source strengths (i.e. mass flux), vertical distributions of sediments and sediment grain-size distributions to represent losses (loads) to the water column from different types of mechanical or hydraulic dredges, sediment dumping practices or other sediment disturbing activities such as jetting or ploughing for cable or pipeline burial. Multiple sediment types or fractions can be simulated simultaneously; as can discharges from moving sources.

### 3.1.1 Model Theory

SSFATE addresses the short-term movement of sediments that are disturbed during mechanical ploughing, hydraulic jetting, dredging and other processes where sediment is resuspended into the water column. The model predicts the path and fate of the sediment particles based on sediment properties, sediment loading characteristics and environmental conditions (bathymetry and currents). The computational model utilizes a Lagrangian (or particle-based) scheme to represents the total mass of sediments suspended over time. The particle-based approach provides a method to track suspended sediment without any loss of mass as compared to Eulerian (continuous) models due to the nature of the

numerical approximation used for the conservation equations. Thus, the method is not subject to artificial diffusion near sharp concentration gradients and can easily simulate all types of sediment sources.

Sediment particles in SSFATE are divided into five size classes (Table 5. ), each having unique behaviors for transport, dispersion, and settling. The model represents the total mass of sediments suspended over time by a defined sub-sample of Lagrangian particles, allocating an equal proportion of the mass to each particle (e.g. 1/1000$^{th}$ of the total release if 1000 particles are used). The initial size distribution of the sediments is used to apportion the sample of Lagrangian particles to size classes.

Table 5. Sediment size classes used in SSFATE

| **Class** | **Type** | **Size Range (microns)** |
|---|---|---|
| 1 | Clay | 0-7 |
| 2 | Fine silt | 8-35 |
| 3 | Coarse silt | 36-74 |
| 4 | Fine sand | 75-130 |
| 5 | Coarse sand | >130 |

Horizontal transport, settling, and turbulence-induced suspension of each particle is computed independently by the model for each time step. Particle advection is based on the relationship that a particle moves linearly (in 3-dimensions) with a local velocity obtained from the hydrodynamic field, for a specified model time step. Diffusion is assumed to follow a simple random walk process. The diffusion distance is defined as the square root of the product of an input diffusion coefficient and the time step is decomposed into X and Y displacements via a random direction function. The vertical Z diffusion distance is scaled by a random positive or negative direction.

Particle settling rates are calculated using Stokes equations and based on the size and density of each particle class. Settling of mixtures of particles is a complex process due to interaction of the different size classes, some of which tend to be cohesive and thus clump together to form larger particles that have different settling rates than would be expected from their individual sizes. Enhanced settlement rates due to flocculation and scavenging are particularly important for clay and fine-silt sized particles (Teeter 1998, Swanson 2004) and these processes have been implemented in SSFATE. These processes are bound by upper and lower concentrations limits, defined through empirical studies, which contribute to flocculation for each size class of particles. Above and below these limits, particle collisions are either too infrequent to promote aggregation, or so numerous that the interactions hinder settling.

Deposition is calculated as a probability function of the prevailing bottom stress and local sediment concentration and size class. The bottom shear stress is based on the combined velocity due to waves (if used) and currents using the parametric approximation by Soulsby (1998). Matter that is deposited may be subsequently resuspended into the lower water column if critical levels of bottom stress are exceeded, and the model employs two different resuspension algorithms. The first applies to material deposited in the last tidal cycle (Lin et al. 2003). This accounts for the fact that newly deposited material will not have had time to consolidate and will be resuspended with less effort (lower shear force) than consolidated bottom material. The second algorithm is the established Van Rijn method (Van Rijn, 1989) and applies to all other material that has been deposited prior to the start of the last tidal cycle. Swanson et al. (2007) summarizes the justifications and tests for each of these resuspension schemes. Particles initially released by operations are continuously tracked for the length of the simulation, whether suspended or deposited.

For each model time step the suspended concentration of each sediment class as well as the total concentration is computed on a concentration grid. The concentration grid is a uniform rectangular grid with user-specified cell size that is independent of the resolution of the hydrodynamic data used to calculate transport, thus supporting finer spatial differentiation of plume concentrations and avoiding underestimation of concentrations caused by spatial averaging over larger volumes/areas. Model outputs include water-column concentrations in both horizontal and vertical planes, time-series plots of suspended sediment concentrations at points of interest, and thickness contours of sediment deposited on the sea floor. Deposition is calculated as the mass of sediment particles that accumulate over a unit area. Because the amount of water in the sediment deposited is not known, SSFATE by default converts deposition mass to thickness by assuming no water content.

For detailed description of the SSFATE model equations governing sediment transport, settling, deposition, and resuspension, the reader is directed to Swanson et al. (2007).

## 3.2 SSFATE Application for the SFWF and SFEC

Offshore construction activities associated with development of the SFWF include the following, all of which will be located on the OCS: (i) installation of up to 15 wind turbine generators (WTG) and associated foundations; (ii) construction of an offshore substation on similar foundation as the WTGs; and (iii) installation and burial of inter-array cables connecting the WTGs and the offshore substation. Construction relating to the SFEC is divided into onshore and offshore activities. The SFEC onshore segment will run between the onshore substation in East Hampton, NY and a sea-to-shore transition vault. Along this segment the cable will be installed using horizontal directional drilling (HDD) under the beach and intertidal water, exiting the seabed at a location approximately 650 m offshore. The SFEC offshore

segment will extend from the sea-to-shore transition vault to the SFWF offshore substation, crossing both New York State territorial waters (SFEC – NYS) and federal waters (SFEC – OCS). This segment will be buried to a target depth of 1.85 m (6ft) below the seabed. Installation of a temporary cofferdam may be required at the sea-to-shore transition point, where the offshore and onshore segments of the SFEC will be spliced together.

SSFATE was used to perform a series of simulations to assess suspended sediment concentration and seabed deposition resulting from the cable burial and other Project activities. The simulations presented within this report evaluate sediment releases from a range of construction activities that include:

1. Burial of the SFEC between the sea-to-shore transition at Beach Lane and the SFWF offshore substation (approximately 98.3 km) using a hydraulic trencher/mechanical plow.
2. Burial of a representative segment of the inter-array cable between two potential WTG locations (approximately 1.4 km apart) using a hydraulic trencher/mechanical plow.
3. Excavation of the HDD exit pit offshore Beach Lane using a suction dredger.[1]

Details describing the process by which each of the construction activities is implemented in the model are discussed below.

### 3.2.1 Description of SSFATE Model Set-up

Setup of the SSFATE model consists of defining how each construction activity will be parameterized and establishing the sediment source terms. For each scenario, this includes defining:

- The geographic extent of the activity (point release vs. line source)
- The dates and duration of the activity
- The volumes and cross-sectional areas of the trench or excavation pit
- The production rate for each dredge/trenching method
- Loss rates for each dredge/trench method
- The grain size distribution along the route
- The vertical distribution of sediments as they are initially released to the water column

The model uses hydrodynamics, and bathymetry sources from the HYDROMAP application described in Section 2. As described above, concentration gridding in SSFATE is independent of the resolution of the hydrodynamic data used to calculate transport. As the Project will include a range of sediment disturbing activities that occur as both point sources of sediment release (e.g. HDD pit excavation), as well as moving

[1] Although two locations are being considered for the shore landing, this study examined sediment dispersion from the SFEC landing at a single landing site (Beach Lane). Due to similarities in the nearshore currents and sedimentary environments, results are expected to be comparable to the alternate (Hither Hills State Park) landfall.

line sources (hydraulic trenching) across a wide range of spatial scales, a series of local grids were developed to efficiently compute concentrations while maintaining fine resolution near each Project activity.

Construction and installation of the SFWF and SFEC is currently scheduled to occur in 2021 and 2022, respectively, with the Project commissioned and operational by the end of 2022. Activities that may result in temporary sediment resuspension (as presented in the Construction and Operations Plan) include the following:

- Winter/Spring 2022 - Sea-to-shore construction (excavation of HDD pit/cofferdam installation)
- Spring-Summer 2022 - SFEC Offshore Cable Installation
- Summer 2022 - Inter-array cable installation

Hydrodynamic output from the year 2016 were used to represent currents for the construction period. As described in Section 2.2.4.1, this range of dates was selected after analyzing the most recent ten years of local wind speed records for the region. In the study area, currents vary primarily due to tides and winds, which do not change substantially on an inter-annual basis but may exhibit variations in monthly-averages due to episodic meteorological events or river flow. For these reasons, RPS chose to use a simulation period (2016) over which the monthly-averaged wind speeds in the study area most closely matched the 10-year record averages, with no extreme outliers. Hydrodynamic fields from this period were used as forcing for the predictive modeling of the sediment transport and dispersion associated with the Project.

#### 3.2.1.1 Sediment Source Terms

Two different subsea excavation techniques are being employed for the construction activities listed above. Sediment losses from each of these activities were represented in SSFATE by characterizing the source strength, vertical distribution, and grain-size distribution of the sediment load. Details describing the parameterization of each method are provided below.

Hydraulic trenching

Submarine cables including the SFWF inter-array cable and the offshore portion of the SFEC will be buried beneath the seafloor using a simultaneous trench and lay process. The installation will utilize a self-propelled hydro-plow vehicle (e.g. SeaREX), equipped with a series of hydraulic jets that are used to fluidize the seabed sediments as the cable is simultaneously laid on the seafloor. The process allows the cable to lower under its own weight, eliminating the need to directly remove and/or displace the sediments and minimizing sediment resuspension in the process. The vehicle is also equipped with a

mechanical plow that can be utilized, as necessary, to create the trench at locations where hydraulic jetting is not sufficient due to harder subsurface conditions.

The advance speed for installation of the SFEC will ultimately depend on final cable type and seabed conditions but is expected to be approximately between 1.6 and 3.2 km/day. The modeling approach for installation of both the inter-array cable and SFEC assumed that cable burial would be achieved in a single pass of the hydro-plow, operating at a constant production rate of 112 $m^3$/hr. (Production was determined using information provided by DWW indicating the hydro-plow would advance at a rate of 67.1 m/hr while trenching a cross-sectional area of 1.67 $m^2$ of the seabed [1.8 m deep by 0.91 m wide]). Losses from the jet trencher were simulated as a moving line source and were assumed to be 25% of the excavation volume. The vertical distribution of the sediment release was partitioned within the lower 1 m of the water column.

Suction Dredging

A ten-inch suction dredge will be used to excavate the HDD exit pit at the sea-to-shore transition point offshore Wainscott Beach, where the offshore segments of the SFEC will transition to the onshore portion of the SFEC. The dredger uses a vacuum to excavate a sediment slurry from the seabed and the fluidized sediment is released through a discharge pipe to a spoil pile on the nearby seafloor. Contractor estimates indicate that the dredger can operate at a production rate of 90 $m^3$/hr. For implementation in the modeling, it is assumed that 100% of the fluidized sediment will be lost to the water column as it is released from the discharge pipe (i.e. sediment will be side-cast adjacent to the excavation site). The discharged sediment is initialized within the model at a single point in the water column, 1.5 m above the seafloor.

#### 3.2.1.2 Sediment Grain Size Distribution

A total of 80 vibracore samples were collected from the Study area as part of the geotechnical site investigation (Fugro, 2018), of which 66 were used to characterize grain size distributions within the model. (The remainder of vibracores were either [i] collected from locations away from the simulated activities, or [ii] not analyzed for grain size at depths that are applicable to the dredging/trenching activities.) Figure 26 shows the location of each of the samples with respect to the Project work area as well as the relative size distributions (percent gravel, sand, and fines) derived from a composite of the uppermost 1.8 m of sediment from each vibracore. (1.8 m is the depth of sediment disturbance during the SFEC and inter-array cable burial.) Figure 27 shows the same data, binned to the size classes used by SSFATE. As seen in both figures, sediments are generally coarse-grained within the upper ~2m of the seabed. On average, over 90% of material within this sedimentary horizon is classified as sand and gravel.

An increase in the sediment fine fraction occurs where the SFEC route jogs south offshore Montauk and along the eastern extent of the route as the SFEC approaches the offshore substation. Otherwise, grain sizes are fairly uniform throughout the Study area

A total of 187 sediment grain size samples (139 by sieve analysis, 48 by hydrometer) from 66 sediment cores were used to develop the modeling input files. Figure 28 presents an example of grain size distribution curves provided by Fugro (2018) and the corresponding size classes that are used to parameterize the distribution in SSFATE. For each core, a unique size distribution was developed using a weighted average of the samples over a range of excavation depths that are relevant to the Project activities (e.g. 1.8 m for cable trenching, 3.7 m for excavation of the HDD exit pit). SSFATE incorporates this spatially varying information and computes a unique grain size distribution for each location in the model domain using a distance weighted interpolation. In addition, the moisture content and specific gravity of the sediment samples were used to calculate the bulk density of the sediments at each core location.

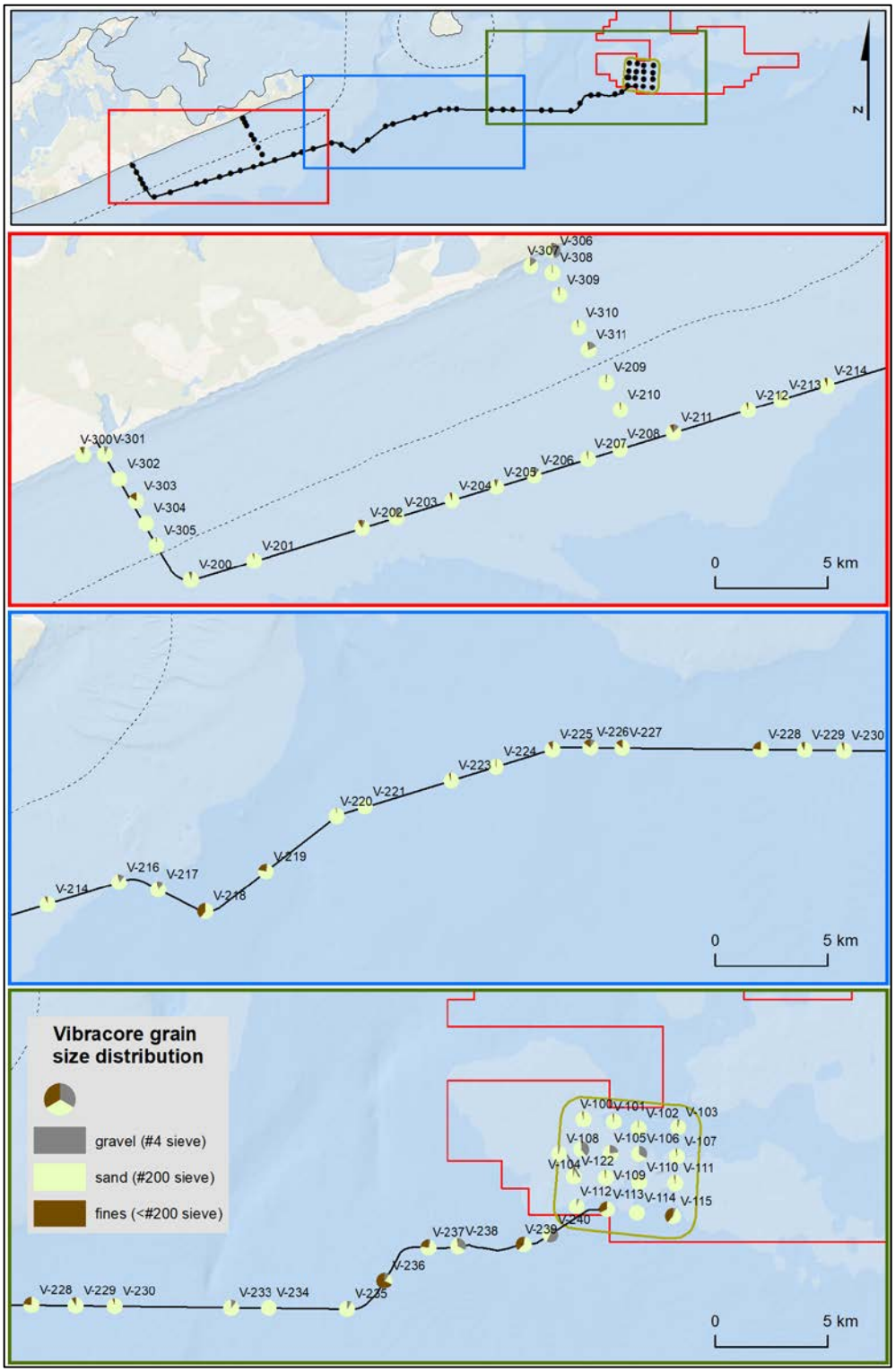


Figure 26. Grain size distributions from vibracores along the SFEC route. Top figure shows full Project extent and bottom three plots show an expanded view based on the extents identified in top plot (west to east).

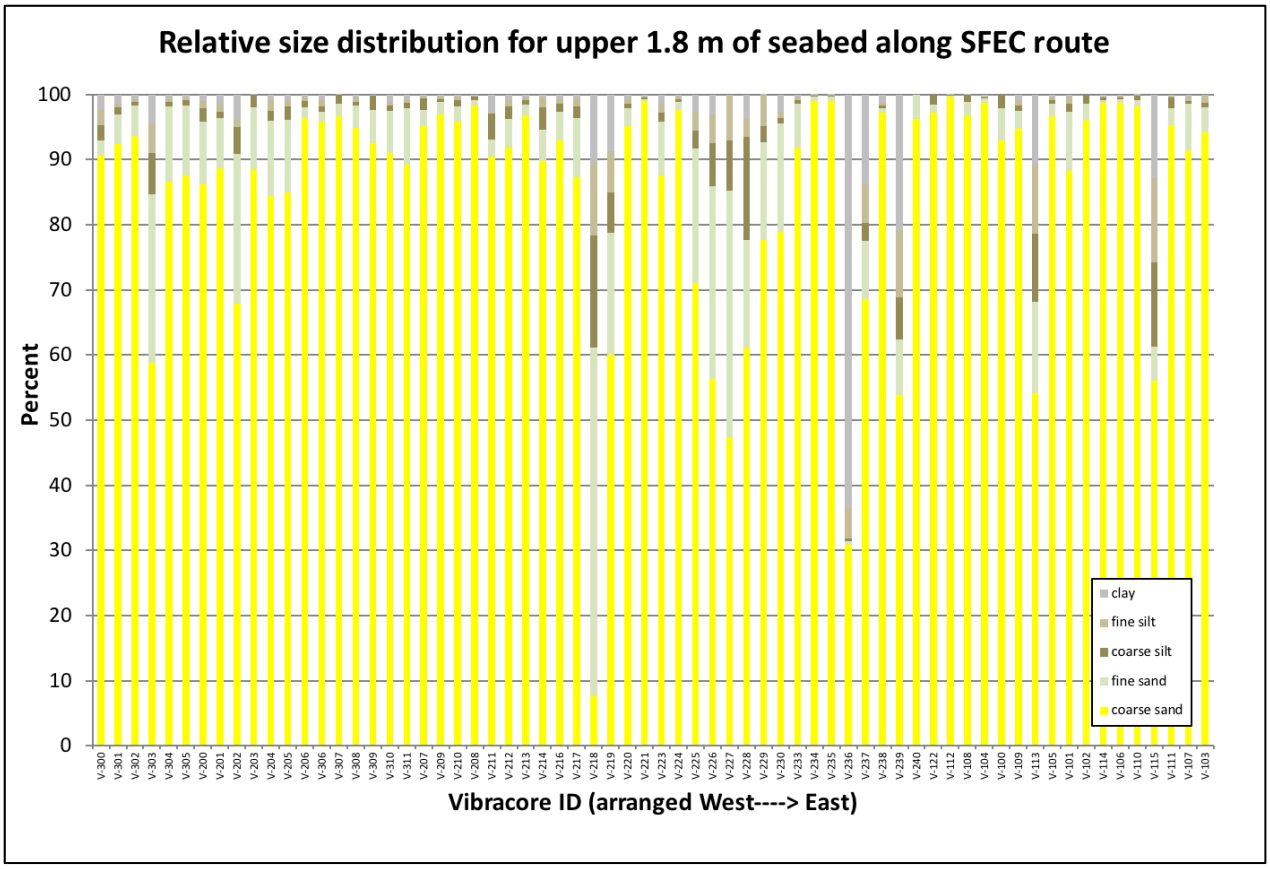


Figure 27. Near-surface sediment grain size distribution along the pipeline route (west to east).

Deepwater Wind South Fork, LLC
Project No. 02.17021080

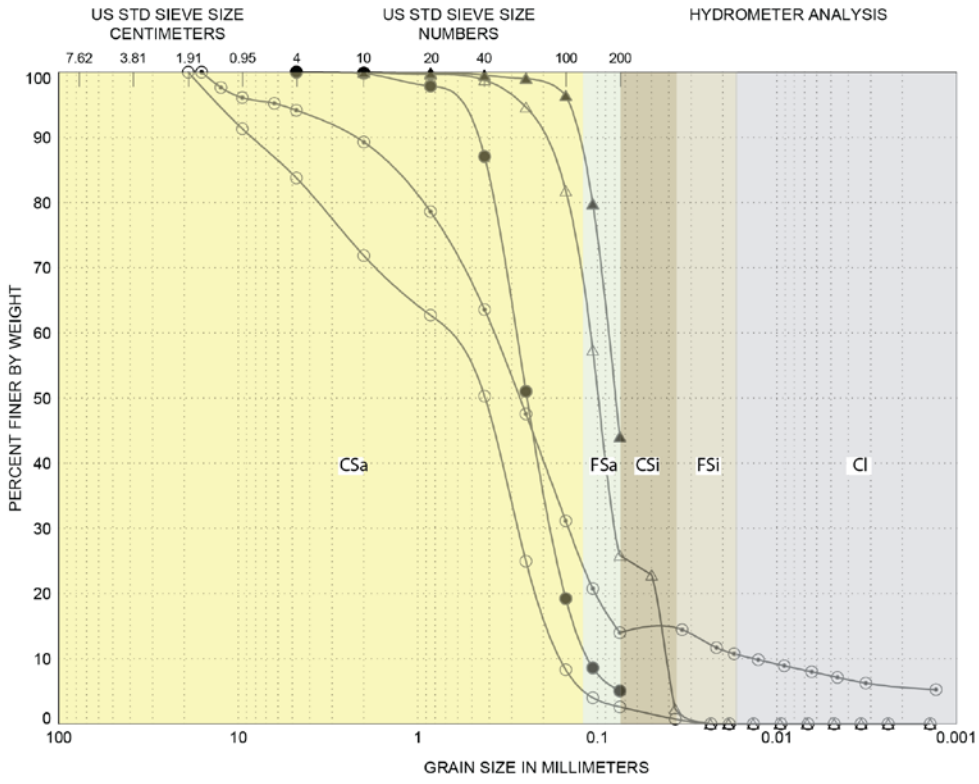


| GRAVEL | | SAND | | | SILT or CLAY |
|---|---|---|---|---|---|
| Coarse | Fine | Coarse | Medium | Fine | |

| LEGEND | | | | Cc | Cu |
|---|---|---|---|---|---|
| | (location) | (depth,m) | | | |
| ○ | V-217 | 0.66 | POORLY GRADED SAND with GRAVEL (SP) fine to medium sand, fine gravel | 0.7 | 4.6 |
| ● | V-217 | 1.50 | POORLY GRADED SAND with SILT (SP-SM) fine sand, non-plastic silt | 1.0 | 2.6 |
| △ | V-218 | 0.00 | *Silty SAND (SM)* | 1.4 | 2.7 |
| ▲ | V-218 | 1.05 | *Silty SAND (SM)* | | |
| ⊙ | V-219 | 0.35 | SILTY SAND (SM) fine to medium sand, non-plastic silt | 4.1 | 28.1 |

**GRAIN SIZE CURVES**
SFWF COP Survey
Offshore NY/RI/MA, Atlantic OCS

Figure 28. Size classes used by SSFATE overlain on grain size distribution curves (Fugro, 2018) from samples collected for the Project. (CSa – coarse sand, FSa – fine sand, CSi – coarse silt, FSi – Fine silt, Cl – clay).

## 3.3 SSFATE Scenarios

Table 6 summarizes the sediment modeling scenarios that RPS has developed in consultation with Jacobs and DWW. The simulations evaluate sediment releases for activities associated with multiple stages of the offshore installation between the sea-to-shore transition vault (offshore Beach Lane) and the SFWF. For stationary activities (point source releases), sediment volumes were based on the construction plan for each stage of excavation. For non-stationary activities (line sources), volumes have been calculated from the trench cross-sectional area and the length over which the installation will occur. The duration of each activity is estimated from the production rates for each of the dredging methods as listed in Section 3.2.1.1. Due to the relatively brief construction period for the latter two scenarios (2 and 3), the model was run twice for these activities to ensure that the simulations captured the potential plume and seabed impacts at different stages of the spring/neap tidal cycle, Figure 29 illustrates the location of each scenario in a map view.

Table 6. Description of activities being simulated for each modeling scenario.

| Scenario | Construction Activity | Equipment Type | Point/Line Source | Location | Excavation/Trench Volume ($m^3$) | Duration (day) |
|---|---|---|---|---|---|---|
| Scenario 1 | SFEC installation between sea-to-shore transition vault and SFWF | hydro-plow | Line | SFEC corridor | 164,366 | 61.1 |
| Scenario 2 | Burial of inter-array cable (representative section) | hydro-plow | Line | WTG 11 to WTG 9 | 2,342 | 0.9 |
| Scenario 3 | Excavation of seafloor for access to HDD pilot hole offshore Beach Lane | suction dredger | point | HDD exit pit | 650 | 0.3 |

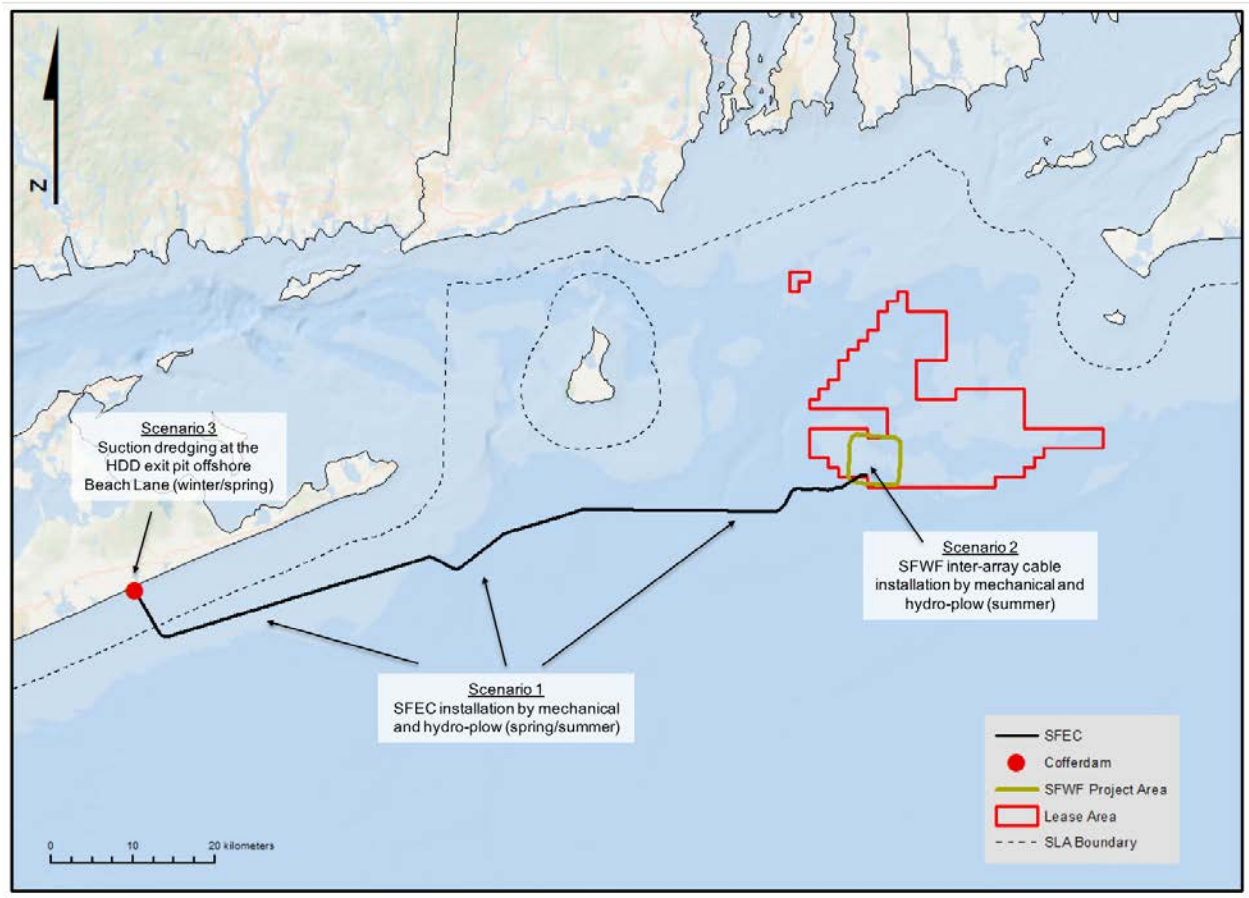


Figure 29. Map view showing sediment modeling scenario locations and simulation periods.

## 3.4 SSFATE Results

SSFATE simulations were performed for each construction activity in Table 6. All modeling assumed continuous operation for each phase of the construction. Computations of instantaneous water column concentrations were performed every 10-minutes, with output saved at a 10-minute time step for the suction dredging (Scenario 3) and at 20 minutes for cable burial (Scenarios 1 and 2) due to the longer duration of the hydro-plow activities. Sediment concentrations were computed on a grid with resolution of 20 m x 20 m in the horizontal dimension and 0.5 m in the vertical dimension. Note that reported concentrations are those predicted above the background concentration in the study area.

The results from the model runs are presented below in maps showing the predicted TSS concentrations and subsequent deposition for each activity. Specifically, three sets of graphics were developed for each scenario:

(i) Maximum cumulative TSS concentrations (mg/L), which show peak TSS for any cell at any time step in the model domain throughout full water column.

(ii) Cross-sections showing the predicted extent of TSS concentrations vertically through the water column for each activity.

(iii) Seabed deposition (thickness in mm) following the modeled activity.

For comparison purposes, each set of figures maintains a consistent spatial scale (with the exception of Figure 37, which shows the cumulative plume footprint over the entire SFEC route). Where applicable, the jurisdictional boundary between state and federal waters is indicated in the figures with a dashed line. Table 7 presents a summary of the model results for each simulation, including:

- the maximum distances of TSS plumes at select concentration thresholds,
- time for TSS concentrations to return to ambient following the modeled activity,
- maximum distance of deposition contours that exceeds selected thicknesses,
- areal extent of the deposit that exceeds selected thicknesses.

Scenario-specific details describing the sediment release, timing, and other assumptions for each simulation are described below.

### 3.4.1 Scenario 1 – South Fork Export Cable Installation

The scenario included simulation of the SFEC burial between the sea-to-shore transition at Beach Lane and the SFWF offshore substation (98.3 km) using a simultaneous trench and lay process. The first 5.6 km of the SFEC will be buried in New York state waters (SFEC-NYS) with the remainder in federal waters (SFEC-OCS). The installation will utilize a self-propelled mechanical and hydro-plow vehicle (e.g. SeaREX), equipped with a series of hydraulic jets that are used to fluidize the seabed sediments as the cable is simultaneously laid on the seafloor. The seabed footprint of sediment resuspension from hydro-plow trenching is approximately 0.9 m (trench surface width), and as the vehicle advances, the cable is lowered to its burial depth (maximum 1.8 m of cover). The total volume of the SFEC trench is estimated to be 164,366 $m^3$ although most of this material will remain undisturbed at the seabed since the jet trencher does not directly excavate sediment from the trench. For modeling, it was assumed that the equipment would operate continuously at a production rate of 112 $m^3$/hr (based on an advance rate of 67 m/hr).

The activity was simulated as a line source and assumed that full burial of the cable would be achieved with a single pass of the trencher. The simulation begins at the sea-to-shore transition vault and advances eastward along the cable route continuously for approximately 61 days. While weather, vehicle repositioning, and other operational factors may periodically interrupt the cable lay/burial process, the

model assumed continuous installation (24 hours/day) for the complete duration of construction. The continuous operation could be considered a "worst case" condition for sustained TSS concentrations.

The SFEC installation is planned for Spring/Summer 2022 and a model period of May 1 – June 30 (yr 2016) was selected based on the current construction schedule. Resuspension of sediment from this activity was set to 25% of the total trench volume - a conservative assumption of sediment loss which also coincides with the resuspension parameter for DWW's analysis of the Block Island Transmission System (RPS ASA, 2012). In the model, mass lost to the water column was partitioned equally into five layers within the lowermost 1 m of the seafloor. In total, the simulation included the release of 41,091 $m^3$ of sediment over the course of 1,466 hours of active production.

Maximum integrated TSS concentration and subsequent seabed deposition from the SFEC installation are presented in a series of overlapping maps along the route (Figure 30 through Figure 44), and results of the full simulation are summarized in Table 7. (Results have been grouped to present impacts to NY state waters and federal waters separately.) The sediment plume that arises during trenching is transient, and generally oscillates with the tide. In New York waters (near the start of the route) the plume is oriented in a NE/SW configuration, reflecting the tidal current patterns near the site, which are aligned with the nearshore topography. As the trencher moves into deeper waters, past Montauk, the plume assumes more of a N/S orientation. The highest TSS concentrations are predicted to occur in locations where the hydro-plow passes over pockets of finer sediments (e.g. between VC-217 and VC-220, and again between VC-235 and the end of the route) but concentrations above 30 mg/L otherwise remain within ~100 m of the source during the simulation. The cross-section view presented in Figure 37 (bottom) suggests that peak TSS concentrations will remain near the seabed, and plumes above 10 mg/L are not predicted to extent vertically beyond 3 meters of the source at any time during the simulation.

Sedimentation (Figure 38 through Figure 44) is limited to the area immediately adjacent to the burial route (typically within 100 m) and the pattern of deposition appears more uniform when compared with the TSS concentrations in the water column. This indicates that a large portion of the mass being resuspended is composed of coarse-grained material that settles rapidly near the trencher and that sediments which remain in suspension (producing the tidally-oscillating plumes shown in Figure 37) disperse widely, settling on the seabed at concentrations below detection by the model (<0.1 mm).

As described above, the first 5.5 km of the cable route extends through NY state waters (SFEC-NYS). The maximum predicted TSS concentration during this portion of the simulation is 578 mg/L. TSS concentrations at or above 100 mg/L are predicted to extend a maximum of 120 m from the source and TSS concentrations are predicted to remain elevated above ambient levels (>10 mg/L) for 1.3 hours after

the trencher passes into federal waters. Sediment deposition does not reach the level of 1.0 cm within NY state territorial waters (maximum predicted deposition thickness resulting from the SFEC-NYS is 9.9 mm).

For the portion of the installation in federal waters (SFEC-OCS) the maximum predicted TSS concentration is 1,347 mg/L. TSS concentrations at or above 100 mg/L are predicted to extend a maximum of 340 m from the source and TSS concentrations are predicted to remain elevated above ambient levels (>10 mg/L) for 1.4 hours after the conclusion of trenching. The maximum predicted deposition thickness is 11.4 mm. Sedimentation at or above 1.0 cm extends a maximum of 9 m from the burial route and covers a cumulative area of 1.74 ha of the seabed.

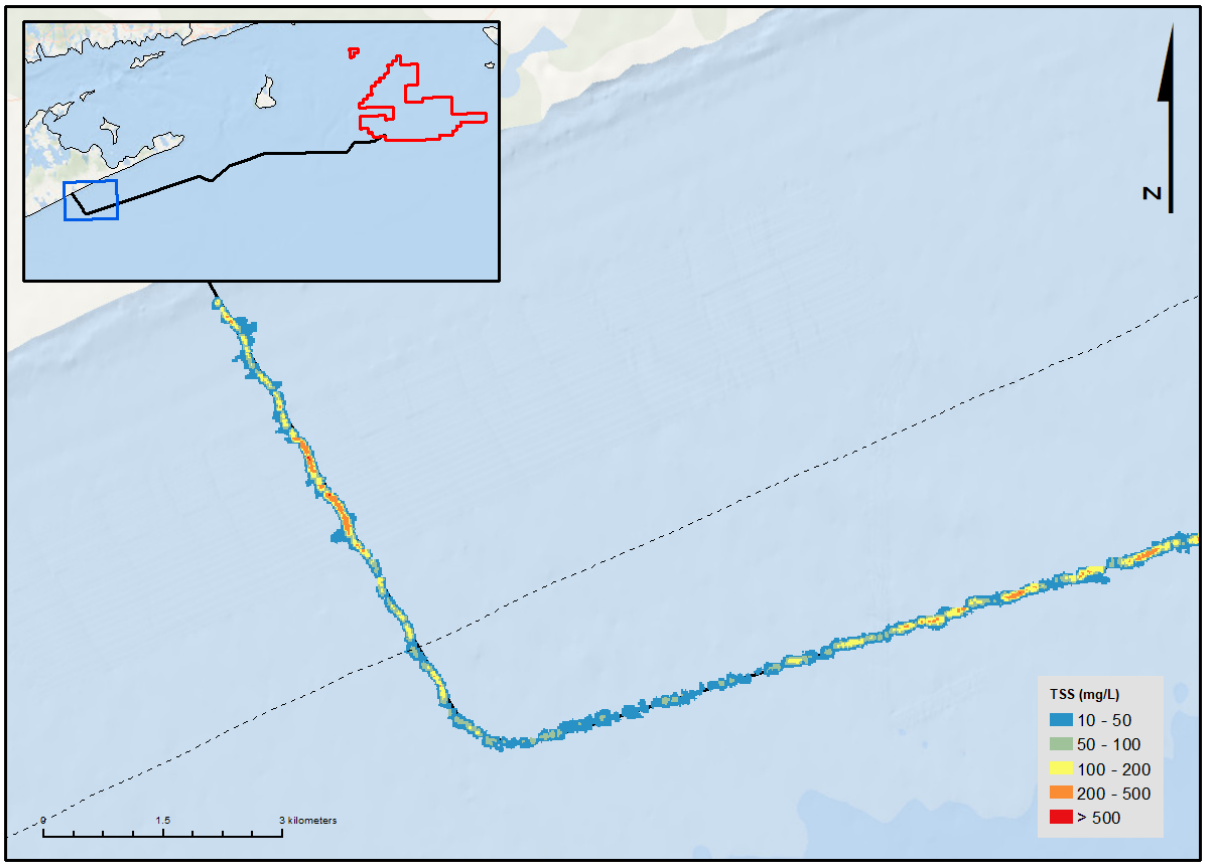


Figure 30. Cumulative TSS concentrations (mg/L) for Scenario 1 - SFEC burial over the full simulation period. TSS concentrations are depth- and time-integrated and show maximum concentrations for any cell at any time step in the model domain. (Map 1 of 7 – refer to inset for location relative to full Project extent.)

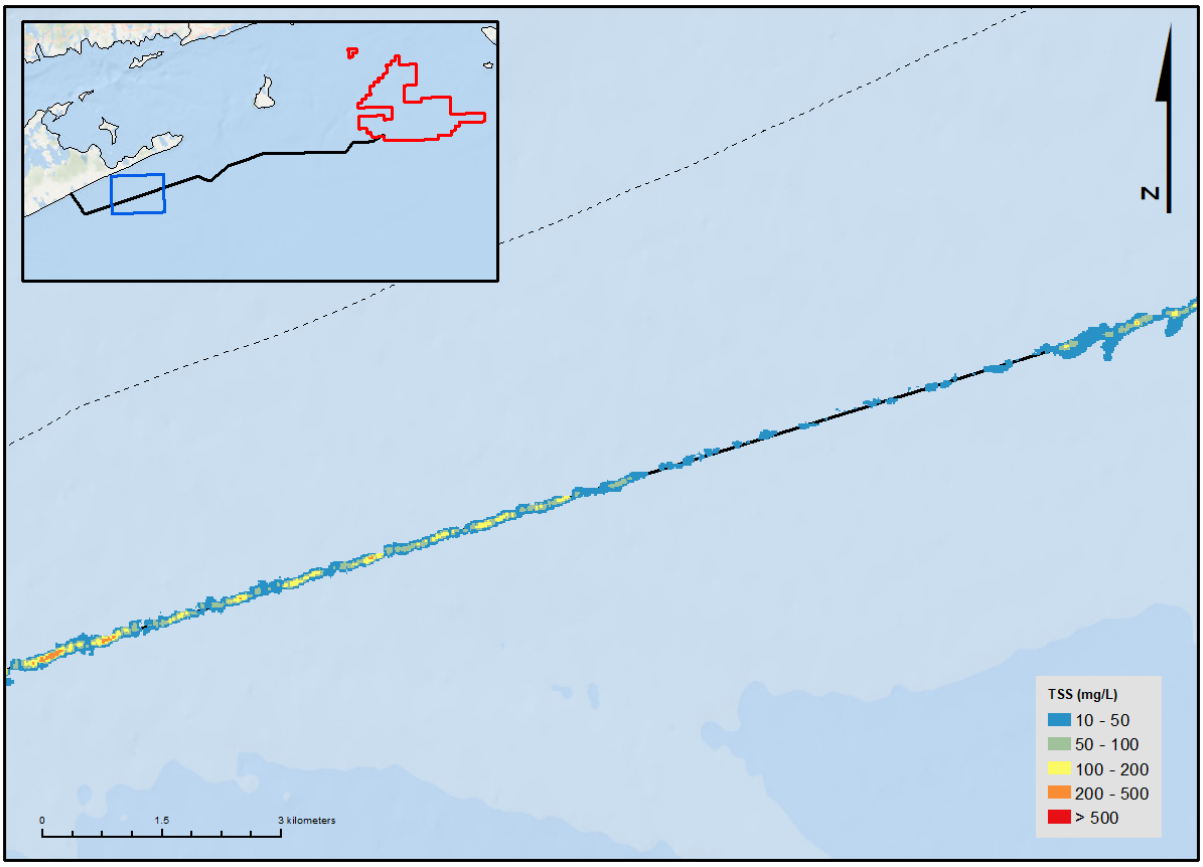


Figure 31. Cumulative TSS concentrations (mg/L) for Scenario 1 - SFEC burial over the full simulation period. TSS concentrations are depth- and time-integrated and show maximum concentrations for any cell at any time step in the model domain. (Map 2 of 7 – refer to inset for location relative to full Project extent.)

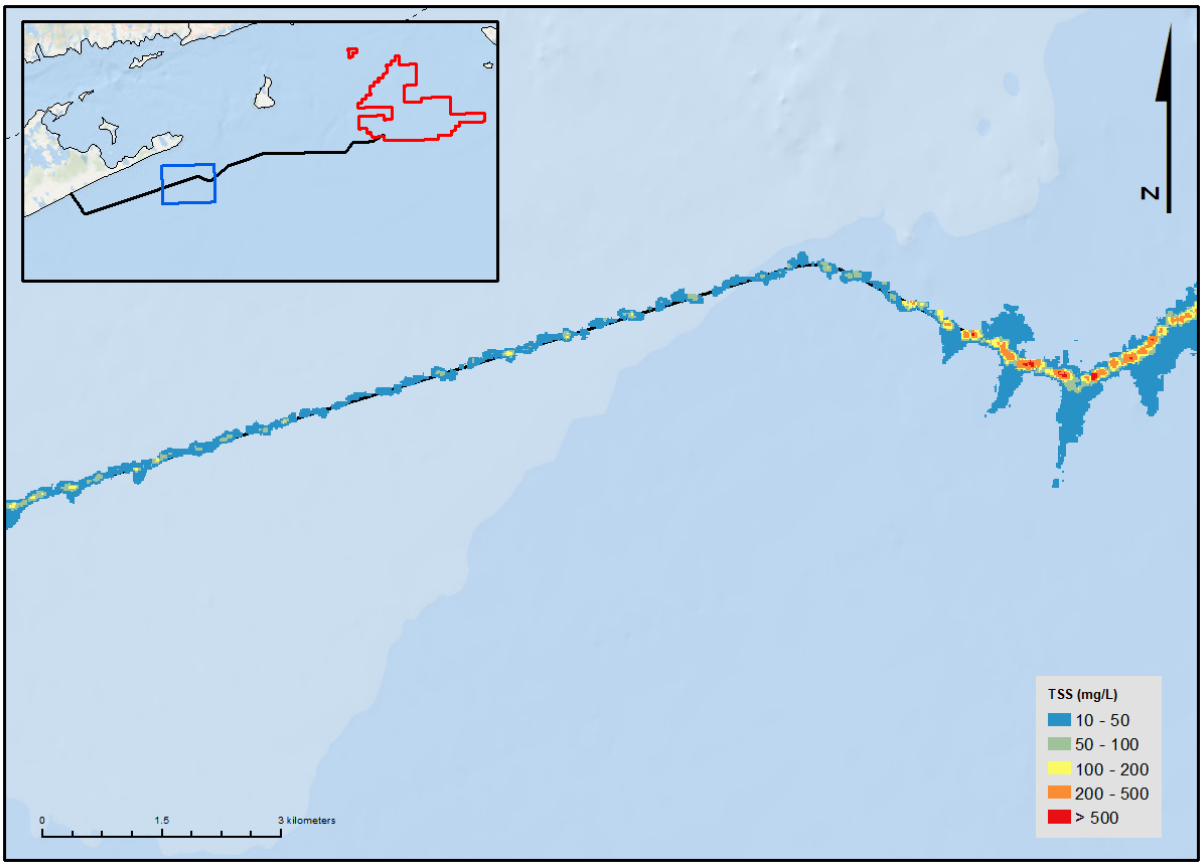


Figure 32. Cumulative TSS concentrations (mg/L) for Scenario 1 - SFEC burial over the full simulation period. TSS concentrations are depth- and time-integrated and show maximum concentrations for any cell at any time step in the model domain. (Map 3 of 7 – refer to inset for location relative to full Project extent.)

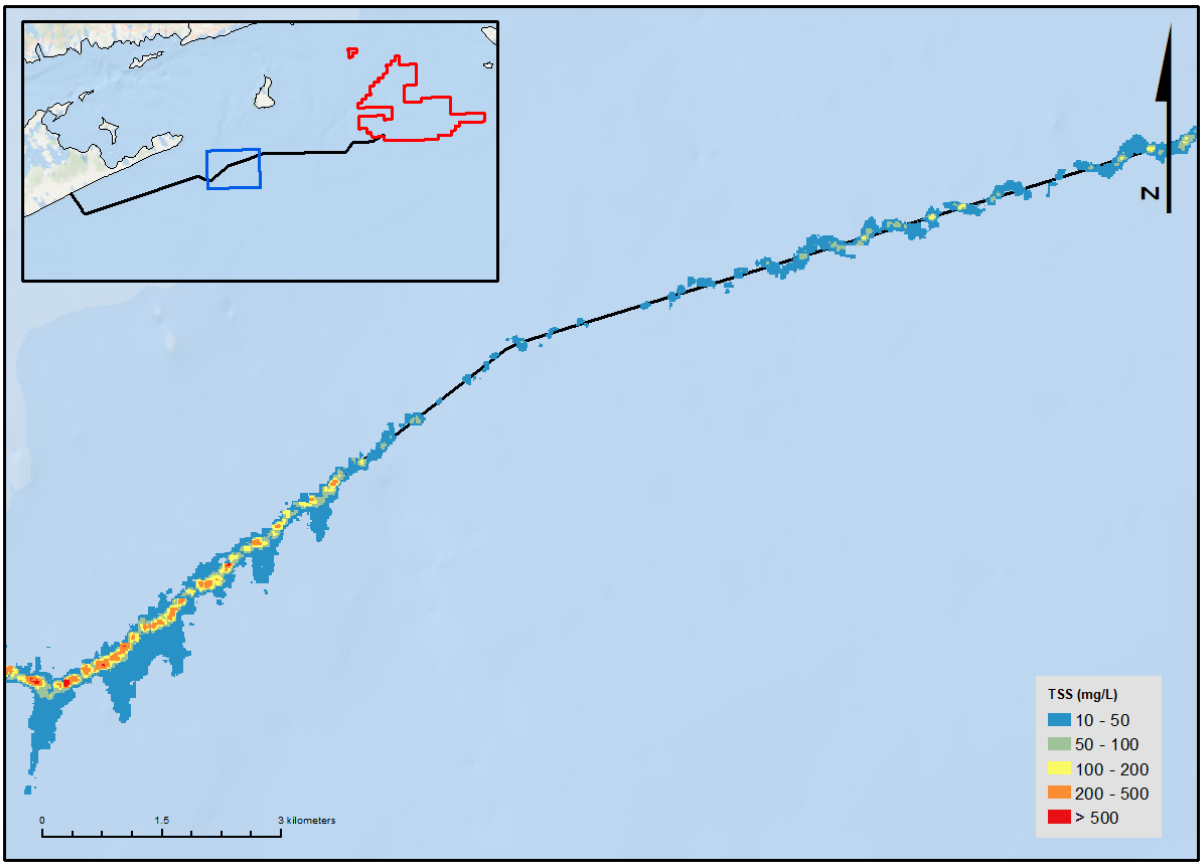


Figure 33. Cumulative TSS concentrations (mg/L) for Scenario 1 - SFEC burial over the full simulation period. TSS concentrations are depth- and time-integrated and show maximum concentrations for any cell at any time step in the model domain. (Map 4 of 7 – refer to inset for location relative to full Project extent.)

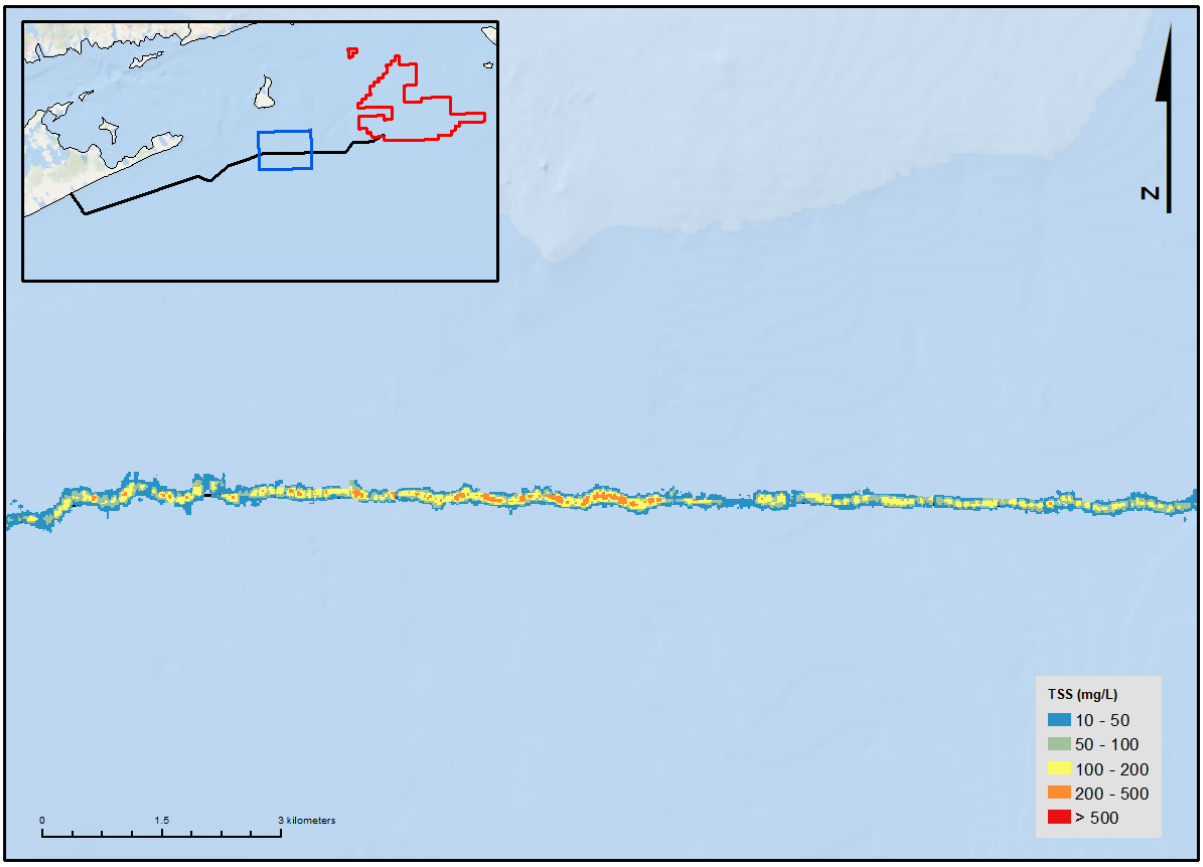


Figure 34. Cumulative TSS concentrations (mg/L) for Scenario 1 - SFEC burial over the full simulation period. TSS concentrations are depth- and time-integrated and show maximum concentrations for any cell at any time step in the model domain. (Map 5 of 7 – refer to inset for location relative to full Project extent.)

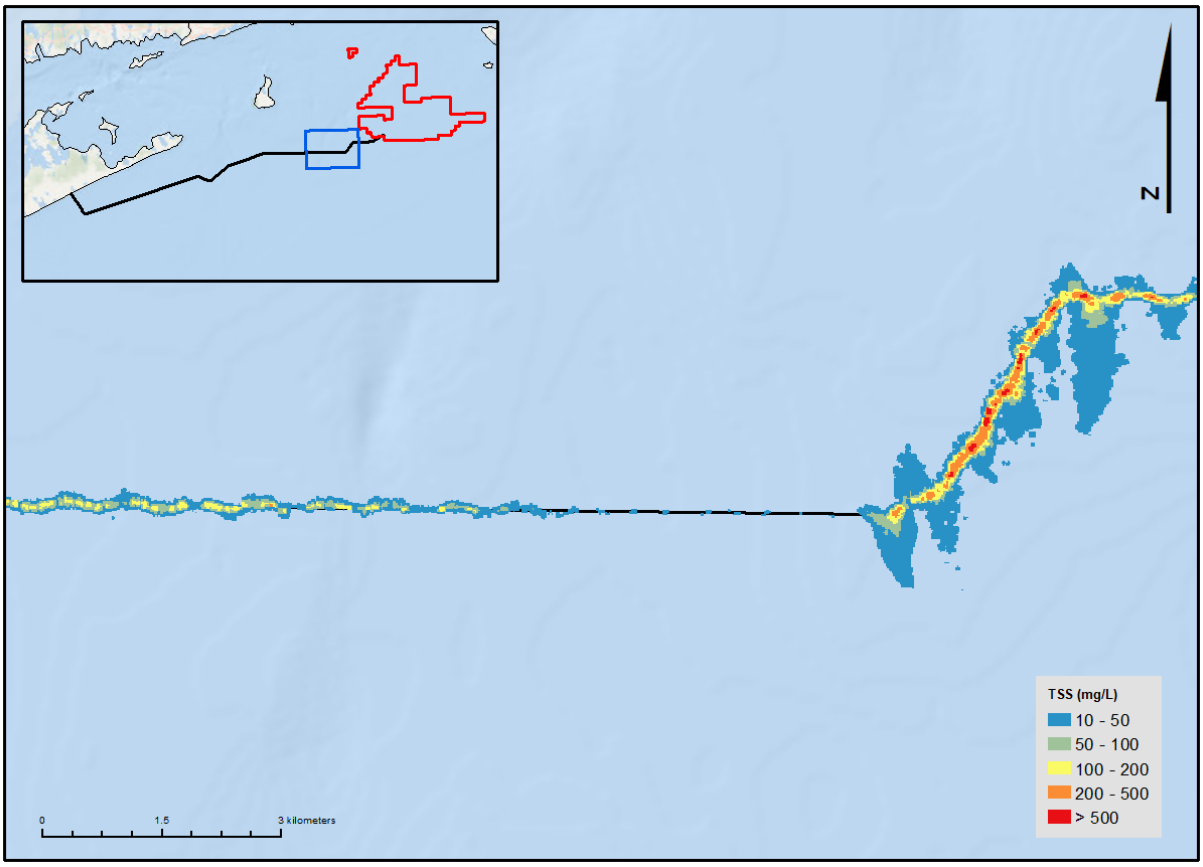


Figure 35. Cumulative TSS concentrations (mg/L) for Scenario 1 - SFEC burial over the full simulation period. TSS concentrations are depth- and time-integrated and show maximum concentrations for any cell at any time step in the model domain. (Map 6 of 7 – refer to inset for location relative to full Project extent.)

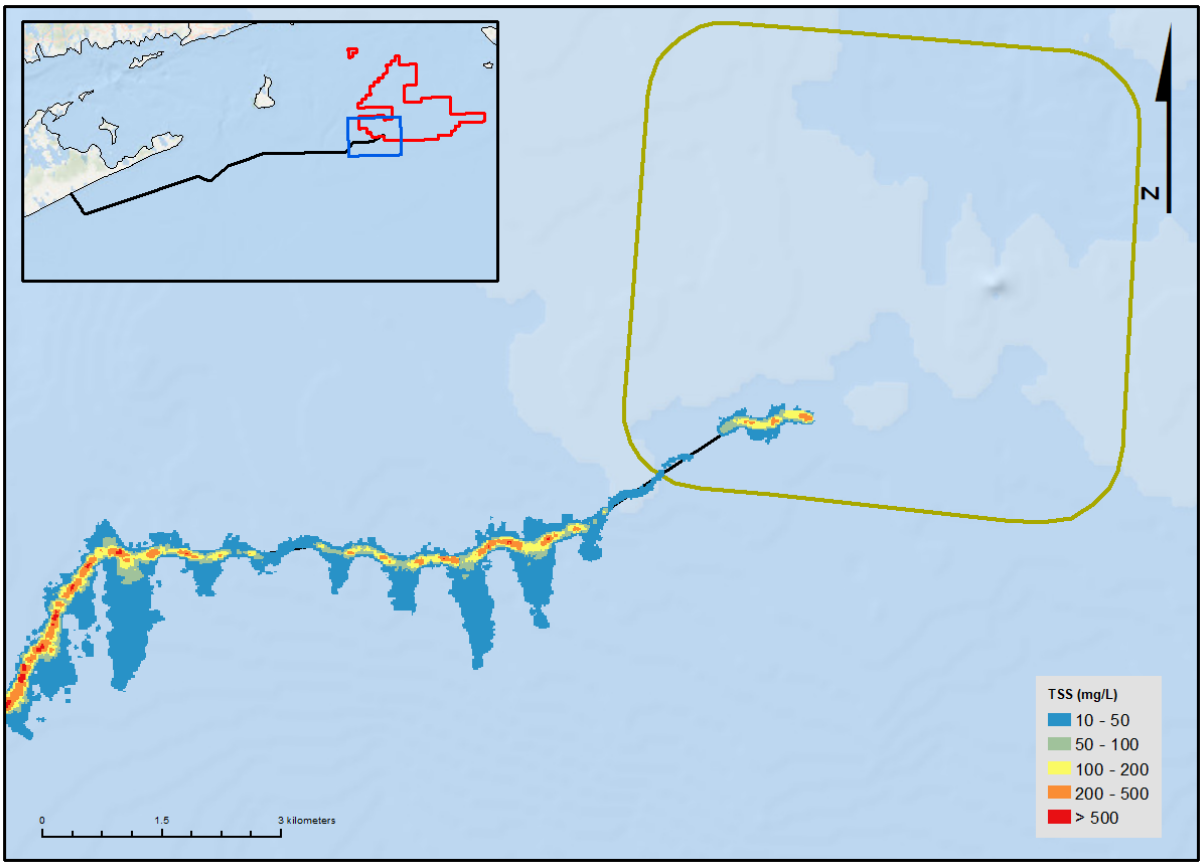


Figure 36. Cumulative TSS concentrations (mg/L) for Scenario 1 - SFEC burial over the full simulation period. TSS concentrations are depth- and time-integrated and show maximum concentrations for any cell at any time step in the model domain. (Map 7 of 7 – refer to inset for location relative to full Project extent.)

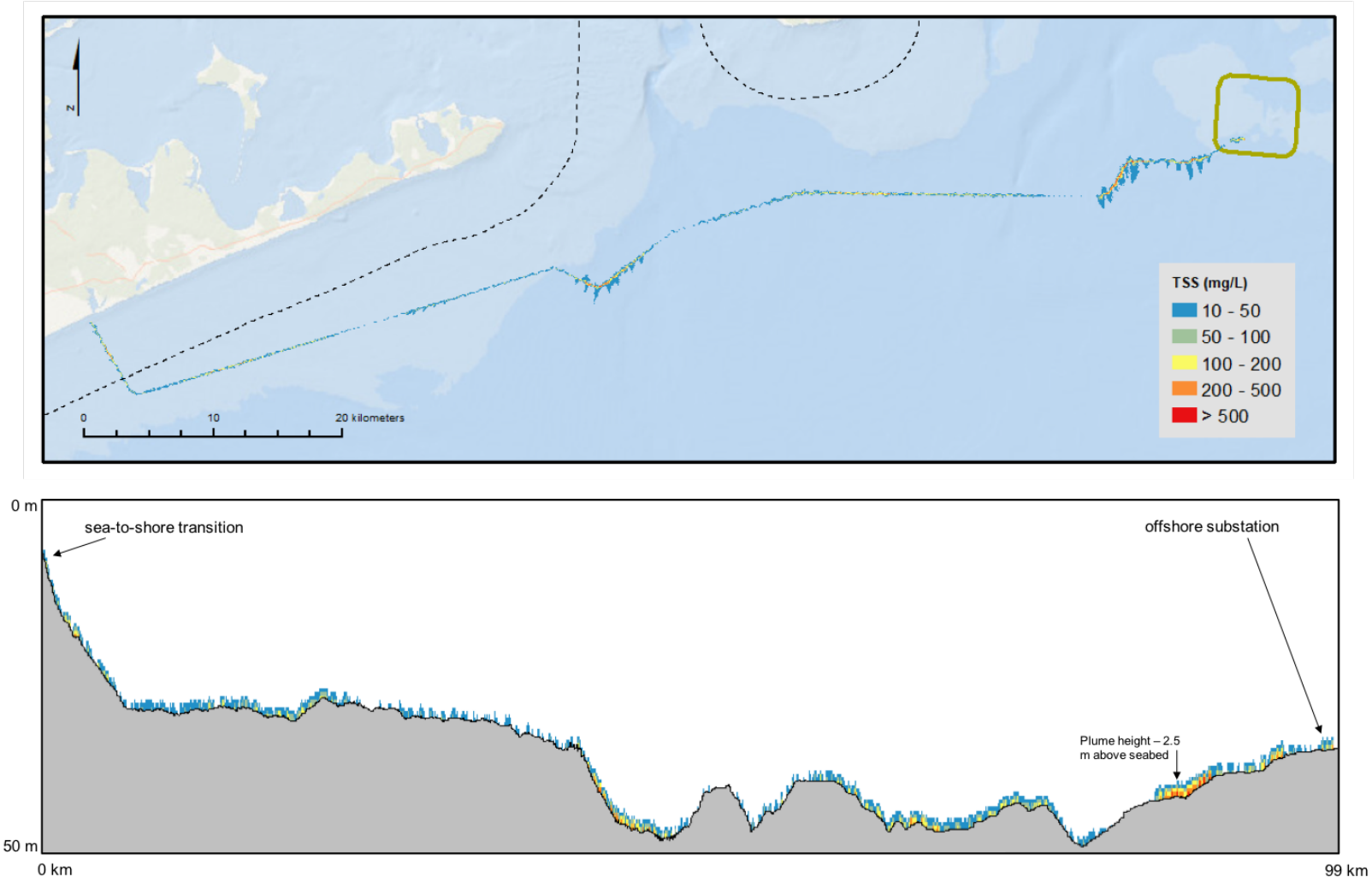


Figure 37. Cumulative TSS concentrations (mg/L) for Scenario 1 - SFEC burial over the full simulation period. Top: plan view showing concentrations over the full burial route; bottom: cross section views along the SFEC corridor between the sea-to-shore transition (left) and offshore substation at the SFWF (right). The maximum TSS concentration over the full simulation period is 1,347 mg/L.

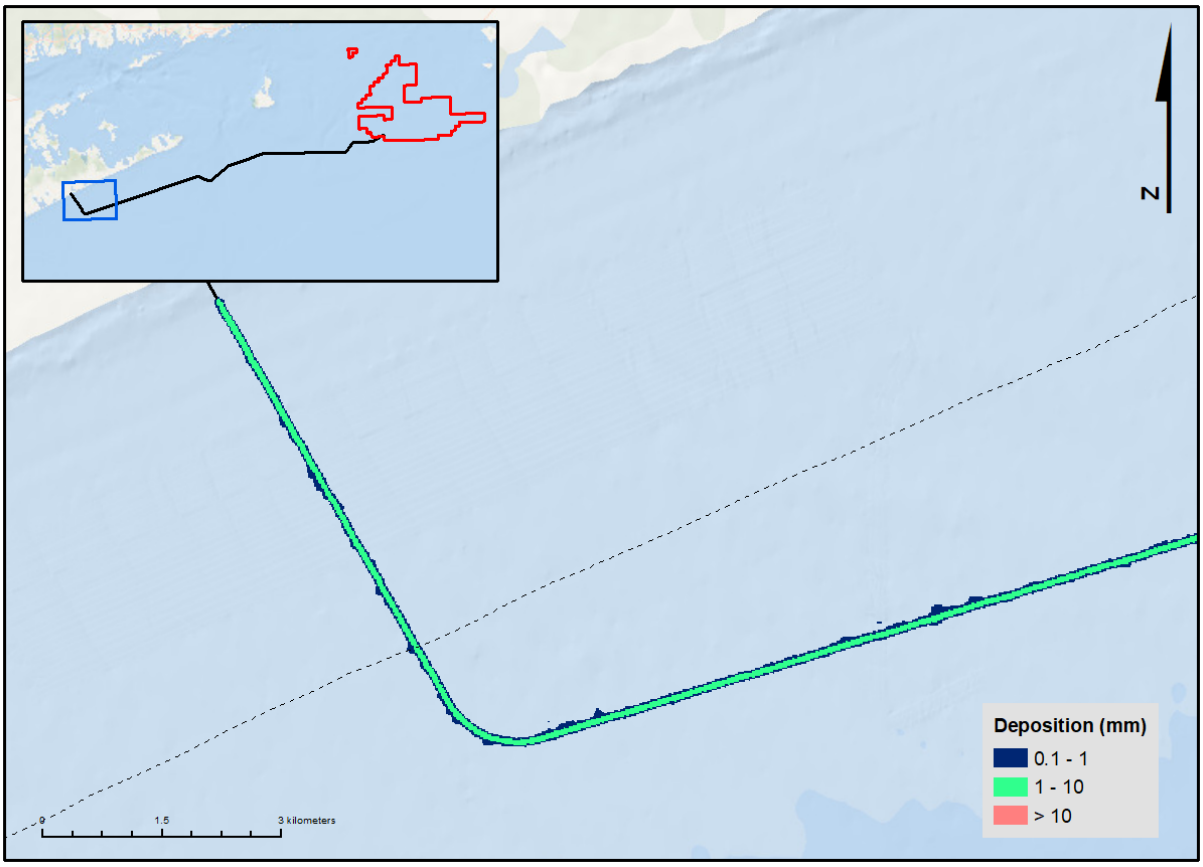


Figure 38. Extent of seabed deposition above 0.1 mm resulting from Scenario 1 – SFEC burial. (Map 1 of 7 – refer to inset for location relative to full Project extent.)

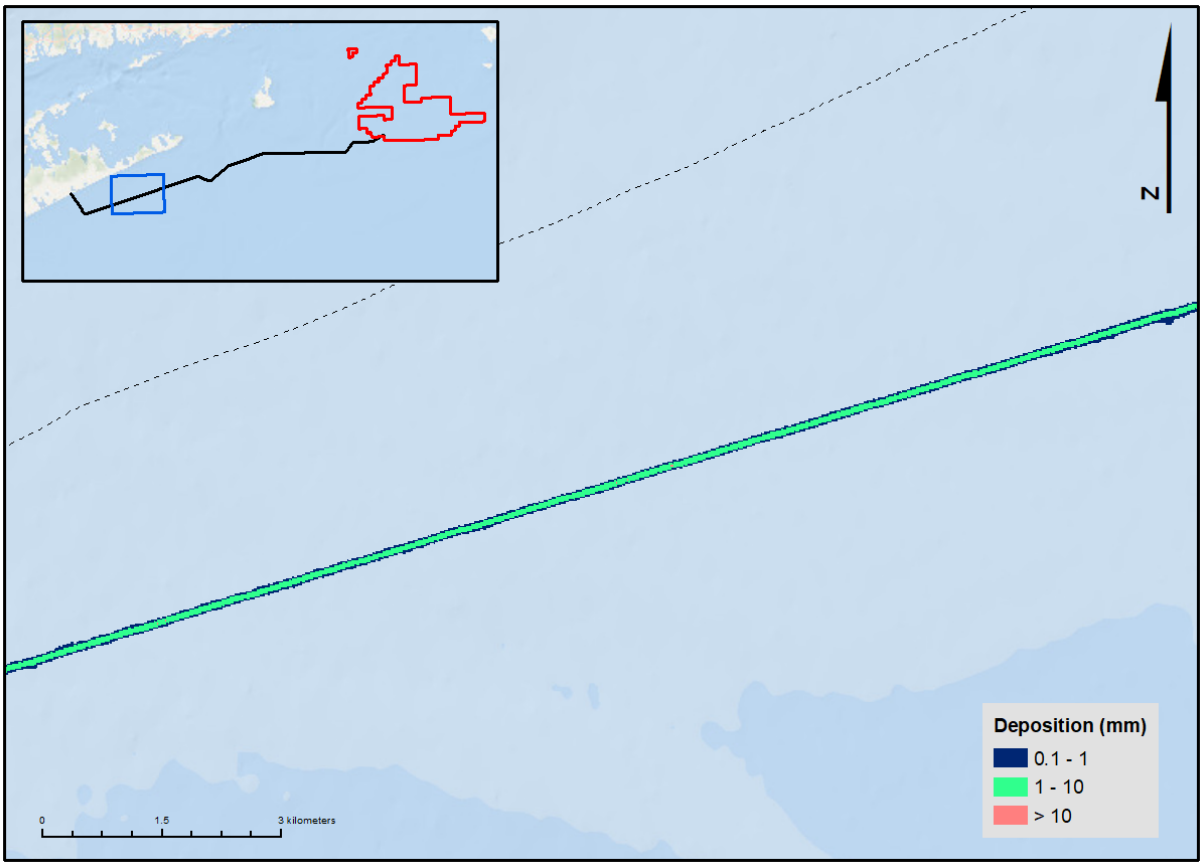


Figure 39. Extent of seabed deposition above 0.1 mm resulting from Scenario 1 – SFEC burial. (Map 2 of 7 – refer to inset for location relative to full Project extent.)

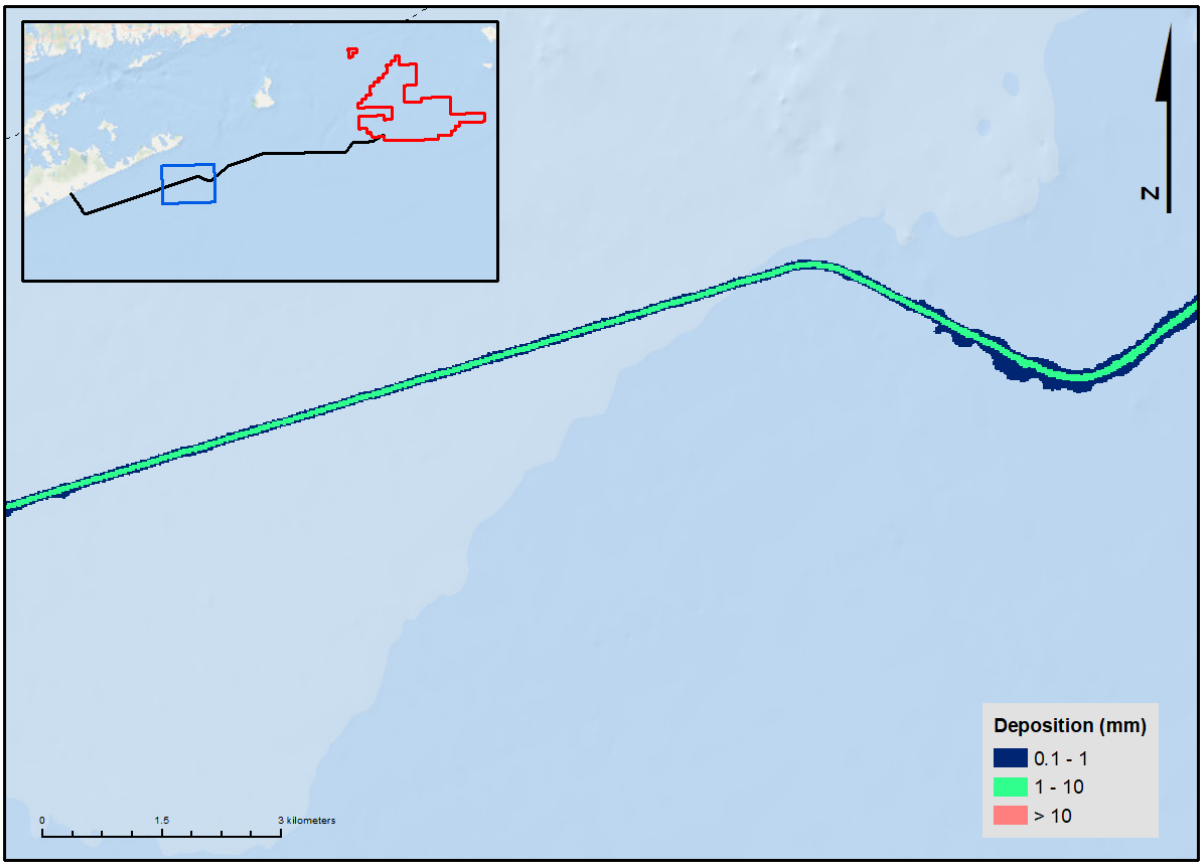


Figure 40. Extent of seabed deposition above 0.1 mm resulting from Scenario 1 – SFEC burial. (Map 3 of 7 – refer to inset for location relative to full Project extent.)

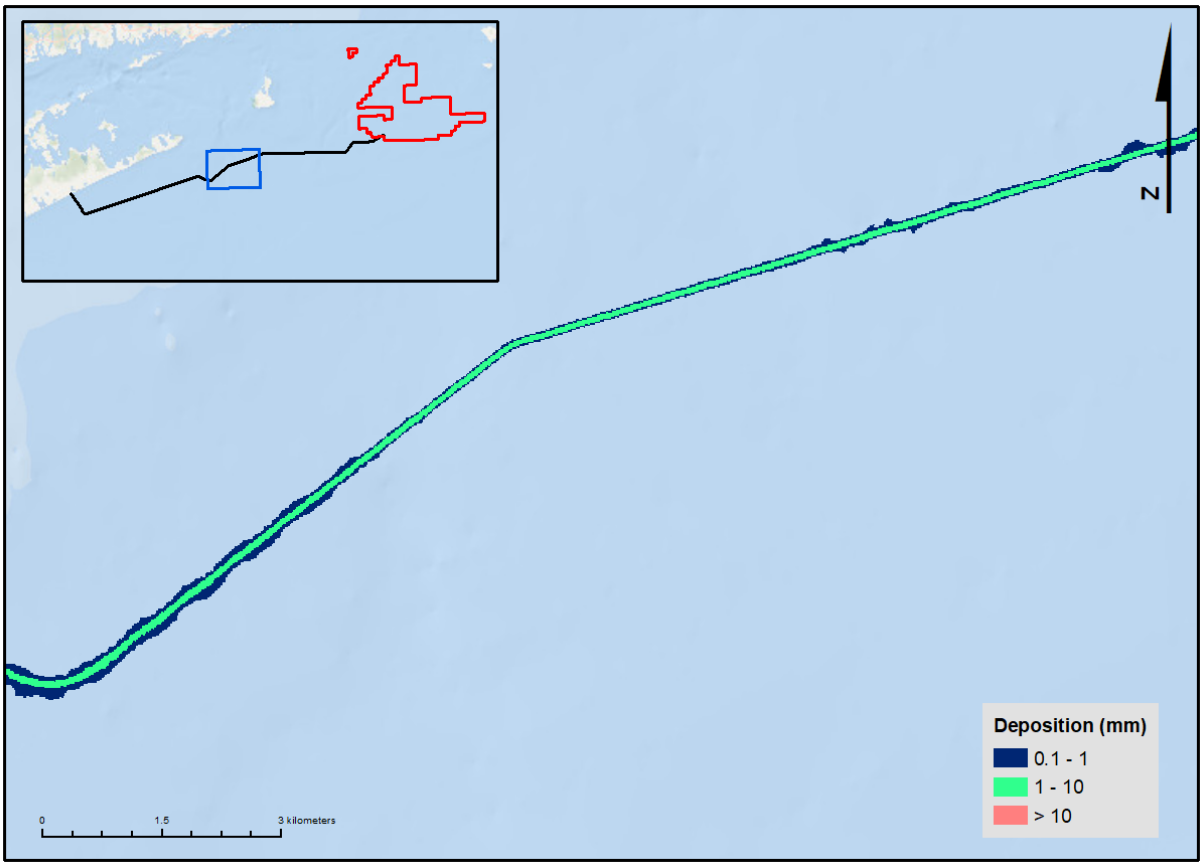


Figure 41. Extent of seabed deposition above 0.1 mm resulting from Scenario 1 – SFEC burial. (Map 4 of 7 – refer to inset for location relative to full Project extent.)

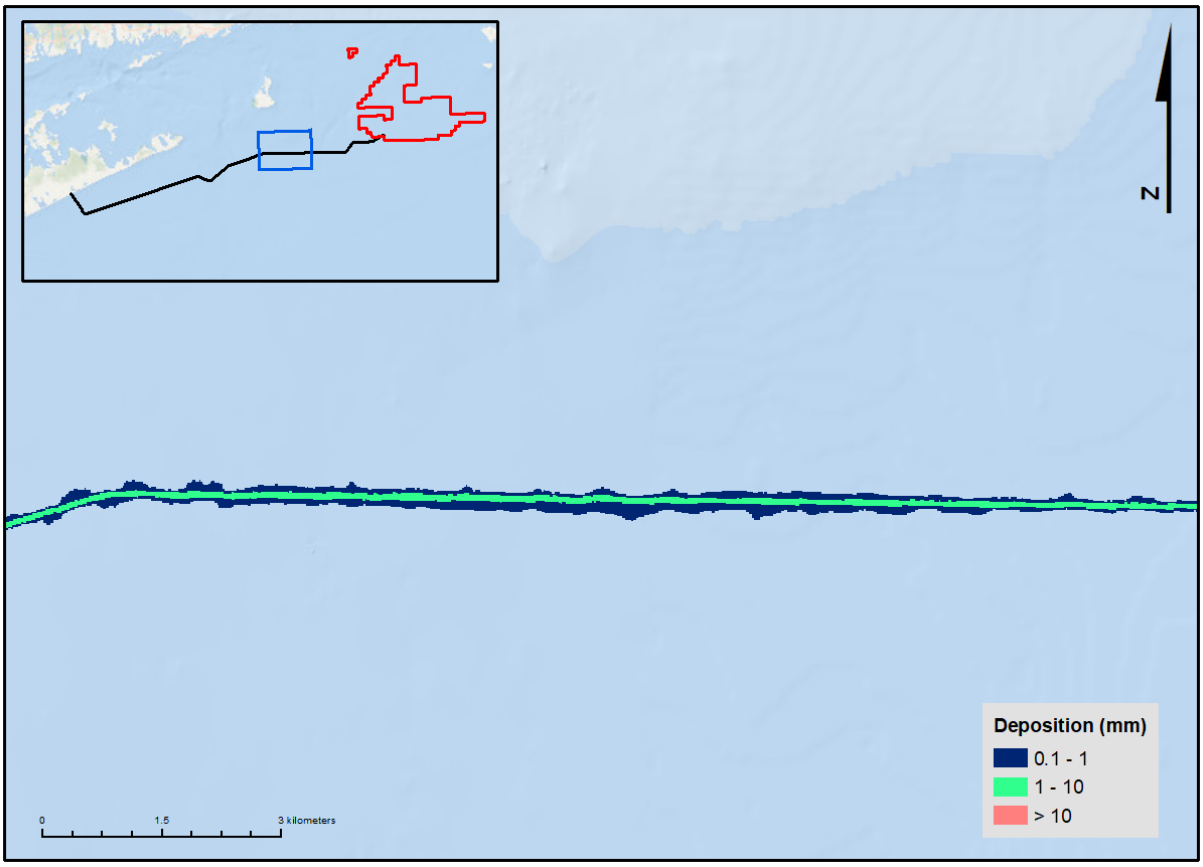


Figure 42. Extent of seabed deposition above 0.1 mm resulting from Scenario 1 – SFEC burial. (Map 5 of 7 – refer to inset for location relative to full Project extent.)

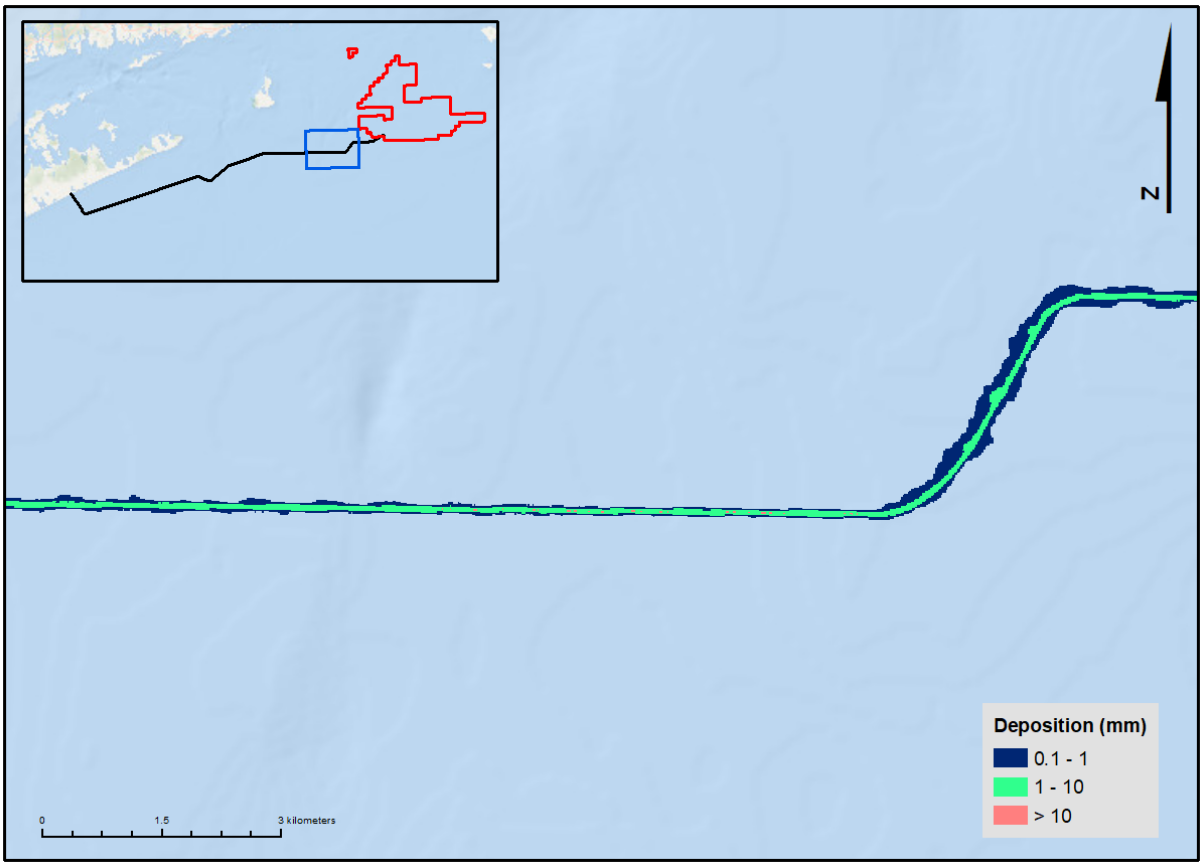


Figure 43. Extent of seabed deposition above 0.1 mm resulting from Scenario 1 – SFEC burial. (Map 6 of 7 – refer to inset for location relative to full Project extent.)

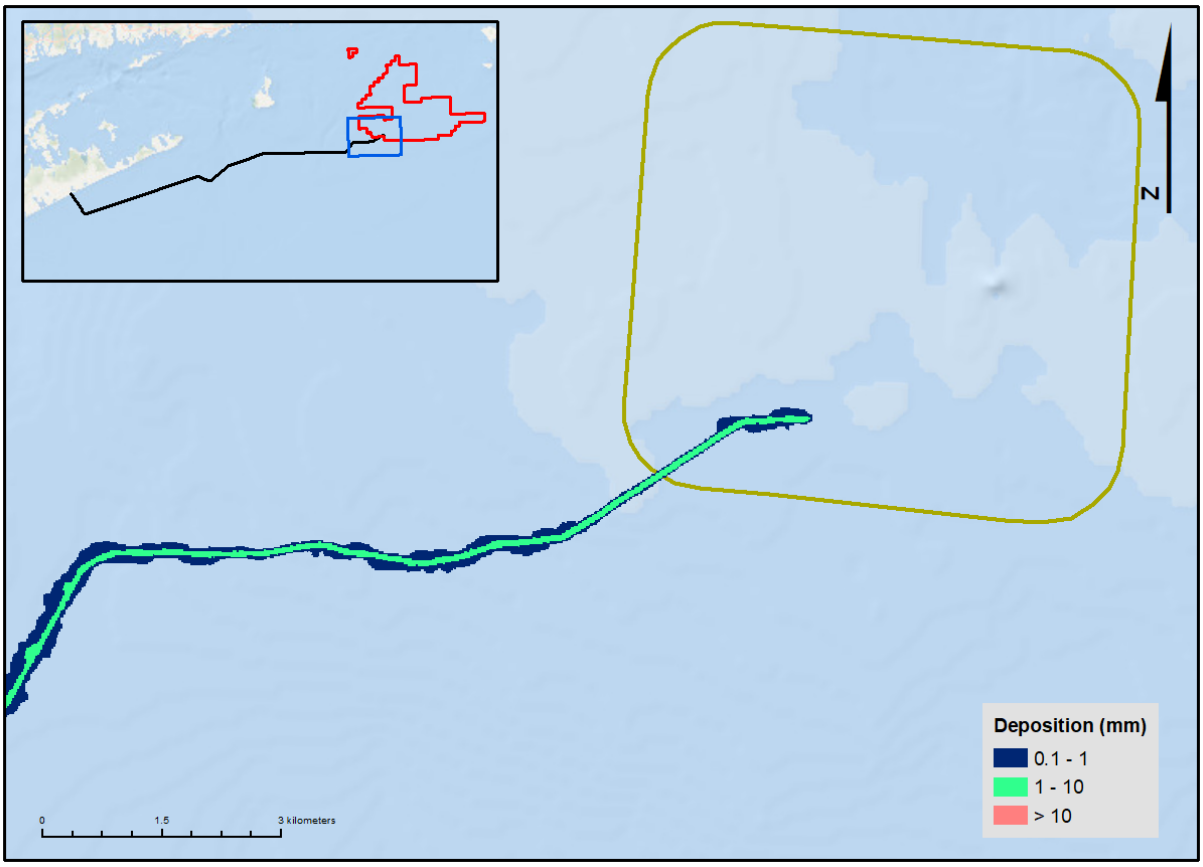


Figure 44. Extent of seabed deposition above 0.1 mm resulting from Scenario 1 – SFEC burial. (Map 7 of 7 – refer to inset for location relative to full Project extent.)

### 3.4.2 Scenario 2 – Inter-Array Cable Installation

Scenario 2 included simulation of installation activities for the inter-array cable network, specifically for a representative section of the cable between two potential WTG locations (approximately 1.4 km apart) in the SFWF work area in federal waters. As with the SFEC burial, the installation will utilize a self-propelled hydro-plow vehicle to simultaneously bay and bury the cable beneath the seafloor. The seabed footprint of sediment resuspension from hydro-plow trenching is approximately 0.9 m (trench surface width), and as the vehicle advances, the cable is lowered to its burial depth (maximum 1.8 m of cover). The total volume of the trench between the two locations is estimated to be 2,342 $m^3$ although, as described before, most of this material will remain undisturbed at the seabed since the jet trencher does not directly excavate sediment from the trench. For modeling, it was assumed that the equipment would operate at a constant production rate of 112 $m^3$/hr (based on an advance rate of 67 m/hr).

The activity was modeled as a line source and assumed full burial of the cable would be achieved with a single pass of the trencher. The simulation originates at the southern WTG location (41.074851N, 71.156538W) and advances northward 1.4 km along the cable route to the next WTG (41.086992N, 71.155759W). As previously described, the model assumed continuous installation (24 hours/day) over the complete duration of construction to replicate “worst case” conditions for sustained TSS concentrations.

Unlike the SFEC installation, cable burial along this reach of the inter-array network will occur relatively quickly (<1 day for the hydro-plow to advance between the two WTGs). For this reason, simulations of the inter-array cable burial were executed for two different periods – each sampling a different tidal regime – to capture some degree of variability in the offshore hydrodynamic conditions. The inter-array cable installation is currently planned Summer 2022 and based on guidance from DWW, the model was run assuming installation would occur during the month of July. Specifically, two model periods were selected representing: (i) spring tide conditions (start date of July 3, 2016; Figure 25), and (ii) neap tide conditions (start date of July 12, 2016). Resuspension of sediment from this activity was set to 25% of the total trench volume. In the model, mass lost to the water column was partitioned equally into five layers within the lowermost 1 m of the seafloor. In total, each simulation included the release of 585 $m^3$ of sediment over the course of 20.9 hours of active production.

Maximum integrated TSS concentration and subsequent seabed deposition from the inter-array cable installation are presented in a series maps centered on the SFWF work area (Figure 45 through Figure 48), and results of the full simulation are summarized in Table 7. The water column and seabed impact from this activity remain entirely within federal waters. The sediment plume that arises during trenching largely

reflects behavior of the currents for each period. During spring tide conditions, the plume oscillates SE and NE of source, while during the neap conditions, the plume exhibits more of a N/S orientation. Due to the relatively consistent grain sizes along this portion of the inter-array cable route plume concentrations do not vary considerably between the two periods. Overall, the plume extends further, maintaining lower TSS concentrations during spring tide, and appears more compact and concentrated during neap conditions. These differences are negligible, however, when compared to the larger project footprint, and are mostly seen in concentrations below 30 mg/L. The cross-section view presented for both periods indicates that elevated TSS concentrations are expected to remain very close the seabed, and plumes are not predicted to extent vertically beyond three meters of the source at any time during the simulation (nowhere in the model domain were concentrations above 10 mg/L predicted above 33 m depth).

As with the results from the SFEC burial, sedimentation (Figure 47 and Figure 48) is limited to the area immediately adjacent to the burial route (typically within 60 m of the hydro-plow track). Maps of deposition from the two simulations are nearly indistinguishable, again suggesting that most sediments are settling very close to the source.

Considering both periods of analysis, the maximum predicted TSS concentration from the inter-array cable burial activities is 100 mg/L. Water column concentrations of 100 mg/L are predicted to extend up to 40 m from the source and TSS concentrations are predicted to return to ambient levels (<10 mg/L) within 0.3 hours from the conclusion of trenching. The maximum predicted deposition thickness is 10.8 mm. Sedimentation at or above 1.0 cm extends a maximum of 8 m from the burial route and covers a cumulative area of only 0.04 ha of the seabed.

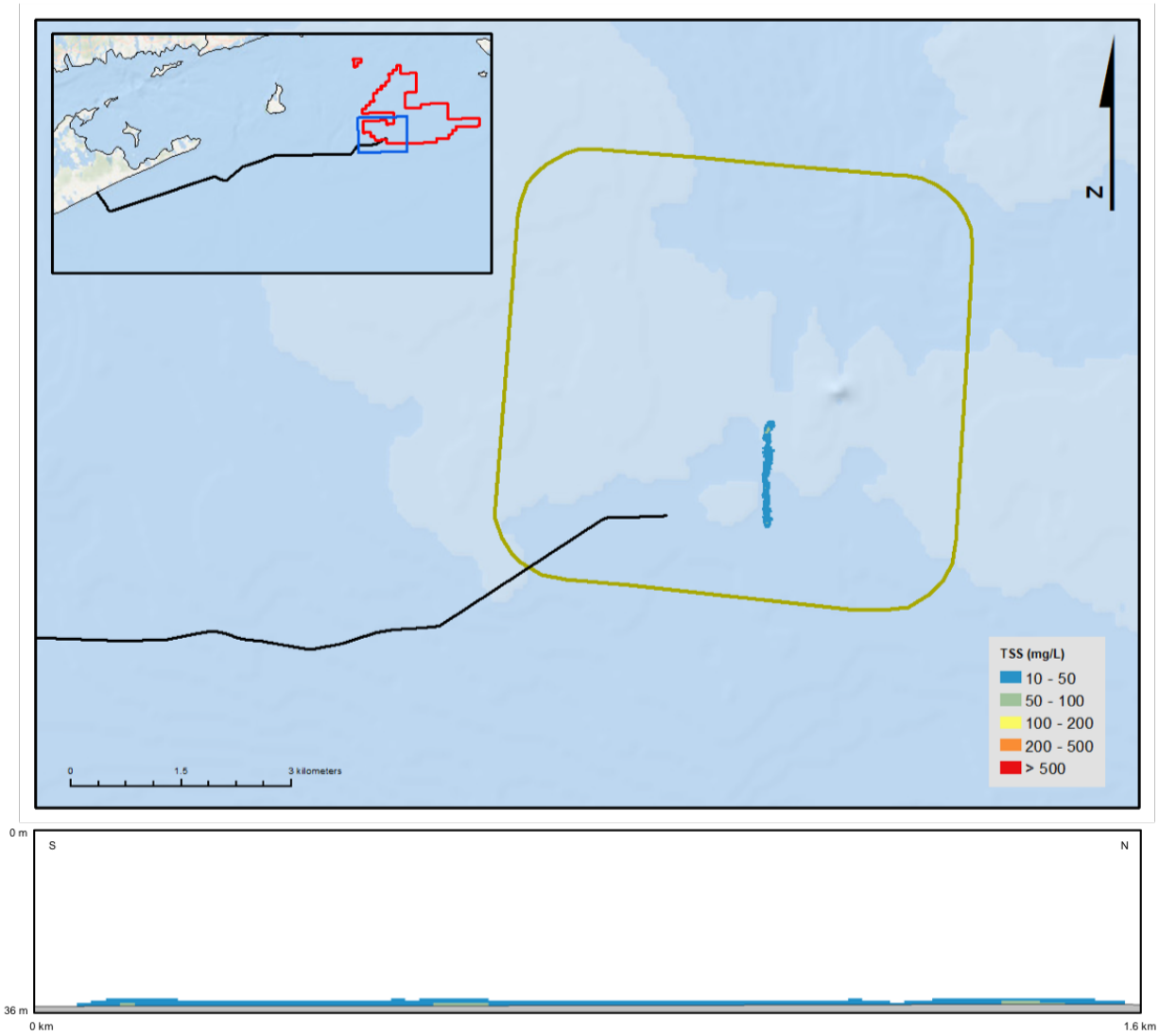


Figure 45. Cumulative TSS concentrations (mg/L) for Scenario 2 – inter-array cable burial between two potential WTG locations (Period 1 – spring tide conditions). Top: plan view showing concentrations within the SFWF work area; bottom: cross section views along the burial route between the southern WTG (left) and the northern WTG (right). The maximum TSS concentration during this period is 82 mg/L.

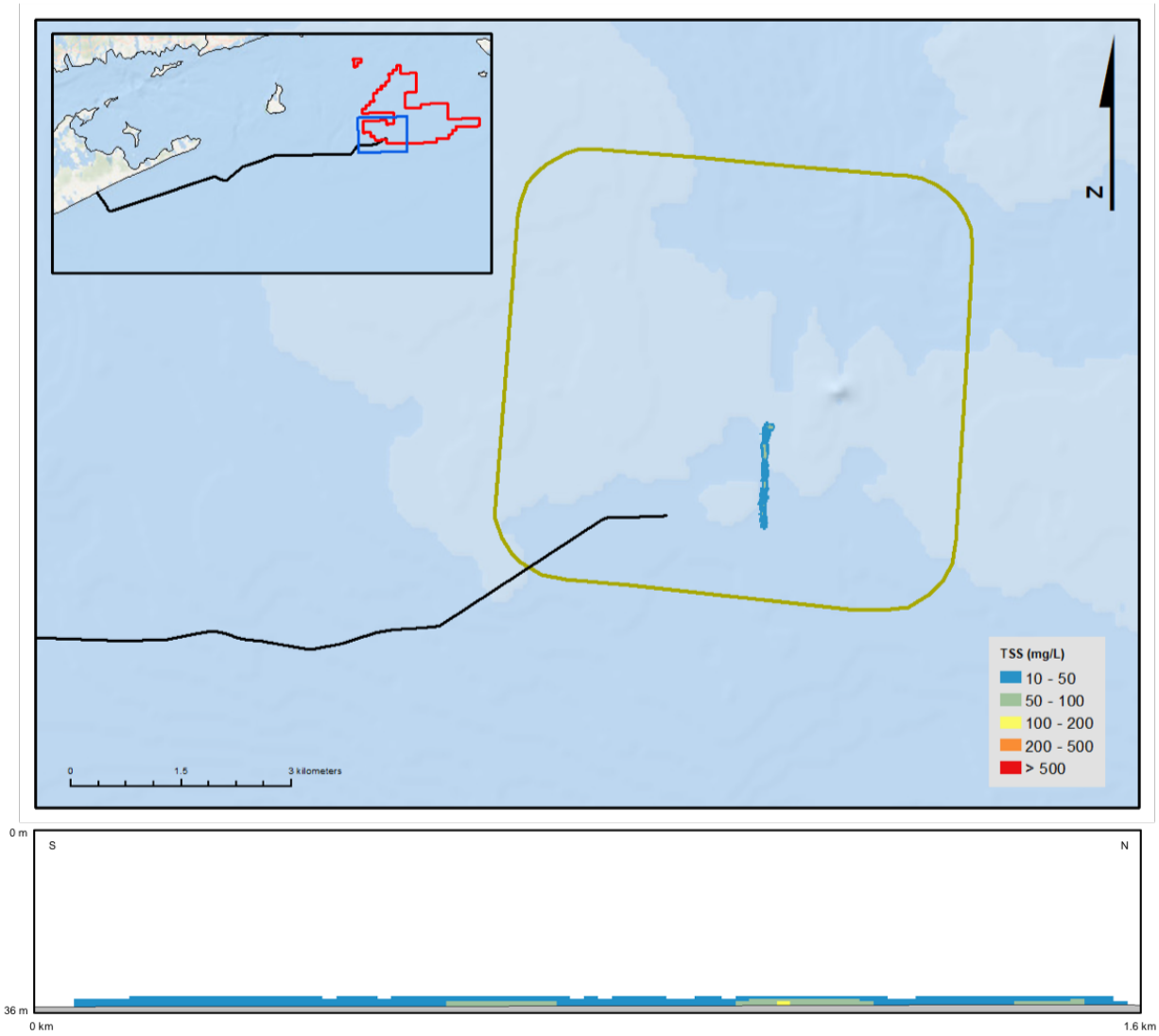


Figure 46. Cumulative TSS concentrations (mg/L) for Scenario 2 – inter-array cable burial between two potential WTG locations (Period 2 – neap tide conditions). Top: plan view showing concentrations within the SFWF work area; bottom: cross section views along the burial route between the southern WTG (left) and the northern WTG (right). The maximum TSS concentration during this period is 100 mg/L.

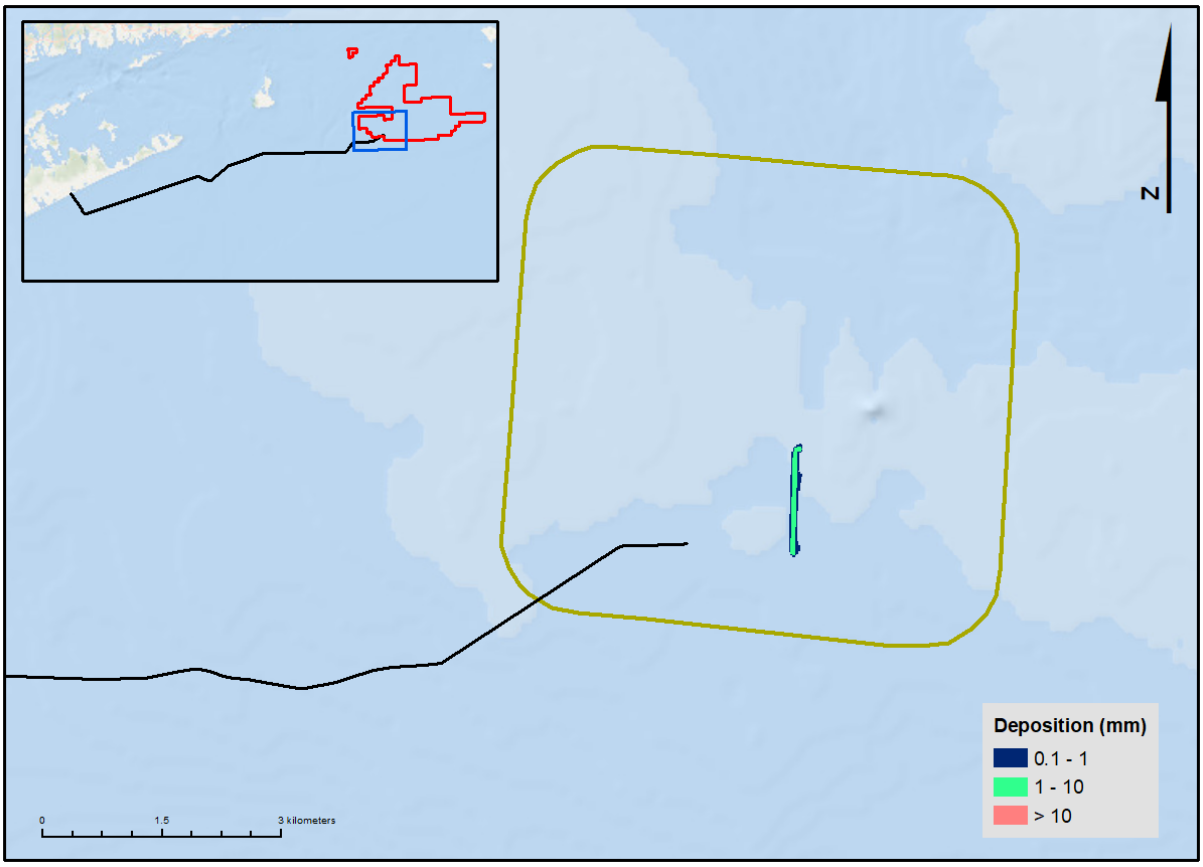


Figure 47. Extent of seabed deposition above 0.1 mm resulting from Scenario 2 – inter-array cable burial between two potential WTG locations (Period 1 – spring tide conditions). Inset shows location relative to full Project extent.)

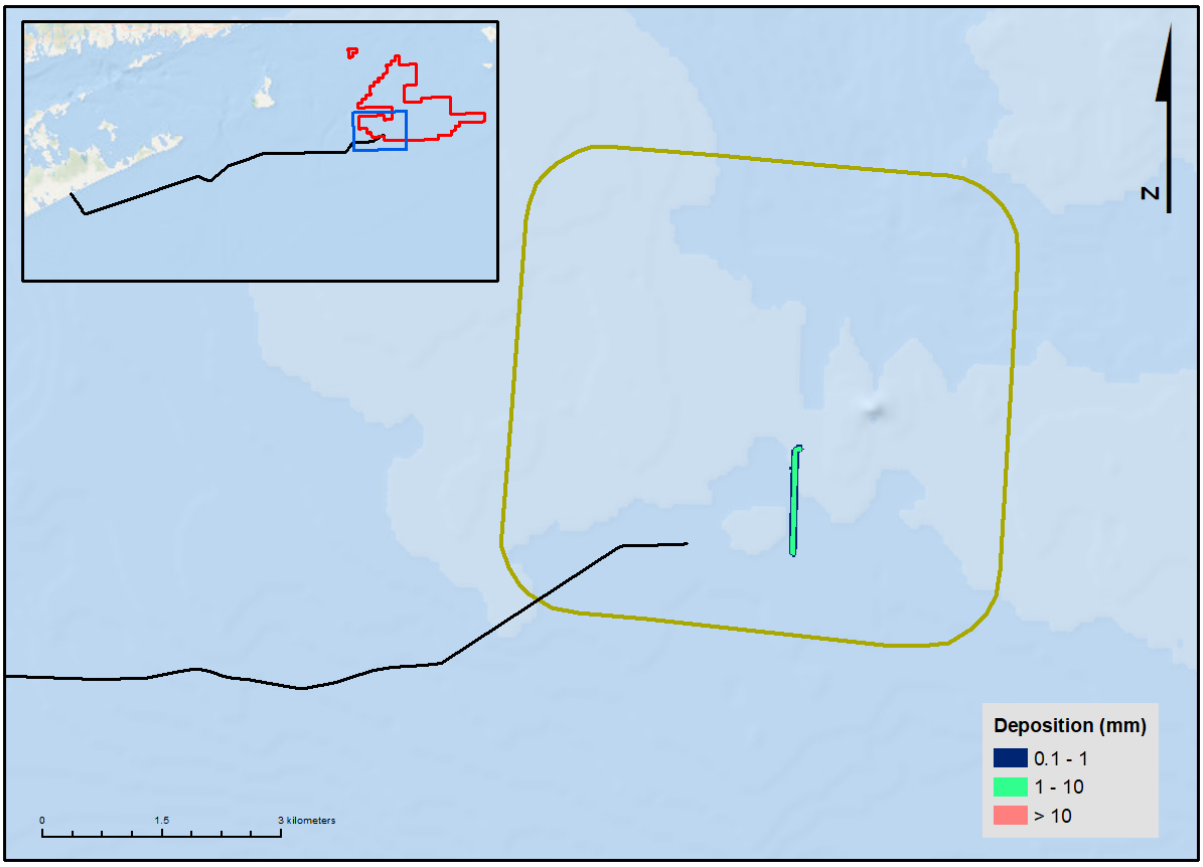


Figure 48. Extent of seabed deposition above 0.1 mm resulting from Scenario 2 – inter-array cable burial between two potential WTG locations (Period 2 – neap tide conditions). Inset shows location relative to full Project extent.)

### 3.4.3 Scenario 3 – Excavation of the HDD Pit

Scenario 3 included simulation of dredging and side-casting at the sea-to-shore transition vault offshore Beach Lane. This activity will occur entirely within NY state jurisdictional waters. A ten-inch suction dredge will be used to excavate the HDD exit pit at a location approximately 650 m from the shoreline, where the offshore segments of the SFEC will transition to the onshore segment. The suction dredger uses a vacuum to excavate a sediment slurry from the seabed and the fluidized sediment is released through a discharge pipe to a spoil pile on the nearby seafloor. The activity was modeled as a point source originating from the HDD exit location (40.922844N, 72.231346W).

It is possible that a temporary offshore cofferdam will be installed at the transition point, prior to the HDD installation, both to serve as containment for the drilling returns and to keep the excavation area from silting back in. The cofferdam would enclose an area around the exit pit approximately 22.9 m long by 7.6 m wide and up to 3.7 m deep. For modeling, it was assumed that 650 $m^3$ of sediment will be removed from the pilot hole and simultaneously side-cast adjacent to the excavation site. (650 $m^3$ includes the full cofferdam area [637 $m^3$] rounded up slightly to include potential over-dredge volumes.) As the entirety of the sediment from suction dredging will be side-cast, resuspension from this activity was set to 100% of the total volume. The discharged sediment is initialized within the model at a single point in the water column, 1.5 m above the seafloor. Contractor estimates indicate that the suction dredger can operate at a production rate of 90 $m^3$/hr.

As with installation of the inter-array cable, dredging at the HDD site will take place over a relatively short construction window (<1 day assuming constant production). For this reason, simulations of dredging were executed for two different periods – each sampling a different tidal regime – to capture some degree of variability in the hydrodynamic conditions. The sea-to-shore construction (which includes excavation of the HDD pit and cofferdam installation) is currently planned for Winter/Spring 2022. Accordingly, two model periods were selected representing: (i) a neap tide conditions (start date of March 2, 2016; Figure 25), and (ii) spring tide (start date of April 8, 2016). For both simulations, the modeling assumed that the suction pump would operate continuously for the duration this activity - 7.2 hours.

Maximum integrated TSS concentration and subsequent seabed deposition from suction dredging at the HDD site are presented in a series of maps below (Figure 49 through Figure 52), and results of the full simulation are summarized in Table 7. The water column and seabed impact from this activity remain entirely within NY state waters. The sediment plume that arises during suction dredging dissipates in the alongshore direction (SW or NE, depending on the phase of the tide). At its largest, the plume extends up to 700 m from the pit location, although concentrations above 30 mg/L remain within 300-400 m of the

site. And while the plume orientation changes between the two model periods, the difference reflects the semi-diurnal (ebb/flood) behavior of the currents, as opposed to any difference in the spring/neap tidal cycle. (To that end, it is important to consider that plume orientation is largely a function of the currents and in actuality may extend away from the source in multiple directions depending on the phase of the tide during construction.) The cross-section view presented for both periods indicates that elevated TSS concentrations are predicted to remain within the lower half of the water column, and plumes are not predicted to extent vertically beyond 3 meters of the source at any time during the simulation. Maximum concentrations are predicted directly above the seabed at the discharge pipe.

Sedimentation is limited to the area immediately adjacent to the exit pit (within 200 m of the source). Unlike previous scenarios where sediment is resuspended along a linear path, the dredge and side-cast operation occurs from a single point within the model domain. For this reason, the deposit is thicker, but is far more limited in extent and is almost difficult to detect at the scale presented in Figure 51 and Figure 52. Results between the two simulations are similar, although in this case the deposition footprints are slightly aligned with the current field for each model period, particularly at lower thickness levels.

Considering both periods of analysis, the maximum predicted TSS concentration from suction dredging at the HDD site is 562 mg/L. Water column concentrations at or above 100 mg/L are predicted to extend up to 145 m from the source and TSS concentrations are predicted to return to ambient levels (<10 mg/L) within 1.1 hours from the conclusion of dredging. The maximum predicted deposition thickness is 318.3 mm. Sedimentation at or above 1.0 cm extends a maximum of 54 m from the side-cast point and covers a cumulative area of only 0.56 ha of the seabed.

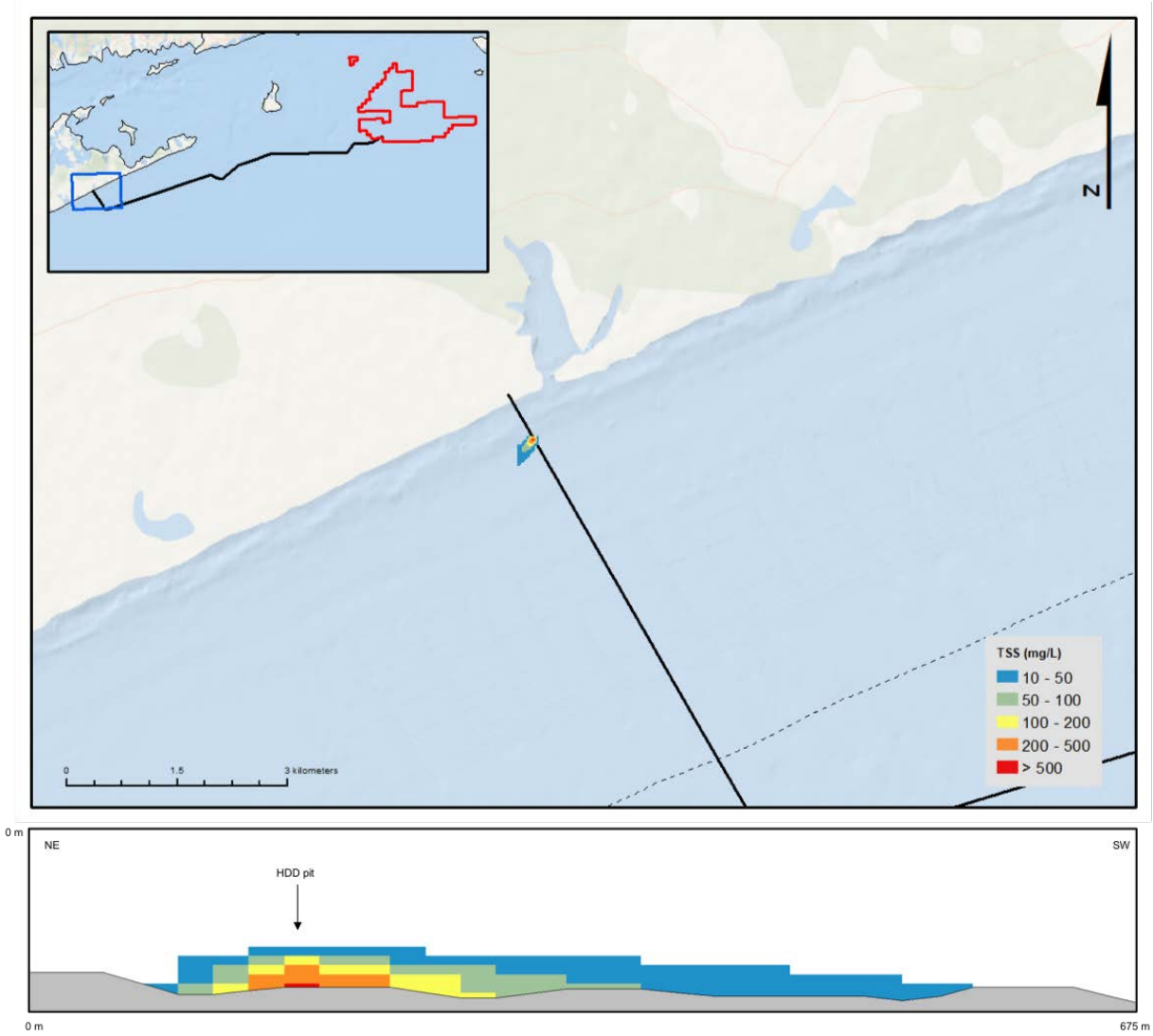


Figure 49. Cumulative TSS concentrations (mg/L) for Scenario 3 – suction dredging of the HDD exit pit at the sea-to-shore transition (Period 1 – neap tide conditions). Top: plan view showing concentrations near the dredging site; bottom: cross section view extending southwest from the dredging location. The maximum TSS concentration during this period is 561 mg/L. The plume is approximately 560 m from the shoreline at its closest point.

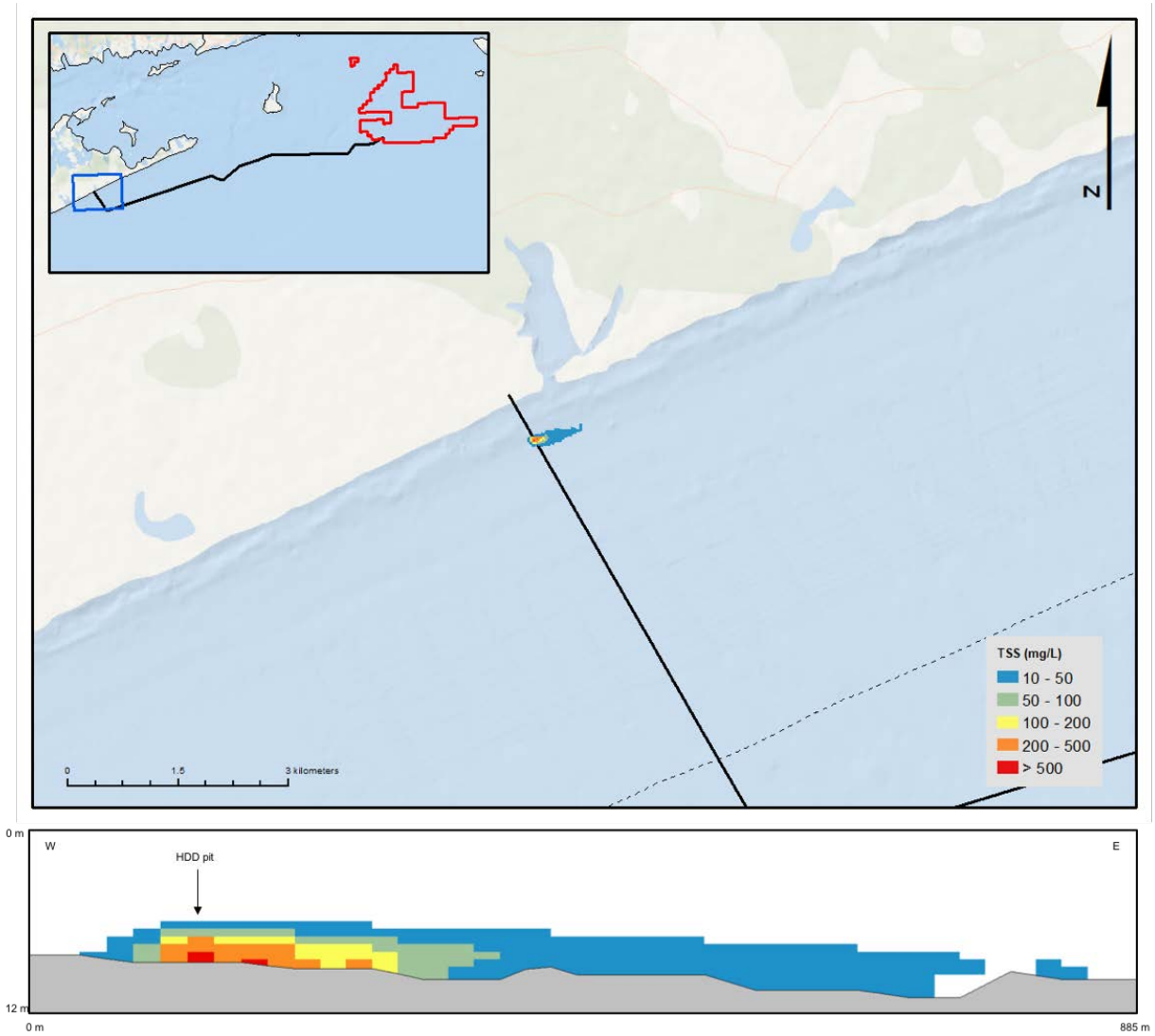


Figure 50. Cumulative TSS concentrations (mg/L) for Scenario 3 – suction dredging of the HDD exit pit at the sea-to-shore transition (Period 2 – spring tide conditions). Top: plan view showing concentrations near the dredging site; bottom: cross section view extending southwest from the dredging location. The maximum TSS concentration during this period is 562 mg/L. The plume is approximately 570 m from the shoreline at its closest point.

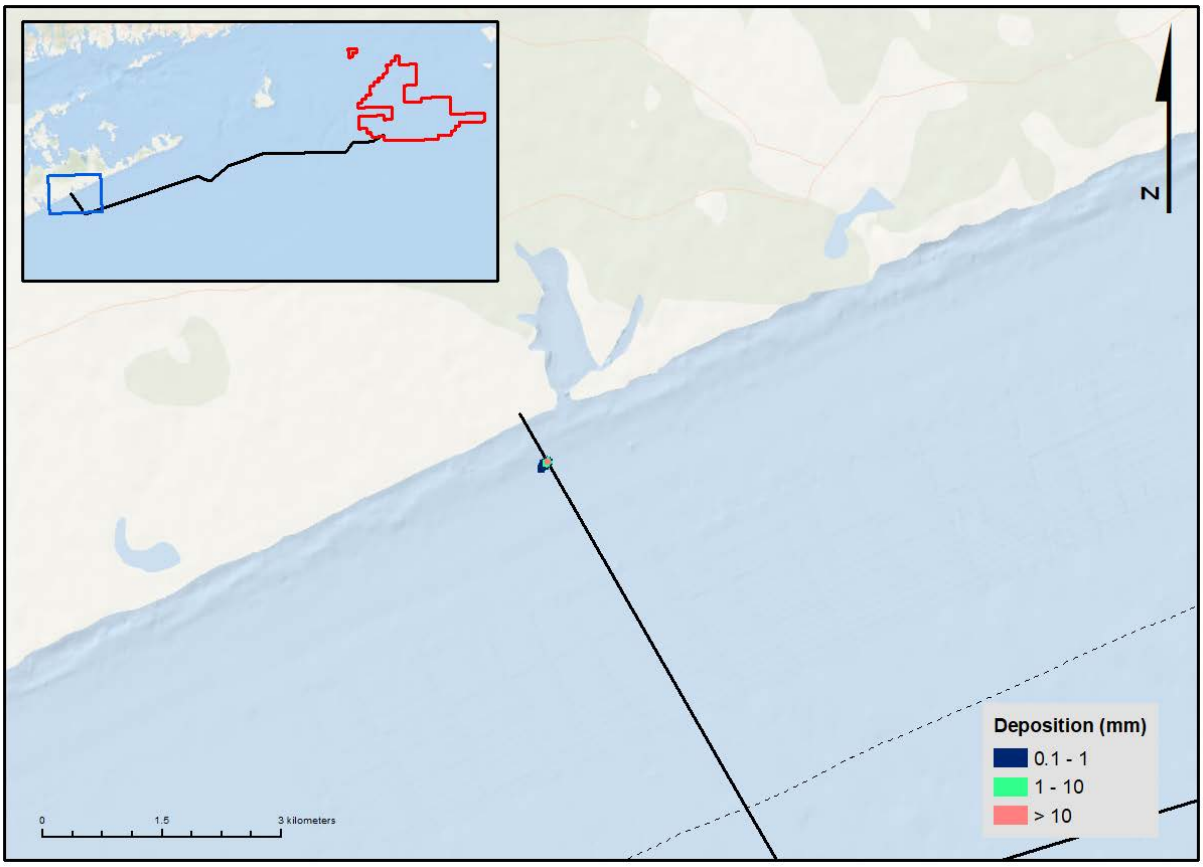


Figure 51. Extent of seabed deposition above 0.1 mm resulting from Scenario 3 – suction dredging of the HDD exit pit at the sea-to-shore transition (Period 1 – neap tide conditions). Inset shows location relative to full Project extent.)

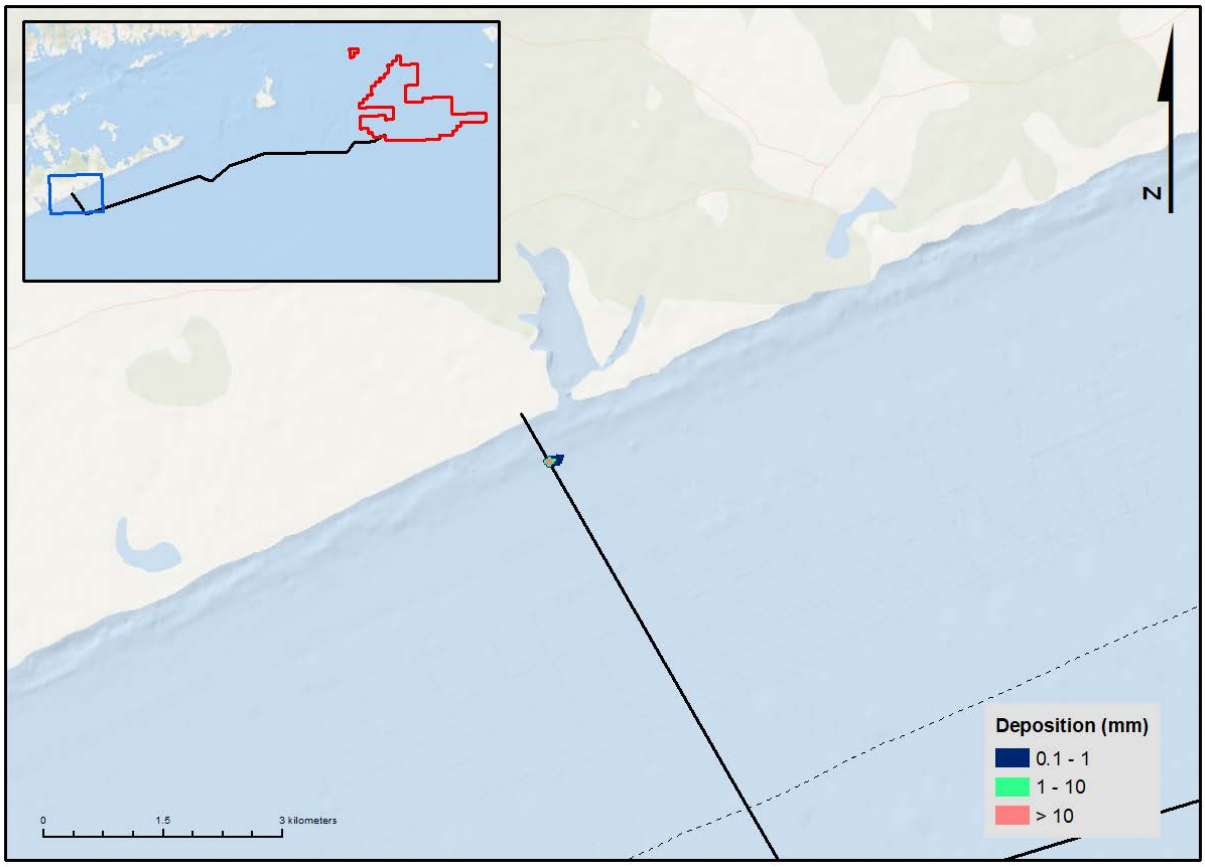


Figure 52. Extent of seabed deposition above 0.1 mm resulting Scenario 3 – suction dredging of the HDD exit pit at the sea-to-shore transition (Period 2 – spring tide conditions). Inset shows location relative to full Project extent.)

Table 7. Summary of SSFATE simulation results.

| Scenario | Construction Activity | Equipment Type | Location | Production rate (m3/hr) | Duration of modeled activity (hr) | Resuspension factor (%) | Total volume released (m3) | Time For TSS to return to ambient (hrs) | Max Distance of TSS Plume exceeding ambient (m) | | Max Distance of deposition exceeding (m) | | | Area of deposition exceeding (ha) | | |
|---|---|---|---|---|---|---|---|---|---|---|---|---|---|---|---|---|
| | | | | | | | | | 50 mg/L | 100 mg/L | 0.3 cm | 1.0 cm | 3.0 cm | 0.3 cm | 1.0 cm | 3.0 cm |
| Scenario 1 | SFEC installation - NYS waters (SFEC-NYS) | hydro-plow | SFEC corridor | 112 | 75.1 | 25 | 2,106 | 1.3 | 135 | 120 | 30 | 0 | 0 | 21.64 | 0.00 | 0.00 |
| | SFEC installation - federal waters (SFEC-OCS) | hydro-plow | SFEC corridor | 112 | 1,390.7 | 25 | 38,938 | 1.4 | 460 | 340 | 35 | 9 | 0 | 396.06 | 1.72 | 0.00 |
| Scenario 2 | Burial of inter-array cable (representative section) | hydro-plow | WTG 11 to WTG 9 | 112 | 20.9 | 25 | 585 | 0.3 | 90 | 40 | 39 | 8 | 0 | 3.28 | 0.04 | 0.00 |
| Scenario 3 | Excavation of seafloor for access to HDD pilot hole offshore Beach Lane | suction dredger | HDD exit pit | 90 | 7.2 | 100 | 650 | 1.1 | 260 | 145 | 65 | 54 | 44 | 0.96 | 0.56 | 0.48 |

# 4 References

Anderson, E.L., Johnson, B., Isaji, T., and E. Howlett, 2001. SSFATE (Suspended Sediment FATE), a model of sediment movement from dredging operations. WODCON XVI World Dredging Congress, 2-5 April 2001, Kuala Lumpur, Malaysia.

Codiga, D.L and A.E. Houk. (2002). Current profile time series from the FRONT moored array. Technical Report, Department of Marine Sciences, University of Connecticut, 19 pp.

Codiga, D.L and D.S Ullman. (2010). Characterizing the Physical Oceanography of Coastal Waters Off Rhode Island, Part 1: Literature Review, Available Observations, and A Representative Model Simulation in the Rhode Island Ocean SAMP study area (p. 14). Technical Report 2.

Connecticut Department of Energy & Environmental Protection. (Accessed 2017). CT_TOWN.shp [Shapefile]. Retrieved from http://www.ct.gov/deep/gisdata/

Davies, A. M. (1977). The numerical solution of the three-dimensional hydrodynamic equations, using a B-spline representation of the vertical current profile. Elsevier Oceanography Series, 19, 1-25.

Egbert, G. D., Bennett, A. F., & Foreman, M. G. (1994). TOPEX/POSEIDON tides estimated using a global inverse model. *Journal of Geophysical Research: Oceans*, *99*(C12), 24821-24852.

Egbert, G. D., & Erofeeva, S. Y. (2002). Efficient inverse modeling of barotropic ocean tides. *Journal of Atmospheric and Oceanic Technology*, *19*(2), 183-204.

Fugro (2017). Geophysical and Geotechnical Survey Plan BOEM Lease OCS-A 0486. Fugro Project No.: 02.81170001. Prepared for Deepwater Wind. May 5, 2017.

Fugro (2018). Geotechnical Data Report - South Fork Wind Farm and Export Cable. South Fork Wind Farm COP Survey Offshore Rhode Island / Massachusetts Atlantic OCS. Fugro Document No.: 02.17021080. Prepared for Deepwater Wind. January 31, 2018.

Gordon, R. B. (1982). *Wind-driven circulation in Narragansett Bay* (Doctoral dissertation, University of Rhode Island).

Grilli, S., Harris, J., Sharma, R., Decker, L., Stuebe, D., Mendelsohn, D., Crowley, D., & Decker, S. (2010). High resolution modeling of meteorological, hydrodynamic, wave and sediment processes in the Rhode Island Ocean SAMP study area (p. 119). Technical Report 6.

Isaji, T. H., Howlett, E, Dalton C. and Anderson E. (2001).,Stepwise-Continuous-Variable-Rectangular Grid. In *Proc. 24th Arctic and Marine Oil Spill Program Technical Seminar* (pp. 597-610).

Isaji, T., & Spaulding, M. L. (1984). A model of the tidally induced residual circulation in the Gulf of Maine and Georges Bank. *Journal of physical oceanography*, *14*(6), 1119-1126.

Johnson, B.H., E. Anderson, T. Isaji, and D.G. Clarke, 2000. Description of the SSFATE numerical modeling system. DOER Technical Notes Collection (TN DOER-E10). U.S. Army Engineer Research and Development Center, Vicksburg, MS. http: //www.wes.army.mil/el/dots/doer/pdf/doere10.pdf.

Lin, J.; Wang, H.V.; Oh, J-H.; Park, K.; Kim, S-C.; Shen, J., and Kuo, A.Y., 2003. A new approach to model sediment resuspension in tidal estuaries. Journal of Coastal Research, 19(1), 76-88.

MassGIS. (Accessed 2017). OUTLINE25K_POLY.shp [Shapefile]. Retrieved from https://www.mass.gov/get-massgis-data

NDBC. (Accessed 2017). Historic Meteorological Observations [ASCII Text Files]. Retrieved from http://www.ndbc.noaa.gov/station_page.php?station=buzm3

NOAA. (Accessed 2017).ENC Data [Multiple geodatabase files]. Retrieved from https://encdirect.noaa.gov/

NOAA. (Accessed 2017). Harmonic Constituents [ASCII Data]. Retrieved from https://tidesandcurrents.noaa.gov/

NY GIS Clearinghouse. (Accessed 2017). Counties_Shoreline.shp [Shapefile]. Retrieved from http://gis.ny.gov/gisdata/inventories/details.cfm?DSID=927

Owen, A. (1980). A three-dimensional model of the Bristol Channel. *Journal of Physical Oceanography*, *10*(8), 1290-1302.

Pawlowicz, R., Beardsley, B., & Lentz, S. (2002). Classical tidal harmonic analysis including error estimates in MATLAB using T_TIDE. *Computers & Geosciences*, *28*(8), 929-937.

RIGIS. (Accessed 2010). Towns.shp [Shapefile]. Retrieved from http://www.rigis.org/

RPS ASA (2012). Sediment Transport Analysis of Cable Installation for Block Island Wind Farm and Block Island Transmission System. ASA Project: 2011-243. Prepared For: Tetra Tech EC. 03 May 2012

Soulsby, R.L., 1998. Dynamics of Marine Sands. Thomas Telford, England.

Spaulding, M. L., & Gordon, R. B. (1982). A nested NUMERICAL tidal model of the Southern New England Bight. *Ocean Engineering*, *9*(2), 107-126.

Swanson, J. C., 1986. A three dimensional numerical model system of coastal circulation and water quality. Ph.D. Thesis, Dept. of Ocean Engineering, University of Rhode Island, Kingston, RI.

Swanson, J.C., M. Spaulding, J-P. Mathisen and O.O. Jenssen, 1989. A three dimensional boundary fitted coordinate hydrodynamic model, Part I: development and testing. Dt. hydrog, Z. 42, 1989, p. 169-186.

Swanson, J.C., T. Isaji, M. Ward, B.H. Johnson, A. Teeter, and D.G. Clarke, 2000. Demonstration of the SSFATE numerical modeling system. DOER Technical Notes Collection (TN DOER-E12). U.S. Army Engineer Research and Development Center, Vicksburg, MS. http://www.wes.army.mil/el/dots/doer/pdf/doere12.pdf.

Swanson, C., and T. Isaji, 2004. Modeling Dredge-Induced Suspended Sediment Transport and Deposition in the Taunton River and Mt. Hope Bay, Massachusetts. Western Dredging Association Annual Meeting and Conference, March 26, 2004.

Swanson, C., H.-S. Kim, and S. Sankaranarayanan, 2006. Modeling of temperature distributions in Mount Hope Bay due to thermal discharges from the Brayton Point Station. In Natural and Anthropogenic Influences on the Mount Hope Bay Ecosystem, Northeastern Naturalist, Vol 13, Special Issue 4, 145-172.

Swanson, C., T. Isaji, and C. Galagan, 2007. Modeling the Ultimate Transport and Fate of Dredge-Induced Suspended Sediment Transport and Deposition. Proceedings of WODCON 2007, Lake Buena Vista, Florida.

Swanson, C., D. Mendelsohn, D. Crowley, and Y. Kim, 2012. Monitoring and modeling the thermal plume from the Indian Point Energy Center in the Hudson River. Proceedings of the Electric Power Research Institute Third Thermal Ecology and Regulation Workshop, Maple Grove, MN, 11-12 October 2011.

Spaulding, M.L., 1984. A vertically averaged circulation model using boundary fitted coordinates. Journal of Physical Oceanography, May, pp. 973-982.

Teeter, A.M., 2000. Clay-silt sediment modeling using multiple grain classes: Part I: Settling and deposition. Proceedings in Marine Science, 3, 157-171.

Van Rijn L.C., 1989, *Sediment Transport by Currents and Waves,* Report H461, Delft Hydraul. Lab., Delft, Netherlands.